1-1-2009

Nonlinear Instability and Reliability Analysis of Composite Laminated Beams

Alireza Fereidooni
Ryerson University

NONLINEAR INSTABILITY AND RELIABILITY ANLYSIS OF COMPOSITE LAMINATED BEAMS

by

ALIREZA FEREIDOONI,

MASc. (Mechanical Engineering)

Ryerson University, 2004

A thesis

presented to Ryerson University

in partial fulfillment of the requirement for the degree of

Doctor of Philosophy

in the Program of

Aerospace Engineering

Toronto, Ontario, Canada, 2009

AUTHOR'S DECLARATION

I hereby declare that I am the sole author of this dissertation.

I authorize Ryerson University to lend this dissertation to other institutions or individuals for the purpose of scholarly research.

I further authorize Ryerson University to reproduce this dissertation by photocopying or by other means, in total or in part, at the request of other institutions or individuals for the purpose of scholarly research.

ABSTRACT

NONLINEAR INSTABILITY AND RELIABILITY ANLYSIS OF COMPOSITE LAMINATED BEAMS

Doctor of Philosophy

in the Program of

Aerospace Engineering

Ryerson University

The wide range of high performance engineering applications of composite laminated structures demands a proper understanding of their dynamics performance. Due to the complexity and nonlinear behaviour of such structures, developing a mathematical model to determine the dynamic instability boundaries is indispensable and challenging. The aim of this research is to investigate the dynamic behaviour of shear deformable composite laminated beams subjected to varying time conservative and nonconservative loads. The dynamic instability behaviour of non-conservative and conservative system are dissimilar. In case of conservative loading, the instability region intersects the loading axis, but in case of non-conservative loads the region will be increased with loading increases.

The extended Hamilton's principle and the first order shear deformation theory are employed in this investigation to establish the integral form of the equation of motion of the beam. A five node beam model is presented to descritize the integral form of the governing equations. The model has the capability to capture the dynamic effects of the transverse shear stress, warping, and bending-twisting, bending-stretching, and stretching-twisting couplings. Also, the geometric and loading nonlinearities are included in the equation of system. The beam model incorporates, in a full form, the non-classical effects of warping on stability and dynamic response of symmetrical and unsymmetrical composite beams. In case of nonlinear elasticity, the resonance curves are bent toward the increasing exciting frequencies.

The response of the stable beam is pure periodic and follow the loading frequency. When the beam is asymptotically stable the response of the beam is aperiodic and does not follow the loading frequency. In unstable state of the beam response frequency increases with time and is higher than the loading frequency, also the amplitude of the beam will increases, end to beam failure. The amplitude of the beam subjected to substantial excitation loading parameters increases in a typical nonlinear manner and leads to the beats phenomena.

The principal regions of dynamic instability are determined for various loading and boundary conditions using the Floquet's theory. The beam response in the regions of instability is investigated. Axially loaded beam may be unstable not just in load equal to critical load and/or loading frequency equal to beam natural frequency. In fact there are infinite points in region of instability in plane load vs.

frequency that the beam can be unstable. The region of instability of the shear deformable beams is wider compare to the non-shear deformable beams. The lower bound of the instability region of the shear deformable beams changes faster than upper bound.

Probabilistic stability analysis of the uncertain laminated beams subject to both conservative and nonconservative loads is studied. The effects of material and geometry uncertainties on dynamics instability of the beam, is investigated through a probabilistic finite element analysis and Monte Carlo Simulation methods. For non-conservative systems variations of uncertain material properties has a smaller influence than variations of geometric properties over the instability of the beam.

ACKNOWLEDGEMENTS

I would like to sincerely and wholeheartedly thank my supervisors, Professor Kamran Behdinan and Professor Zouheir Fawaz who have been very supportive. I wish to thank them for their valuable guidance and scientific suggestions throughout this research. Their patience as advisors, boundless energy while reviewing all my writing and passion for this research are to be commended and worth emulating.

Financial support of National Sciences and Engineering Research Council of Canada (NSERC) and Ryerson Graduate Scholarship and Award (RGS/ RGA) to carry out this research is gratefully acknowledged.

Also, I am indebted to my friendly colleagues at Ryerson University, for their help and support.

DEDICATION

To my family, with love, admiration, and gratitude

TABLE OF CONTENTS

LIST OF FIGURES

LIST OF TABLES

NOMENCLATURE

Roman

A	extensional stiffness matrix
A_m	vector independent of time
b	width of beam
B	extensional-bending stiffness matrix
B_m	vector independent of time
C	damping matrix
D	bending stiffness matrix
e	Green-Lagrange strain
E	elastic modulus
E	strain energy
F	applied force
F	loading vector
f	forces acting on surface of beam
f_{nc}	non-conservative force vector
$F(\chi)$	probability density function
G	displacement gradient
G	shear modulus
h	height of beam
I	unit matrix
J	Jacobian determinent

i, j	numerical increment
$\boldsymbol{I}$	moment of inertia
$\mathrm{K_L}$	loading stiffness matrix
$\mathrm{K_E}$	elastic stiffness matrix
$\mathrm{K_G}$	geometric stiffness matrix
k	shear correction factor
l	length of beam
l_e	length of beam element
L	probabilistic loading matrix
$\boldsymbol{M}$	bending and twisting moment
$\mathbf{M}$	mass matrix
$\mathbf{M^e}$	element mass matrix
$\boldsymbol{N}$	in-plane forces
N	number of plies
N	Shape function
P	varying time load applied on beam
P_0	amplitude of static term of applied load on beam
P_t	amplitude of dynamic term of applied load on beam
P_{cr}^{w}	critical load of non-shear deformable beam
P_{cr}	critical load of shear deformable beam
$\boldsymbol{Q}$	shear forces
$\bar{Q}$	transformed reduced stiffness
$\boldsymbol{S}$	engineering stress

S_i	PK2 stress
$\hat{S}$	shear stiffness
t	time
T	generalized stress vector
T	time period of motion
u_1	axial displacement
u_2	lateral displacement
u_3	transverse displacement
U_i	global displacement
U_i^e	nodal displacement
U^T	mid surface displacement matrix
V_f	fiber volume fraction
δK	virtual kinetic energy
δT	virtual potential strain energy
W_{nc}	virtual work done by non-conservative forces

Greek

α	warping constant
α°	ply angle
ε	true strain
ε_L	linear strain

ε_{NL}	non-linear strain
δ	damping loss factor
δ_l	axial damping loss factor
γ	membrane strain
κ	bending strain
θ	angle between force vector and longitudinal axis of beam
θ	loading frequency
λ_i	eigenfrequency
ψ	shape function
Ψ	nonlinearity function
ν	poisson ratio
χ_i	mean value of probability density function
ω	beam frequency
ω_n	natural frequency
η	conservativeness factor
Λ	amplitude of beam
δK	virtual kinetic energy
δu	virtual displacement
ε_t	total strain
ζ	warping function
ξ	damping coefficient
ξ_{NL}	nonlinear damping

V	volume of body in motion
Θ	nonlinear inertia
A	surface of body in motion
ϕ_1	twist angle
ϕ_2	rotation of transverse normals
ϕ_3	in plane rotation
ρ	mass density
σ	Cauchy true stress
σ_i	variance of i^{th} random variable
σ_p	standard deviation of probability density function
χ	random variable
$\overline{\chi}_i$	mean value of i^{th} random variable
$\Re^{-1}$	inverse of cumulative distribution function
$\wp$	factor of reliability of beam

CHAPTER 1

Introduction

1.1 Motivation

Laminated composite structures have been widely used in the fields of aerospace, civil and mechanical engineering due to their excellent properties. A variety of light-weight heavy load bearing structural components made of composite materials such as aircraft wings, helicopter rotor blades, spacecraft antennae, flexible satellites, robot arms, and long-span bridges can be modeled as laminated beam members.

When a laminated beam subjected to harmonic loads, in specific conditions of loading frequency and loading magnitude the beam becomes unstable leading to large deflections and internal stresses and eventually beam failure. Therefore a better understanding of the behaviour of laminated composite beams under dynamic loading is essential to satisfy their design requirements. This research intends to present a comprehensive study of the dynamic analysis of laminated beams to determine when they will be unstable, not just in critical loading conditions but also in other situations and further to establish their regions of instability and response of the beams under such conditions.

Extensive studies can be found in stability analysis of linear beams which are applicable only in a very restrictive domain such as when the vibration amplitude is very small. To gain a better understanding of the dynamic behaviour of a composite beam under general conditions, it is essential to present the nonlinearities in the mathematical model. There are very few comprehensive studies in the field of nonlinear performance of composite laminated beams.

The fibre orientation, the number of layers and their lay-up in laminated composites introduce many complicated nonlinear dynamic behaviours such as twisting-bending, extension-bending, and twisting-extension couplings. To capture all of these nonlinear couplings, a new beam element is derived to perform dynamic and stability analysis through the nonlinear finite element analysis.

Mechanical properties of laminated composite structures can become uncertain due to changes in various manufacturing conditions such as fibre orientations, curing temperature and curing pressure. Thus, for predicting the instability regions of an uncertain beam, it is extremely important to identify and use an appropriate statistical model. In this study the probabilistic finite element method and Monte Carlo simulation are used to predict the structural behaviour of the composite beams with geometrical and material property uncertainties.

1.2 Objectives

The objective of this study is to investigate the dynamic instability behaviour of laminated composite beams subjected to axial periodic loads. Also, the influence of the uncertain material and geometric properties on the region of instability and response of the imperfect beam will be studied.

The above objectives may be broken into four parts. The first part deals with the formulation of the governing equation of motion of a laminated beam with large deflection and small strain. The second part concerns the development of a new beam element to descitize the equation of motion to a set of Mathieu type differential equations and variety of numerical applications is presented to test the developed beam model. In the third part the boundary parametric resonance frequencies of the motion (instability regions) are determined by using the Floquet theory, various loading patterns, arbitrary lamination, and general boundary conditions are studied. The fourth part addresses the problem of the probabilistic dynamic analysis of the uncertain laminated beam. A developed probabilistic finite element analysis and Monte Carlo simulation are used to predict the effects of imperfections on the stability and failure of such structures.

1.3 Literature Review

Composite laminated beams have been increasingly used over the past few decades in the field of engineering as structural components because of the

high strength-stiffness to weight ratios, the ability of having different strengths in different directions and the nature of being tailored to satisfy the design requirements. For these reasons the dynamic behaviours of laminated composite beams have received widespread attention and have been investigated extensively by many researchers.

1.3.1 Composite Laminated Beams

Earlier studies of the dynamic behaviour of composite laminated beams were largely based on the composite laminated materials, which neglects the effects of out-of-plane deformation. Abarcar and Cunniff (1972) conducted a free vibration analysis of a simple laminated composite beam without the effects of shear deformation. Miller and Adams (1975) studied the vibration characteristics of the orthotropic clamped-free beams using the classical lamination theory. Vinson and Sierakowski (1986) obtained the exact solutions of a simply-supported composite beam based on the classical lamination theory. Banerjee and Williams (1995) developed the exact dynamic stiffness matrix for a uniform, straight and bending–torsion coupled composites. Mahapatra et al. (2000) studied the axial–flexural coupled wave propagation in multiply connected slender composite beams based on Bernoulli–Euler beam theory.

Teoh and Huang (1976) introduced the effects of shear deformation and rotary inertia on the free vibration of the orthotropic cantilever beam based on an energy approach. They presented two finite element models based on the

first-order shear deformation theory for the free vibration analysis of the fixed-free beams of general orthotropy. Chen and Yang (1985) introduced a finite element method to predict the free vibration of the laminated beams with the shear deformation included. Kapania and Raciti (1989) compiled a survey of developments in the vibration analysis of laminated composite beams. Chandrashekhara et al. (1990) presented the exact solutions for the free vibration of symmetrically laminated composite beam including the shear deformation for some arbitrary boundary conditions. Bhimaraddi and Chandrashekhara (1991) modeled the laminated beams by a systematic reduction of the constitutive relations of the three-dimensional anisotropic body and obtained the basic equations of motion of the beam theory based on the parabolic shear deformation theory. Numerical results for the natural frequencies and buckling load were presented. Soldatos and Elishakof (1992) developed a third-order shear deformation theory for the static and dynamic analysis of an orthotropic beam incorporating the effects of transverse shear and transverse normal deformations. Abramovich (1992) presented the exact solutions for symmetrically laminated composite beams with ten different boundary conditions, where shear deformation was included in the analysis. Krishnaswamy et al. (1992) presented the analytical solutions to the free vibration of generally layered moderately thick composite beams by the Lagrange multipliers method. Rotary inertia and shear deformation effects were included in the formulation. But to get convergent solutions, the theory required 80 or more terms of the assumed series. Chandrashekhara and Bangera (1992)

studied the free vibration characteristics of the laminated composite beams using the finite element analysis and a higher order beam theory. Abramovich and Livshits (1994) studied the free vibration of non-symmetric cross-ply laminated composite Timoshenko beams. Khdeir and Reddy (1994) employed the transfer matrix method in the free vibration analysis of the cross-ply laminated beams based on the various shear deformation theories. Nabi and Ganesan (1994) presented the finite element method based on the first-order shear deformation theory for the free vibration analysis of the composite beam. Eisenberger et al. (1995) utilized the dynamic stiffness analysis to study the free vibration of the laminated beams using a first-order shear deformation theory. Teboub and Hajela (1995) adopted the symbolic computation technique to analyze the free vibration of generally layered composite beam on the basis of a first-order shear deformation theory. Abramovich et al. (1995) applied the exact element method to determine the natural frequencies, the buckling loads, and the influence of the axial load on the natural frequencies and mode shapes of nonsymmetric laminated composite beams based on a first-order deformation theory including the effects of rotary inertia, shear deformation, and coupling between the longitudinal and the transverse displacements. Song and Waas (1997) studied the buckling and free vibration of stepped laminated composite beams using a simple higher-order theory which assumed a cubic distribution for the displacement field through the thickness. Kant et al. (1997) presented an analytical method for the dynamic analysis of the laminated beams using the higher-order refined theory. Banerjee (1998) performed the free vibration

analysis of axially loaded composite Timoshenko beams by using the dynamic stiffness matrix method with the effects of axial force, shear deformation, rotary inertia and coupling between the bending and the torsional deformations taken into account. Shimpi and Ainapure (1999) studied the free vibration of two-layered laminated cross-ply beams using the variational consistent layer-wise trigonometric shear deformation theory. Yildirim et al. (2000) studied the in-plane and out of plane free vibration problem of symmetric cross-ply laminated composite straight beams using the transfer matrix method. Yildirim (2000) used the stiffness method for the solution of the purely in-plane free vibration problem of symmetric cross-ply laminated beams with the rotary inertia, axial and transverse shear deformation effects included by the first-order shear deformation theory. Rao et al. (2001) proposed a higher-order mixed theory for determining the natural frequencies of a diversity of laminated simply-supported beams. Matsunaga (2001) investigated the natural frequencies, buckling stresses and interlaminar stresses of multilayered composite beams by using the one-dimensional global higher-order theories. Chakraborty et al. (2002) presented a new refined locking free first-order shear deformable finite element and demonstrated its utility in solving the free vibration and wave propagation problems in the laminated composite beam structures with symmetric as well as asymmetric ply stacking. Goyal (2002) proposed the formulations to study the static responses, free vibration and buckling of laminated composite beams based on the first order shear deformation theory and principle of virtual work. He employed an accurate model to obtain the transverse shear correction factor.

Mahapatra and Gopalakrishnan (2003) presented a spectral finite element model for the analysis of the axial– flexural–shear coupled wave propagation in thick laminated composite beams and derived an exact dynamic stiffness matrix. Chen et al. (2004) presented a new method of state-space-based differential quadrature for free vibration of generally laminated beams. Ruotolo (2004) developed a spectral element for anisotropic, laminated composite beams. The axial–bending coupled equations of motion were derived under the assumptions of the first-order shear deformation theory.

The above literature analysis on the subject shows that there appears to be very few works reported on the dynamic instability of laminated composite beams including the influences of shear effect, axial force and shear deformation, and all the stretching-bending, twisting-bending, and twisting-stretching in a unitary manner. The dynamic behaviours of axially loaded generally laminated beams are not well-investigated and there is a need for further studies.

1.3.2 Finite Element Analysis

Finite element methods are widely used in engineering applications to determine stresses and strains in complicated mechanical systems. Finite element analysis (FEA) or finite element modeling (FEM) are generally synonymous terms for computer-based methods of stress analysis which are used when the shapes, numbers or types of materials, or the loading history are

too complicated to yield to analytical methods. The study of fiber-reinforced laminated composite beams using the finite element analysis is of great interest to researchers.

In the last two decades, some attention has been paid to the development of laminated beam elements. A twelve degree of freedom element was developed by Chen and Yang (1985) to study the static and dynamic behaviour of the deterministic symmetric laminated beam. Later Kapania and Raciti (1989) developed a 20 degree of freedom element to study static, free vibration, buckling, and nonlinear vibrational analysis of unsymmetrically laminated beams. However, no derived beam elements were available to obtain all three displacements (axial, transverse, and lateral), in-plane rotations, warping effects, and shear effects.

Bassiouni et al. (1999) used a finite element model to obtain the natural frequencies and mode shapes of laminated composite beams, which consisted of five nodes. The displacement components were lateral displacement, axial displacement, and rotational displacement, and closed form solutions for stiffness and mass matrices were given. Although this is one of the most complete beam elements, it does not take into account inplane shear, shear deformations, transverse deflections, and torsional effects.

Some research has been focused on deriving beam elements for laminated composites using higher order shear deformation theories (HSDT). Manjunatha and Kant (1993) developed a set of higher-order theories for the analysis of composite and sandwich beams. By incorporating a more realistic nonlinear

displacement variation through the beam thickness, they eliminated the need for shear correction coefficients.

Subramanian (2001) developed a two-node finite element of eight degrees of freedom per node, using a HSDT, for flexural analysis of symmetric laminated composite beams.

Goyal (2002) developed a twenty-one degree-of-freedom beam element, based on the first order shear deformation theory, and principle of virtual work, to study the static response, free vibration and buckling of laminated composite beams. In his model and formulation, the dynamic stiffness matrix is not included in the formulation, because of that his model can not capture the effects of the dynamic part of varying time loading stiffness matrix. Therefore a beam model and formulation to include both static and dynamic varying time loading is desired.

Averill and Yip (1996) developed an accurate, simple, and robust two node finite elements based on shear deformable and layerwise laminated beam theories. The two node element has only four degrees of freedom per node, and the formulation is only valid for small deformations.

Only few researchers have worked on nonlinear analysis of laminated beams using the finite element method. Murin (1995) formulated a nonlinear stiffness matrix of a finite element without making any simplifications. The matrix includes the quadratic and cubic dependencies of the unknown increments of the generalized nodal displacements into the initially linearized

system of equations. However, the formulation is limited to isotropic materials and not applied to laminated composites.

After reviewing most of the works done in this field there appears to be no shear deformable laminated beam element for the study of large deflection, including torsional and warping effects, lateral displacement, and inplane displacement of the composite laminated beams. Thus, a much improved laminated beam for the dynamic analysis of large deflections of laminated composite beams is greatly needed. An element that does not require numerical integration, but uses symbolic manipulators such as MATLAB© to discretize the equation of motion of the beam is also needed. One of the contributions of this study is to present a new beam element to study large deflection with small strain of an axially loaded generally layered composite beam on the basis of first-order shear deformation theory.

1.3.3 Dynamics Instability Analysis of composite Beams

Beams may become unstable when the loading frequency matches the resonance frequency and/or the loading reaches a specific fraction of the critical load. In these situations, stability analysis becomes a significant tool when it comes to design and analysis of beams. A retrospective on the important developments in dynamic stability theory was presented by Bolotin (1964).

A literature review on the subject shows that there appears to be very few studies reported on the free vibration and stability analysis of laminated

composite beams, including the influences of axial force conservativeness and shear deformation in a unitary manner. The dynamic behaviours of axially loaded laminated beams are not well-investigated and there is a need for further study. This problem is addressed in the current study. The contribution of this study is to extend the derivation of the dynamic stiffness matrix for an axially loaded layered composite beam on the basis of first-order shear deformation theory which assumes a constant distribution of the transverse shear strain over the thickness of the whole beam by using the extended Hamilton's principle. Furthermore the dynamic stiffness matrix for determining the natural frequencies and mode shapes of the composite beams is formulated from the general solutions of the governing differential equations of motion. Finally, the effects of axial force, boundary conditions, and natural frequencies of the beam on instability regions are extensively studied using Floquet theory.

1.3.4 Probability Analysis of composite Beams

Composite laminates are made of fibers and matrix which are of two different materials. The way in which the fibres and matrix materials are combined to make a lamina, as well as the lay-up and curing of lamina, are complicated processes and may involve a lot of uncertainties. These uncertainties result in dispersion in the material and geometry properties of the composite laminates.

In the presence of inherent scatter in the material and geometry properties an accurate prediction of instability and failure of composite structures has become more challenging to designers. For reliability assessment and failure analysis it is important to model the problem with random material and lay up properties for accurate prediction of instability and failure load of the structure.

Various methods exist to analyze an uncertain structure by integrating probabilistic aspects into the finite element modeling. Specifically, there has been a growing interest in applying these methods to better understand laminated composite structures by integrating the stochastic nature of the structure in the finite element analysis, Schueller (1997).

Recently, a number of researchers have studied the failure probability of composite laminates subjected to both transverse and in-plane loads. Cassenti (1984) investigated the failure probability and probabilistic location of failure in composite beams based on weakest-link hypothesis. Cederbaum et al. (1991) studied the reliability of laminated plates subjected to in-plane random static loads based on failure criterion for unidirectional fibre composites. Engelstad et al. (1992) and Kam and Cheng (1992) studied the reliability of linear and non-linear laminated composite plates subjected to transverse loading. Reddy (1992) used different failure criteria to investigate linear and non-linear first-ply failure load based on first-order shear deformation plate theory. Kam and Jan (1995) used layer-wise linear displacement plate model to obtain a more accurate first-ply failure load on the basis of several failure criteria. Both investigations were basically done in deterministic environment only. Nakayasu and Maekawa

(1997) proposed stochastic failure envelope diagrams to evaluate the stochastic behaviour of a composite laminate with any lamination angle under in-plane multi axial load. Lin (2002) used the stochastic finite element method to predict the reliability of angle-ply laminates with different types of buckling failure modes subject to in-plane edge random load which were not applied simultaneously. Wu et al. (2002) used the Monte Carlo approach to generate different strengths of composite lamina. Frangopol and Recek (2003) studied the reliability of fibre reinforced composite laminated plates under transverse random loads. The failure criterion was used to predict the failure load and the probability of failure was computed by Monte Carlo simulation.

Goyal (2002) studied the reliability analysis of the composite beams with uncertain axial module of elasticity and ply angle orientation through the probabilistic finite element analysis and Monte Carlo simulation. He did not study the effects of the uncertainties on the region of dynamic instabilities.

In this study both geometric properties (cross-sectional properties and dimensions) and material mechanical properties (modulus and strength), and also dynamic load magnitude are treated as random variables in a stochastic finite element analysis with taking advantage of Monte Carlo method using the Weibull distribution function for predicting the dynamic region of instabilities of composite laminated beams.

1.4 Dissertation organization

The organization of this research is as follows:

Chapter 1 contains a literature review of the references that were most helpful in carrying out the objective of the dissertation. The first and second sections describe the motivation and objectives of this study. The third section contains the references that were most useful for dynamic analysis, finite element analysis, stability analysis, and probabilistic analysis of composite laminated beams. The fourth section describes the dissertation organization.

Chapter 2 establishes the governing equations of motion of laminated composite beams subjected to both conservative and non-conservative varying time loads, using the extended Hamilton's principle. Assumptions used in the derivation are also elaborated on. The derived integral form of equations is used in the finite element analysis in subsequent chapters.

Chapter 3 describes in detail the development of a finite element beam model that allows large deflections and small strain. The beam equation of motion is descritized using a developed beam element. The resulting finite element is required for the calculation of the dynamic stiffness and mass matrices.

Chapter 4 presents the solutions of the nonlinear system of equations that result from the finite element formulation presented in Chapter 3. In this chapter, dynamic stability analysis of the composite laminated structures, with different boundary and loading (conservative and non-conservative) conditions are studied. The effect of damping behaviour on stability of the structure is also

studied. Determination of the boundaries of instability regions is the main objective of this chapter.

Chapter 5 covers a description of the probability approach through an imperfection modeling: then the random variables and their characteristics are studied. The rest of the chapter is dedicated to the explanation of the probabilistic finite element analysis (PFEA), and the Monte Carlo Simulation (MCS). The final part of the chapter covers the use of PFEA to predict the response of the beam, determine its region of instability, and calculate the probability of failure.

Chapter 6 briefly summarizes the findings in this dissertation with the proposed method and some recommendations for future work in the area of dynamic stability analysis of laminated beams with or without geometric imperfections. The last section of this chapter includes areas in which this work can be expanded.

CHAPTER 2

Governing Equations of Motion of Composite Laminated Beams

When a structure is subjected to periodic loads, the forced response may become dynamically unstable under certain circumstances. Therefore for such a problem, stability analysis plays a vital role in design and analysis of structures.

A retrospective attention in dynamic stability analysis of isotropic beams, plates and shells, subjected to periodic in-plane loads, has been investigated by Bolotin (1964), whereas the study related to composite laminates has been fairly attempted by other investigators. All these studies are based on the analysis in which periodic loading is conservative. The boundaries of the instability regions are then obtained using an eigenvalue approach.

2.1 Problem Definition

It is considered a straight composite laminated beam subjected to an axial parametric load undergoes to transversal large deformation. A schematic of the beam is shown in Fig. 2.1, where (x_1, x_2, x_3) denote the orthogonal coordinate system with displacement vectors (U_1, U_2, U_3). For simplification, thermal and piezoelectric effects are ignored. The structure is assumed to have a high length-to-width and length-to-thickness ratios therefore one dimensional beam theory is used to model the structure.

The thickness of the beam is assumed far smaller than the length and the width. As a result, the magnitudes of the stresses acting on the surface parallel to the mid-plane are small compared to the bending and membrane stresses. As a result, the state of stress can be approximated as a state of plane stress. Also a out-of-plane warping will be considered. Laminated composite materials are made of fiber-reinforced lamina of different properties. It is assumed that each lamina is a continuum and there are no empty spaces, voids, internal delaminations, or material defects in the laminated beam.

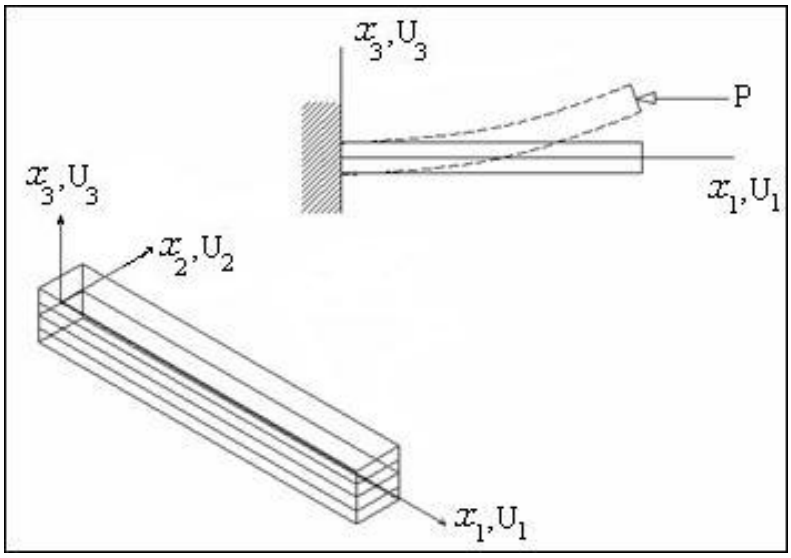

Figure 2. 1 Composite laminated beam geometry and local coordinate system.

If laminated structures is not symmetric and experiences a large bending-extension coupling, the effect of curvature may arise during the curing process (Kollar and Springer 2003). However, this effect is ignored and the present formulation assumes a perfectly straight laminated beam in its initial configuration.

2.2 Sources of Nonlinearities

If there is any discontinuity in the system or if dependent variables and their derivatives appear in the equations of motion, then the system should be considered as nonlinear. In theory, nonlinearity exists in a system whenever there are products of dependent variables and their derivatives in the equations of motion, boundary conditions, and/or constitutive laws, and whenever there are any sort of discontinuities.

In structural mechanics, nonlinearities can arise in numerous ways; three of the most common in structural applications are material nonlinearity, geometric nonlinearity, and loading nonlinearity. The plastic forming of a component related to stress-strain relations is an example of the material nonlinearity. In the systems undergoing large deformations or deflections usually result in nonlinear strain-displacement relations. This type of nonlinearity is called geometric nonlinearity. The follower loads applied on structure is an example of loading nonlinearity. The effect of the nonlinearities is seen in the equations governing the structural response and stability. In this study, the geometric and forces nonlinearities will be considered. The geometric nonlinearities will be used to analyze laminated beams with large displacements and small strains. Under small strains composite laminates do not typically show any nonlinear material behaviour. The effects of following loads on stability analysis of system will be investigated as well.

2.3 Beam Theories for composite laminated beams

Two popular beam theories in use to analyze the beams are: 1- The Euler-Bernoulli beam theory, and 2- The Timoshenko beam theory. The Euler-Bernoulli beam theory (Shames 1985) assumes that plane cross sections, normal to the neutral axis before deformation, continue to remain plane and normal to the neutral axis and do not undergo any strain in their planes. In other words, the warping and transverse shear-deformation effects and transverse normal strains are considered to be negligible and hence ignored. These assumptions are valid for slender beams. In this case the rotation of the cross sections is just due to bending alone. But for problems where the beam is made up of a composite material, the transverse shear is not negligible. Incorporating the effect of transverse shear deformation into the Euler-Bernoulli beam model gives us the Timoshenko beam theory (Timoshenko, 1921,1922; Meirovitch, 2001; Shames and Dym, 1985). In this theory, to simplify the derivation of the equations of motion, the shear strain is assumed to be uniform over a given cross section. In turn, a shear correction factor is introduced to account for this simplification, and its value depends on the shape of the cross section (Timoshenko, 1921). In the presence of transverse shear, the rotation of the cross section is due to both bending and transverse (or out-of-plane) shear deformation. The method of analyzing layered beams is to use a Timoshenko like formulation, the so called first-order shear deformation theory, with appropriate transverse shear stiffness and shear correction factors and then complete a post-processing calculation in which the in-plane stresses are used to determine approximations for the

transverse shear stresses; that is, the procedure outlined above for the classical and shear deformation models (J.S. Hansen, CANCAM 2007).

A linear beam model would suffice when dealing with small deformations. But when the deformations are moderately large, for accurate modeling, several nonlinearities also need to be included.

2.4 Kinematics methodology for the beams with large deformations and small strains

A large deformation of a beam does not necessarily mean the presence of large strains. Under large rigid-body rotations, structures like beams may undergo large deformations but small strains. Even when the rigid-body rotations are small, deformations will still be large for long structures. With respect to a coordinate system co-rotated with the rigid-body movement, the relative displacements are small and the problem becomes linearly elastic. But the large deformations give rise to geometric nonlinearities due to nonlinear curvature and/or mid-plane stretching, leading to nonlinear strain-displacement relations. When the deformation is small, the small deformation linear strains and the Cauchy stresses can be used. But in case of large deformation strain measures, stress measures, and the constitutive equations for nonlinear system shall be considered.

The first step in defining large deformation strain measures is to define the relationship between what is known as the reference, initial or undeformed configuration of a body, and the deformed configuration of the body. The

reference or undeformed configuration is the condition of the body in 3D space before loads have been applied to it. The deformed configuration is the location and shape of the body after loads have been applied to it. It is important to note that the body may undergo rigid body motion in addition to strain when loads are applied on it. An illustration of the relationship between the initial and deformed configuration is shown in Fig. 2.2.It is noted that the relationship between the two position vectors in space is the displacement vector *u*. It can be directly written the relationship between the position vectors in the initial and deformed configuration $x_i = x_i^{\circ} + u_i$.

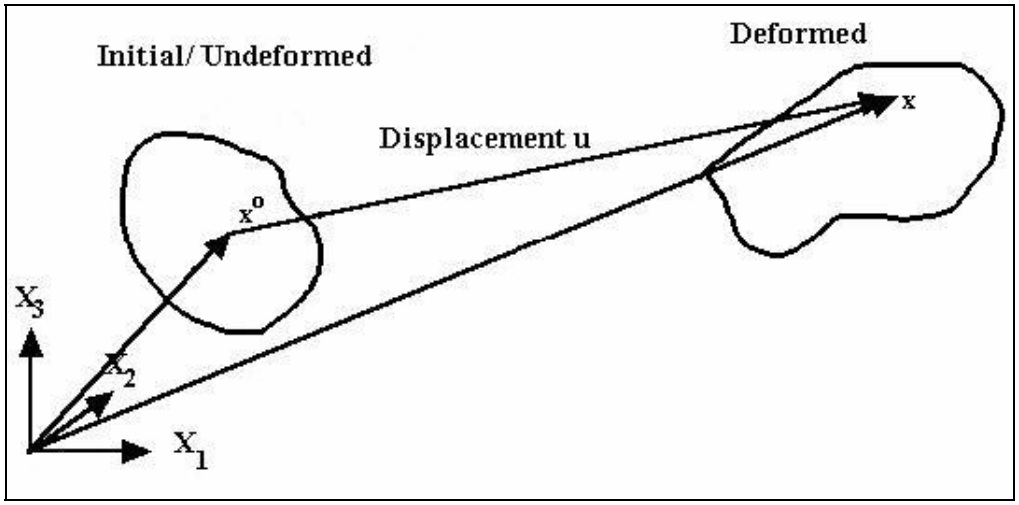

Figure 2. 2 Deformation of a body from undeformed to the deformed configuration.

2.5 Beam Displacement

To measure the beam displacement at any point of the beam the strains need to be converted into displacement at that point. Orthotropic and anisotropic materials exhibit directional characteristics and thus bring shear-extension coupling into the analysis. When laminates are unsymmetrically stacked, bending-stretching coupling is added to the analysis. The bending-stretching coupling will cause unsymmetric laminates to warp out-of-plane. The differences in elastic properties between fiber filaments and matrix materials lead to inplane-shear coupling. The high ratio of in-plane modulus to transverse shear modulus makes the classical lamination theory, which neglects the effect of out-of-plane strains, inadequate for the analysis of multilayered composites. In such a case, one should use a theory which includes transverse shear deformation, an example being the first order shear deformation theory.

For symmetric laminates, the classical lamination theory (CLT) has been used successfully in most cases. Classical lamination theory assumes that the Kirchhoff's hypothesis is valid for the laminate and that the through-the-thickness effects and geometric nonlinearities are negligible. (Kapania et al.) The CLT assumptions and the integration of the laminae constitutive equations lead to the well-known A, B, and D matrices. For symmetric laminates, the B matrix is identically zero, and therefore the inplane and out-of-plane effects are uncoupled. Although the bending-stretching coupling is present only in unsymmetric laminates, the stretching-shearing and the bending-twisting coupling may characterize both symmetric and unsymmetric laminates. The

effect of the stretching-shearing coupling is to induce shear when a stretching force is applied to the laminate and vice versa. The effect of bending-twisting coupling is to induce twisting when a bending moment is applied to the laminate and vice versa. Thus with the above explanation, a displacement field that would be able to capture the existence of the various coupling effects is desired. In this study, the in-plane displacements are assumed to vary linearly with respect to the thickness coordinate.

Assuming that:

- The deformations of the beam take place in-plane and the displacement components along x_1, x_2, and x_3 are $U_1, U_2,$ and U_3 respectively,

- The cross-section contour is rigid in its own plane.

- The warping distribution is assumed to be given by the Saint–Venant function for the beam.

- The radius of curvature at any point of the beam is neglected.

- Twisting linear curvature of the beam is expressed according

to the classical plate theory.

According to the assumptions and on the basis of the general shear deformable beam theory, the displacements field along with coordinate system shown in Fig.2.1 of any point of the beam is defined as follows:

$$\begin{aligned} U_1(x_1,x_2,x_3,t) &= u_1(x_1,t) - x_2\phi_3(x_1,t) - x_3\phi_2(x_1,t) - \zeta(x_1,x_2,t)(\phi_3(x_1,t) - \phi_2(x_1,t)) \\ U_2(x_1,x_2,x_3,t) &= u_2(x_1,t) - x_3\phi_1(x_1,t) \\ U_3(x_1,x_2,x_3,t) &= u_3(x_1,t) + x_2\phi_1(x_1,t) \end{aligned} \tag{2.1}$$

where,

$u_1(x_1,t) =$ The axial displacement , $u_2(x_1,t) =$ The lateral displacement

$u_3(x_1,t) =$ The transverse displacement ,

$\phi_1(x_1,t) =$ The twist angle,

$\zeta(x_1,x_2,t) =$ The warping function,

$\phi_2(x_1,t) =$ The rotation of the transverse normals with respect to x ,

$\phi_3(x_1,t) =$ The in-plane rotation , and $t =$ time .

The above defined displacement field would be able to capture the existence of the various coupling effects i.e., bending and twisting-extension couplings. All these displacements and rotations are measured to the mid-surface. The generalized displacement vector for each point of the beam can be defined as follows:

$$\mathbf{U}^{\mathrm{T}} = \{u_1, \quad u_2, \quad u_3, \quad \phi_1, \quad \phi_2, \quad \phi_3,\} \tag{2.2}$$

2.6 Displacements independent of time

The governing equations of motion of the nonlinear composite laminated beam can be derived either by the Newtonian approach or by a variational approach. (Doyle 2001). Hamilton's principle is the most widely used variational method to obtain the equations of motion for dynamical problems. Hamilton's principle states that for a system with given configurations of all the varied paths from the prescribed initial configuration at time at time t_1 and final configurations at time t_2, the actual path ds of the Lagrangian motion of

$T-V=\int_0^l lds$ satisfies the function $I=\int_{t_1}^{t_2}(T-V)dt$, where T is the kinetic energy and V is the potential energy and l denotes the length of the beam. The essentially geometric of the system is illustrated in both space and time for the beam shown in Fig. 2.3.

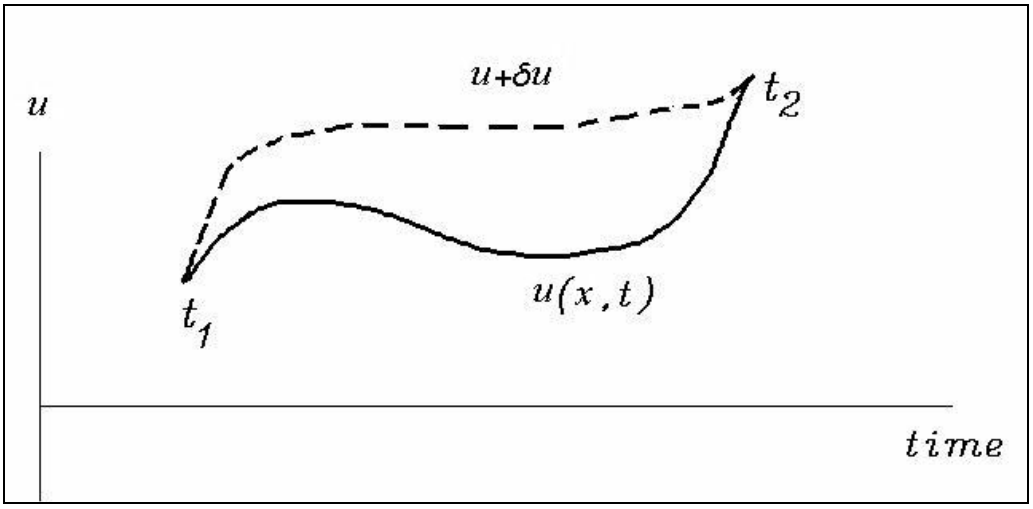

Fig. 2.3 Hamilton's configuration of the beam with varied time path.

The solid line represents the position of a particular point on the beam over time and dotted line gives the path with considering the addition of the virtual displacement $\delta u(x_i,t)$. As it can be seen there are no variations at the extreme times t_1 and t_2. Therefore the displacement in Eq. 2.1 can be independent of time and re-written as follows:

$$\begin{aligned} U_1(x_1,x_2,x_3) &= u_1 - x_2\phi_3 - x_3\phi_2 - \zeta(\phi_3-\phi_2) \\ U_2(x_1,x_2,x_3) &= u_2 - x_3\phi_1 \\ U_3(x_1,x_2,x_3) &= u_3 + x_2\phi_1 \end{aligned} \tag{2.3}$$

2.7 Relationships between Volume and Area in Reference and Deformed Configuration for the Beam with large deformation

Recall from deformation vector relationship: $x_i = x_i^{\circ} + u_i$, the displacement vectors in three directions can be written as:

$$u_i = \begin{Bmatrix} U_1 \\ U_2 \\ U_3 \end{Bmatrix},\ x_i^0 = \begin{Bmatrix} x_1^0 \\ x_2^0 \\ x_3^0 \end{Bmatrix}, \text{ and } x_i = \begin{Bmatrix} x_1 \\ x_2 \\ x_3 \end{Bmatrix} \tag{2.4}$$

The relationship between a volume dV in the deformed configuration and a volume dV^0 in the reference configuration is described as: $dV = \det F dV^0$, where F is the deformation gradient tensor and can be defined as the kroneckor delta plus a displacement gradient:

$$F_{ij} = \delta_{ij} + \frac{\partial u_i}{\partial x_j^0} \tag{2.5}$$

Many texts denote the determinant of F as the Jacobian, and denote the Jacobian as J. This would allow one to rewrite the expression of volume in reference and deformed configurations as:

$$dV = JdV^0 \tag{2.6}$$

The Jacobian J actually represents the ratio of the deformed configuration volume to the reference configuration volume:

$$J = \frac{dV}{dV^0} \tag{2.7}$$

The mapping between areas in the reference and deformed configuration is written with the normal vectors as:

$$n_j dA = JN_i F_{ij}^{-1} dA^0 \tag{2.8}$$

This defines a relationship between normal vectors (N_i) and area (A^0) in the reference configuration to normal vectors (n_j) and area (dA) in the deformed configuration. The displacement gradients referred to the reference configuration x=x^0 become:

$$\begin{aligned}
&\frac{\partial U_1}{\partial x_1} = \frac{\partial u_1}{\partial x_1} - x_2 \frac{\partial \phi_3}{\partial x_1} - x_3 \frac{\partial \phi_2}{\partial x_1} - \frac{\partial \zeta}{\partial x_1}(\phi_3 - \phi_2) - \zeta\left(\frac{\partial \phi_3}{\partial x_1} - \frac{\partial \phi_2}{\partial x_1}\right), \\
&\frac{\partial U_2}{\partial x_2} = \frac{\partial u_2}{\partial x_1} - x_3 \frac{\partial \phi_1}{\partial x_1}, \qquad , \\
&\frac{\partial U_3}{\partial x_3} = \frac{\partial u_3}{\partial x_1} + x_2 \frac{\partial \phi_1}{\partial x_1}
\end{aligned}$$

$$\begin{aligned}
&\frac{\partial U_1}{\partial x_2} = \phi_3, \qquad \frac{\partial U_1}{\partial x_3} = -\phi_2, \\
&\frac{\partial U_2}{\partial x_2} = 0, \text{ and, } \frac{\partial U_2}{\partial x_3} = -\phi_1, \\
&\frac{\partial U_3}{\partial x_2} = \phi_1, \qquad \frac{\partial U_3}{\partial x_3} = 0
\end{aligned} \tag{2.9}$$

2.8 Alternate Stresses

The true or Cauchy's stresses is defined in the deformed configuration and is thus not practical to use for large deformation analysis or experimental measures. Therefore, it is needed to develop alternative stresses. Two often used for large deformation systems are the 1st Piola-Kirchoff (PK1) stress and the 2nd Piola-Kirchoff (PK2) stress tensor.

The PK1 stress is defined such that the total force resulting from the PK1 stress multiplied by the normal and area in the reference configuration is the same as the total force resulting from the Cauchy stress times the normal and area in the deformed configuration. If the total force over the infinitesimal area in both configurations is *dP*, the Cauchy stress as σ, the PK1 stress *T* is expressed as:

$$dP = (\sigma n)\, dA = (TN)\, dA^0 \tag{2.10}$$

or:

$$TN = \frac{dP}{dA^0} \tag{2.11}$$

Physically, this indicates that the PK1 stress is equivalent to dividing the total force in the deformed configuration by the area in the reference configuration.

There are two difficulties with using the 1st Piola-Kirchoff stress. First, it is not energetically appropriate to use with the Green-Lagrange strain tensor. That is, the 1st Piola-Kirchoff stress tensor multiplied by the Green-Lagrange strain will not produce the same strain energy density result as the Cauchy stress multiplied by the small deformation strain tensor. Second, the 1st Piola-Kirchoff stress tensor is not symmetric. The results of multiplying a symmetric stress tensor, the Cauchy stress, by a non symmetric matrix for systems with a generally non-symmetric deformation gradient matrix, will be a non-symmetric matrix. Such non-symmetry makes it difficult to form constitutive models. This

makes it more difficult to use with numerical analyses like the finite element method.

Therefore, a symmetric stress matrix, the PK2 stress, is used for large deformation. The PK2 stress involves one further mapping step between the reference and deformed configuration than the PK1 stress. As such, it does not have such a straightforward physical interpretation as the PK1 stress.

The PK2 stress S is defined such that the traction force resulting from the PK2 stress in the reference configuration multiplied by the area in the reference configuration creates the transformed total force and is expressed in matrix form as:

$$S = JF^{-1}\sigma F^{-T} \tag{2.12}$$

The stress in the reference configuration is obtained via a mapping that preserves the relative relationship between the stress direction and the area normal in the current configuration. If the material rotates without a change in stress state (rigid rotation), the components of the 2nd Piola-Kirchhoff stress matrix will remain constant, irrespective of material orientation.

The difficulty with all the PK2 stresses is how to envision their physical meaning. In truth, the physical meaning of the PK2 stress is hard to interpret. It is mainly used as a vehicle to solve the large deformation problem, after which the Cauchy stress is computed from the PK2 stress.

The 2nd Piola-Kirchhoff stress is energy conjugate to the Green-Lagrange finite strain. These strains can be expressed in terms of the displacement gradients.

2.9 Strain-Displacement relations for beam with large deformation

It is known that rigid-body translations and rotations do not produce any strains; strains are only due to relative displacements. Although the deformation gradient tensor defined above is one measure of how a body changes under load, it cannot be used directly for strain characterization because it contains rigid body motions. For strain and deformation characterization, it is desired a measure that does not contain rigid body motions. It is tried to define a strain measure related to the change in length squared in a material vector in going from one configuration to the deformed configuration. It is noted that this measures should be independent of rigid body rotation. From which it can be directly written the strain tensor in terms of the deformation gradient tensor and deformation gradients as by matching the strain e as follows:

$$e_{ij} = \frac{1}{2}\left(F_{ki}F_{kj} - \delta_{ij} \right) \tag{2.13}$$

The strain tensor gives us deformations independent of rigid body motion. Noting that it has not been made any assumptions about the magnitude of the deformation, the strain tensor given above is thus exact for any size of deformation. The above strain tensor is known as the Green-Lagrange strain tensor. It is also a second order tensor because it has two independent indices.

Substituting the displacement equation for the deformation gradient tensor, it is obtained:

$$e_{ij} = \frac{1}{2}\left(\left(\delta_{ki} + \frac{\partial u_k}{\partial x_i^0} \right) \left(\delta_{kj} + \frac{\partial u_k}{\partial x_j^0} \right) - \delta_{ij} \right) \tag{2.14}$$

then expanding the parentheses results:

$$e_{ij} = \frac{1}{2}\left(\frac{\partial u_k}{\partial x_i^0} + \frac{\partial u_k}{\partial x_j^0} + \frac{\partial u_k}{\partial x_i^0} \frac{\partial u_k}{\partial x_j^0} \right) \tag{2.15}$$

It shows that the large deformation strain tensor contains a quadratic term. This means that all large deformation analyses are *nonlinear*.

The strains associated with the displacement field defined in Equation (2.3) can be expressed in terms of the displacement gradients as follows:

$$\begin{aligned}
e_{11} &= \varepsilon_{11} + x_3\kappa_{11} = \frac{\partial u_1}{\partial x_1} + x_2\frac{\partial \phi_3}{\partial x_1} + x_3\frac{\partial \phi_2}{\partial x_1} - \frac{\partial \zeta}{\partial x_1}(\phi_3 - \phi_2) + \frac{1}{2}[\frac{\partial u_3}{\partial x_1} + y\frac{\partial \phi_1}{\partial x_1}]^2, \\
e_{22} &= \varepsilon_{22} + x_3\kappa_{22} = 0 + \frac{1}{2}(-\phi_1)^2 = \frac{1}{2}\phi_1^2, \\
e_{33} &= \varepsilon_{33} + x_3\kappa_{33} = 0, \\
e_{23} &= \gamma_{23} + x_3\kappa_{23} = 0, \\
e_{13} &= \gamma_{13} + x_3\kappa_{13}, \\
e_{12} &= \gamma_{12} + x_3\kappa_{12}
\end{aligned} \tag{2.16}$$

where $(\varepsilon_{xx}, \varepsilon_{yy}, \gamma_{xz}, \gamma_{xy})$ are the membrane strains and the $(\kappa_{xx}, \kappa_{yy}, \kappa_{xz}, \kappa_{xy})$ bending strains and curvatures.

2.10 Stress-Strain relationship

The stress-strain relations of the laminate can be obtained by using the classical lamination theory. The generalized stresses can be expressed through the constitutive relation in terms of the extensional stiffness matrix **A**, the

extensional-bending coupling stiffness matrix **B** , and the bending stiffness matrix **D** as follows:

$$\begin{Bmatrix} N_x \\ N_y \\ N_{xy} \\ M_x \\ M_y \\ M_{xy} \end{Bmatrix} = \begin{bmatrix} A_{11} & A_{12} & A_{16} & B_{11} & B_{12} & B_{16} \\ A_{12} & A_{22} & A_{26} & B_{12} & B_{22} & B_{26} \\ A_{16} & A_{26} & A_{66} & B_{16} & B_{26} & B_{66} \\ B_{11} & B_{12} & B_{16} & D_{11} & D_{12} & D_{16} \\ B_{12} & B_{22} & B_{26} & D_{12} & D_{22} & D_{26} \\ B_{16} & B_{26} & B_{66} & D_{16} & D_{26} & D_{66} \end{bmatrix} \begin{Bmatrix} \varepsilon_x^0 \\ \varepsilon_y^0 \\ \gamma_{xy}^0 \\ \kappa_x^0 \\ \kappa_y^0 \\ \kappa_{xy}^0 \end{Bmatrix} \tag{2.17}$$

where $\left(N_{xx}, N_{yy}, N_{xy}\right)$ are the in-plane forces, $\left(M_{xx}, M_{yy}, M_{xy}\right)$ the bending and twisting moment. By integration of the stresses throughout the thickness of the laminate the following are obtained:

$$\begin{aligned} N_{xx} &= \int_{-h/2}^{h/2} S_{xx} dz & N_{yy} &= \int_{-h/2}^{h/2} S_{yy} dz & N_{xy} &= \int_{-h/2}^{h/2} S_{xy} dz \\ M_{xx} &= \int_{-h/2}^{h/2} S_{xx} z dz & M_{yy} &= \int_{-h/2}^{h/2} S_{yy} z dz & M_{xy} &= \int_{-h/2}^{h/2} S_{xy} z dz \end{aligned} \tag{2.18}$$

The ε_x^0 , ε_y^0 , and γ_{xy}^0 denotes the mid-plane strains , and κ_x^0 , κ_y^0 and κ_{xy}^0 denotes the bending and twisting curvatures. For the case of laminated beams with taking the effect of transverse shear deformation into account the constitutive relation of the transverse shear resultant simplifies to $Q_{xz} = A_{55}\gamma_{xz}$. The laminate stiffness coefficients A_{ij} , B_{ij} , and D_{ij} for $\left(i, j = 1, 2, 6\right)$ and the transverse shear stiffness A_{55} , which are functions of laminate ply orientation and material property are given by

$$A_{ij} = \int_{-h/2}^{h/2} \bar{Q}_{ij} dz = \sum_{k=1}^{N} \bar{Q}_{ij}^k (z_{k+1} - z_k) \tag{2.19}$$

$$B_{ij} = \int_{-h/2}^{h/2} \bar{Q}_{ij} z dz = \frac{1}{2}\sum_{k=1}^{N} \bar{Q}_{ij}^{k} (z^2{}_{k+1} - z^2{}_{k}) \tag{2.20}$$

$$D_{ij} = \int_{-h/2}^{h/2} \bar{Q}_{ij} z^2 dz = \frac{1}{3}\sum_{k=1}^{N} \bar{Q}_{ij}^{k} (z^3{}_{k+1} - z^3{}_{k}) \tag{2.21}$$

$$A_{55} = k \int_{-h/2}^{h/2} \bar{Q}_{55} dz \tag{2.22}$$

where N is the total number of plies considered, h is the thickness of the beam, and $k = 5/6$ is the shear correction factor that changes with mode number and lamination scheme but it is assumed a constant as by most works.

The relation between the transformed plane stress-reduced elastic coefficients $\bar{Q}$ matrix with PK2 stresses and in-plane strains can be expressed as

$$\begin{Bmatrix} S_{xx} \\ S_{yy} \\ S_{xy} \end{Bmatrix} = \begin{bmatrix} \bar{Q}_{11} & \bar{Q}_{12} & \bar{Q}_{16} \\ \bar{Q}_{12} & \bar{Q}_{22} & \bar{Q}_{26} \\ \bar{Q}_{16} & \bar{Q}_{26} & \bar{Q}_{66} \end{bmatrix} \begin{Bmatrix} \varepsilon_{xx} \\ \varepsilon_{yy} \\ \gamma_{xy} \end{Bmatrix} \tag{2.23}$$

The transformed reduced stiffness constants $\bar{Q}_{ij}\,(i, j = 1, 2, 6)$ and $\bar{Q}_{55}$ with respect to ϑ, the angle between the fiber direction and longitudinal axis of the beam, are given by (Reddy 1997, CRC Press LLC):

$$\begin{aligned}
\bar{Q}_{11} &= Q_{11}\cos^4\vartheta + 2\left(Q_{12} + 2Q_{66}\right)\sin^2\vartheta\cos^2\vartheta + Q_{22}\sin^4\vartheta, \\
\bar{Q}_{12} &= \left(Q_{11} + Q_{22} - 4Q_{66}\right)\sin^2\vartheta\cos^2\vartheta + Q_{12}\left(\sin^4\vartheta + \cos^4\vartheta\right), \\
\bar{Q}_{22} &= Q_{11}\sin^4\vartheta + 2\left(Q_{12} + 2Q_{66}\right)\sin^2\vartheta\cos^2\vartheta + Q_{22}\cos^4\vartheta, \\
\bar{Q}_{16} &= \left(Q_{11} - Q_{12} - 2Q_{66}\right)\sin\vartheta\cos^3\vartheta + \left(Q_{12} - Q_{22} + 2Q_{66}\right)\sin^3\vartheta\cos\vartheta, \\
\bar{Q}_{26} &= \left(Q_{11} - Q_{12} - 2Q_{66}\right)\sin^3\vartheta\cos\vartheta + \left(Q_{12} - Q_{22} + 2Q_{66}\right)\sin\vartheta\cos^3\vartheta, \\
\bar{Q}_{66} &= \left(Q_{11} + Q_{22} - 2Q_{12} - 2Q_{66}\right)\sin^2\vartheta\cos^2\vartheta + Q_{66}\left(\sin^4\vartheta + \cos^4\vartheta\right), \\
\bar{Q}_{55} &= G_{13}\cos^2\vartheta + G_{23}\sin^2\vartheta
\end{aligned} \tag{2.24}$$

The components of the lamina stiffness matrix Q can be expressed in terms of the engineering constants, modulus of elasticity E, Poisson's ratio ν, and shear modulus G:

$$\begin{aligned} Q_{11} &= \frac{E_1}{1-\nu_{12}\nu_{21}}, & Q_{12} &= \frac{\nu_{12}E_2}{1-\nu_{12}\nu_{21}} = \frac{\nu_{21}E_1}{1-\nu_{12}\nu_{21}}, \\ Q_{22} &= \frac{E_2}{1-\nu_{12}\nu_{21}}, & Q_{66} &= G_{12}, \quad Q_{16} = 0, \quad Q_{26} = 0 \end{aligned} \tag{2.25}$$

2.11 Variational Method

To drive the equations governing nonlinear vibration of symmetrical and unsymmetrical laminated composite beams, Hamilton's principle variational formulation is used for the varied paths satisfying the prescribed initial and final configurations. Also by adding the work done by non-conservative forces within the integrand, the extended Hamilton's principle will be obtained. Then for the actual path it can be expressed as:

$$\delta I = \int_{t_1}^{t_2} \left\{ \delta \left(T - V \right) + \delta W_{nc} \right\} dt = 0 \tag{2.26}$$

where W_{nc} denotes the work done by non-conservative forces, such as external following forces or moments. This condition of stationary leads to all of the equations of motion and boundary conditions.

Using the generalized forces along the (x_1, x_2, x_3) axes denoted by $(f_{x_1}, f_{x_2}, f_{x_3})$ respectively (Fig. 2.3), the expression for a can be written as:

$$\delta W_{nc} = \int_0^l \{ f_{x_1} \delta u_1 + f_{x_2} \delta u_2 + f_{x_3} \delta u_3 \} ds \tag{2.27}$$

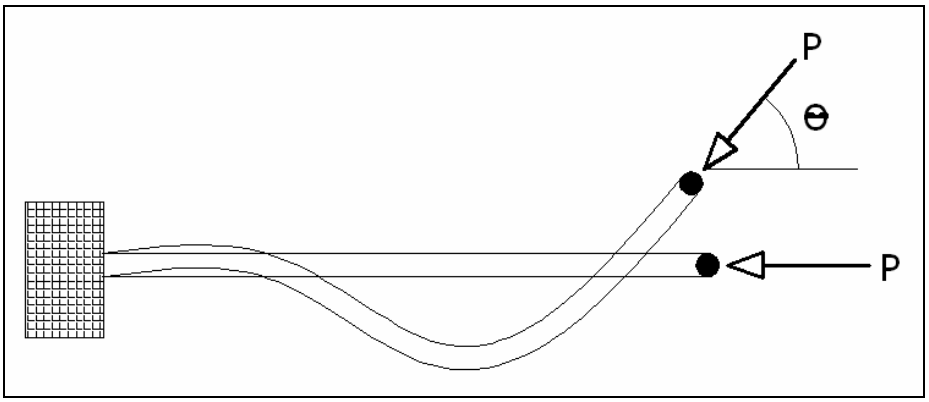

Figure 2. 4 Beam subjected to nonconservative load

In general, the nonconservative force remains parallel to the midsurface, and then $\theta = \phi_2$, then the nonconservative work done by nonconservative load, P acting on the cross section of the beam with width *b* becomes:

$$\delta W_{nc} = P\cos\phi_2 \delta u_1 + P\sin\phi_2 \delta u_3 = P(\cos\phi_2 \delta u_1 + \sin\phi_2 \delta u_3) \tag{2.28}$$

2.11.1 Virtual Kinetic Energy

The virtual kinetic energy is given by (Reddy, 2002):

$$\delta T = \int_A \int_{-h/2}^{h/2} \rho \left(\dot{u}_1 \delta \dot{u} + \dot{u}_2 \delta \dot{u}_2 + \dot{u}_3 \delta \dot{u}_3 \right) dx_1 dx_2 dx_3 \tag{2.29}$$

where ρ is the mass density, *h* the total thickness of the beam, and the superposed dot on the variable indices time derivative. Substituting the displacement field into Eq.(2.29), the virtual kinetic energy can be expressed as:

$$\delta T = \int_0^l \Big\{ \left(I_0 \ddot{u}_1 + I_1 \ddot{\phi}_2 \right) \delta u_1 + \left(I_0 \ddot{u}_2 - I_1 \ddot{\phi}_1 \right) \delta u_1 + \left(I_0 \ddot{u}_3 \right) + \left(-I_1 \ddot{u}_2 + J_{x_1} \ddot{\phi}_1 \right) \delta \phi_1 + \left(I_1 \ddot{u}_1 + I_2 \ddot{\phi}_2 \right) \delta \phi_2 + \left(J_{x_2} \ddot{\phi}_3 \right) \delta \phi_3 \Big\} ds \quad (2.30)$$

where I_0, I_1, I_2 are the mass moments of inertia, J_{x_1} is the polar mass moment of inertia, and J_{x_2} is the in-plane mass moment of inertia and are defined as follows:

$$\begin{aligned}
I_0 &= \int_{-h/2}^{h/2} \int_{-b/2}^{b/2} \rho dy dz && = b \sum_{k=1}^{N} \rho^k \left(z_{k+1} - z_k \right) \\
I_1 &= \int_{-h/2}^{h/2} \int_{-b/2}^{b/2} \rho z dy dz && = b \sum_{k=1}^{N} \rho^k \left(\frac{z^2{}_{k+1} - z^2{}_k}{2} \right) \\
I_2 &= \int_{-h/2}^{h/2} \int_{-b/2}^{b/2} \rho z^2 dy dz && = b \sum_{k=1}^{N} \rho^k \left(\frac{z^3{}_{k+1} - z^3{}_k}{3} \right) \\
J_x &= \int_{-h/2}^{h/2} \int_{-b/2}^{b/2} \rho \left(y^2 + z^2 \right) dy dz && = \frac{b^2}{12} I_0 + I_2 \\
J_y &= \int_{-h/2}^{h/2} \int_{-b/2}^{b/2} \rho y^2 dy dz && = \frac{b^2}{12} I_0
\end{aligned} \quad (2.31)$$

N is the number of plies.

The mass moments of inertia (I_0, I_1, I_2), the polar mass moment of inertia (J_{x_1}), and the inplane mass moment of inertia (J_{x_2}) are expressed as members of mass matrix **M** as follows:

$$\mathbf{M}=\begin{bmatrix} \frac{I_0}{\rho bh} & 0 & 0 & 0 & \frac{I_1}{\rho blh} & 0 \\ 0 & \frac{I_0}{\rho bh} & 0 & -\frac{I_1}{\rho blh} & 0 & 0 \\ 0 & 0 & \frac{I_0}{\rho bh} & 0 & 0 & 0 \\ 0 & -\frac{I_1}{\rho blh} & 0 & \frac{J_{x_1}}{\rho bl^2h} & 0 & 0 \\ \frac{I_1}{\rho blh} & 0 & 0 & 0 & \frac{I_2}{\rho bl^2h} & 0 \\ 0 & 0 & 0 & 0 & 0 & \frac{J_{x_2}}{\rho bl^2h} \end{bmatrix} \tag{2.32}$$

2.11.2 The potential strain energy due to the applied load

The virtual potential strain energy can be written as:

$$\delta V=\iiint_V S_i.\delta e_i.dV \tag{2.33}$$

where S_i are the PK2 stresses and are energetically conjugate to Green-Lagrange strains e_i. The virtual potential strain energy is expressed as

$$\begin{aligned}\delta V=\int_A \Big\{ & N_{x_1x_1}\delta\varepsilon^0_{x_1x_1}+M_{x_1x_1}\delta k^0_{x_1x_1}+N_{x_2x_2}\delta\varepsilon^0_{x_2x_2}+M_{x_2x_2}\delta k^0_{x_2x_2}+N_{x_1x_2}\delta\gamma^0_{x_1x_2} \\ & +M_{x_2x_2}\delta\gamma^0_{x_1x_2}+M_{x_1x_2}\delta k^0_{x_1x_2}+Q_{x_1}\delta\gamma^0_{x_1x_3}+Q_{x_2}\delta\gamma^0{}_{x_2x_3}\Big\}dx_1dx_2\end{aligned} \tag{2.34}$$

where $\varepsilon^0,\gamma^0,k^0$ are midplane strains.

2.11.3 Governing Equations of Motion

The governing equations of the first order beam theory can be derived using the extended Hamilton's principle of Eq. (2.26):

$$\begin{aligned}\delta I = \int_{t_1}^{t_2} \Bigg\{ & \int_0^l \Big\{ \left(I_0 \ddot{u}_1 + I_1 \ddot{\phi}_2 \right) \delta u_1 + \left(I_0 \ddot{u}_2 - I_1 \ddot{\phi}_1 \right) \delta u_1 + \left(I_0 \ddot{u}_3 \right) \\ & + \left(-I_1 \ddot{u}_2 + J_{x_1} \ddot{\phi}_1 \right) \delta \phi_1 + \left(I_1 \ddot{u}_1 + I_2 \ddot{\phi}_2 \right) \delta \phi_2 + \left(J_{x_2} \ddot{\phi}_3 \right) \delta \phi_3 \Big\} dx_1 \\ & - \int_A \Big\{ N_{x_1 x_1} \delta \varepsilon^0_{x_1 x_1} + M_{x_1 x_1} \delta k^0_{x_1 x_1} + N_{x_2 x_2} \delta \varepsilon^0_{x_2 x_2} + M_{x_2 x_2} \delta k^0_{x_2 x_2} + N_{x_1 x_2} \delta \gamma^0_{x_1 x_2} \\ & + M_{x_2 x_2} \delta \gamma^0_{x_1 x_2} + M_{x_1 x_2} \delta k^0_{x_1 x_2} + Q_{x_1} \delta \gamma^0_{x_1 x_3} + Q_{x_2} \delta \gamma^0{}_{x_2 x_3} \Big\} dx_1 dx_2 \\ & + \int_0^l \Big\{ f_{x_1} \delta u_1 + f_{x_2} \delta u_2 + f_{x_3} \delta u_3 \Big\} dx_1 \Bigg\} dt \end{aligned} \tag{2.35}$$

In the next chapter, the above equations will be discretized using finite element method to obtain the equation of motion in Mathieu type differential equation.

2.12 Summary

In this chapter, the Lagrangian motion description is used to derive the equation of motion of the beam.

A displacement field is defined to take into account the various couplings that affect laminated composites: twisting-bending, bending-extension, and in-twisting-extension couplings. The present formulation also includes a warping function.

The Green-Lagrange strains are derived for the given displacement field. The stresses corresponding to the Green-Lagrange strains are the second Piola-Kirchhoff stresses. The laminated constitutive law is expressed in terms of the extensional matrix **A**, the extensional-bending coupling matrix **B**, and the bending stiffness matrix **D**. Since a one dimensional analysis is being considered, the load conditions are prescribed. This leads to the constitutive equations used throughout this dissertation.

Finally the extended Hamilton's principle was employed to derive the governing equations of motion of the beam. In next chapter, these equations will be dicretized using the finite element method.

CHAPTER 3

Finite Element Formulation of Composite Laminated Beams

In this chapter, the integral form of the equation of motion of the beam derived in Chapter 2 is discretized through the finite element formulation of the proposed laminated beam model. This beam model takes into account the existence of various coupling effects and can be used for dynamic analysis of symmetric and unsymmetric beams.

3.1 A proposed beam element

Many investigations and studies have been done in the field of numerical simulation and finite elements analysis of laminated beams. Extensive formulations can be found in literature to solve the equation of motion of nonlinear beams with large deformation and small strains by proposing various beam element.

Goyal (2002), and Goyal and Kapania (2006) proposed a five node twenty-one degree of freedom beam element for the shear deformable beams based on the first order shear deformation theory, and principle of virtual work, to study the static response and free vibration of laminated composite beams. In their model the dynamic loading stiffness matrix resulted from varying time load is neglected and therefore the dynamic instability region of the beam can

not be determined through their model. Loja et al. (2002) proposed a model based on a straight beam finite element with four nodes and fourteen degrees of freedom per node, considering bi-axial bending, extension and twisting effects, but warping has been neglected. Bassiouni et al. (1999) presented a two dimensional ten degrees of freedom finite element model for one lamina with five nodes, two ends, two with same distances from the centre, and one in middle of element. The effect of the warping is neglected in his study as well. Subramanian (2005) developed two node finite elements of eight degrees of freedom per node for the vibration problems of the beams, but not such a warping and other coupling effects has been considered in his theory. Ramtekkar et al. (2002) presented a six-node, plane-stress mixed finite element model by using minimum potential energy principle, which can't include nonconservative loading.

In this study, a particular attention is focused on the stability analysis and behaviour of the laminated beams under either conservative or nonconservative loads. This needs to take into account all the coupling such as bending-extension and even warping functions to analyse the dynamics behaviour and response of such structures to identify the regions of instabilities in accurate manner. To the author's best knowledge previous studies have not proposed a beam model that can include all the above behaviours.

Using the theory of geometrically nonlinear analysis within the classical finite element method a five node hybrid beam element with six degree of freedom for each node is proposed to discretize the integral form of the equation

of motion of the beam. This element consists of four equally spaced nodes and a node at the middle as shown in Figure 3.1.

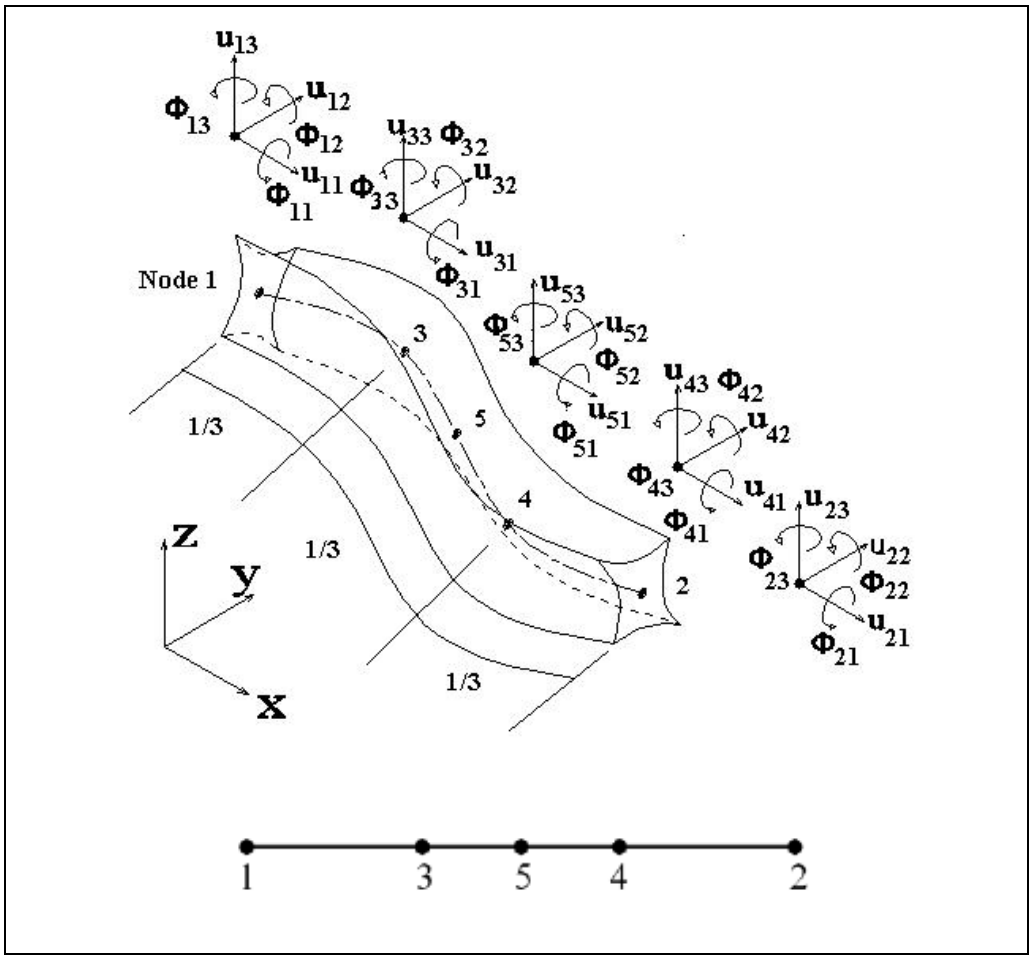

Figure 3. 1 A proposed beam element

The nodal displacements measured at each node are: (i) The axial displacements u_{i1}, $u_{i1,}$ the lateral deflections u_{i2}, u_{i2}, the transverse deflections u_{i3}, $u_{i3,}$ the twist angles ϕ_{i1}, the in-plane bending ϕ_{i2}, and the in-plane rotations ϕ_{i3} where i=1,2,3,4,5. All these nodal displacements are measured at the midplane:

$$\mathbf{U}_t^e = \{u_{i1}, u_{i2}, u_{i3}, \phi_{i1}, \phi_{i2}, \phi_{i3}\} \quad i = 1,2,3,4,5 \tag{3.1}$$

An approximation solution to EQ. 2.35 of the form:

$$u_e(x) = \sum_{i=1}^{n} c_i^e \varphi_i^e(x) \tag{3.2}$$

over the element is defined to determine relations among c_i^e. Since the elements are connected to each other at the nodes, the solutions from various elements connected at a node must have the same value at the node. It is convenient to express the solution over each element in terms of values at *n* nodes of the element:

$$u_e(x) = \sum_{i=1}^{n} u_i^e \psi_i^e(x) \tag{3.3}$$

where u_i^e is the value of $u_e(x)$ at the i^{th} node, and ψ_i^e are the functions satisfy the interpolation. If there are *n* nodes in the element, a polynomial with *n* terms is required to fit the solution at the *n* points. Thus, each ψ_i^e is a (*n*-1) degree polynomial known as Lagrangian interpolation function.

Follow the procedure as the reduced integration of shear stiffness for a slender beam limit, the beam element equations reduce to only one constraint. With a sufficient number of elements in the entire beam domain, one gets a very accurate solution, (Reddy 2002). Based on this and since the beam slope is continuous across the elements, therefore the cubic shape function are selected to approximate the transverse and rotations displacements, The reason for selecting u_i^e to be a cubic polynomial is that; four parameters are needed in the polynomial in order to satisfy all the boundary conditions. Also the quadratic

functions are selected to approximate the axial displacements. The general form of the shape function are defined as:

$$\psi_j^e = \prod_1^n \frac{\left(x - x_n^e\right)}{\left(x_i^e - x_n^e\right)} \tag{3.4}$$

The end points of individual elements are called element nodes and they match with a pair of global nodes that refers to the whole problem as opposed to an element. The relationship between the element nodes and global nodes can be written in matrix form as follows:

$$\mathbf{U} = \mathbf{N}\mathbf{U}^e \tag{3.5}$$

where $\mathbf{N}$ is the shape function matrix, and $\mathbf{U}^e$ is the vector containing the nodal displacements defined in Eq. (3.1).

The virtual displacements corresponding to the nodal virtual displacements Eq.(3.5) can be defined as:

$$\delta\mathbf{U} = \mathbf{N}\delta\mathbf{U}^e \tag{3.6}$$

3.2 Derivation of Element Matrices

The element stiffness and mass matrices are derived using the following procedure as:

Elastic stiffness Matrix: $$\mathbf{K}_{\mathrm{M}}^e = \int_0^{l_e} \int_{-b/2}^{b/2} \mathbf{B}^{\mathrm{T}}\mathbf{D}\mathbf{B}\, dydx \tag{3.7}$$

where l_e the element length.

The geometric stiffness matrix is a function of in-plane stress distribution in the element due to applied loading. Plane stress analysis is carried out using the finite element techniques to determine the stresses and these stresses are used to formulate the geometric stiffness matrices:

Geometric stiffness matrix: $$\mathbf{K}_{\mathrm{G}}^{\mathrm{e}} = \int_0^{l_e} \int_{-b/2}^{b/2} \left\{ \frac{\partial \mathbf{B}^{\mathbf{T}}}{\partial \mathbf{U}^e} \mathbf{T} \right\} dydx \tag{3.8}$$

where $\mathbf{T}$ is the generalized stresses, is defined as:

$$\mathbf{T} = \begin{Bmatrix} N_{xx} \\ N_{xy} \\ M_{xx} \\ M_{xy} \\ Q_x \end{Bmatrix} \tag{3.9}$$

Mass Matrix: $$\mathrm{M}^{\mathrm{e}} = \int_0^{l_e} \int_{-b/2}^{b/2} \mathrm{N}^T [\rho] \mathrm{N} dxdy \tag{3.10}$$

Where B, D, N are the strain-displacement matrix, stress-strain matrix and shape function matrix and $[\rho]$ involves mass density parameters.

3.3 Loading Stiffness Matrix

When the load depends on the response such as wind, aerodynamic, and contact loading, another stiffness matrix, loading stiffness matrix, should be added to the governing equation. The virtual work done by such a nonconservative force of the follower type (i.e., displacement dependent) can be written in terms of the nodal displacements as:

$$\delta W_{\text{nc}} = \delta \mathbf{U}^{e^{\text{T}}} \mathbf{f}_{\text{nc}} \tag{3.11}$$

where $\mathbf{f}_{\text{nc}}$ is the nonconservative force function of the nodal displacements, and $\mathbf{U}^{e}$ are defined for the global system but not locally, and $\delta \mathbf{U}^{e^{\text{T}}}$ are the virtual nodal displacements corresponding to the nodal displacements and the force terms in the vector $\mathbf{f}_{\text{nc}}$. The loading stiffness matrix is then can be written as:

$$\mathbf{K}_{\text{L}} = \frac{\partial \mathbf{f}_{\text{nc}}}{\partial \mathbf{U}} \tag{3.12}$$

The above matrix is zero for conservative loading.

Now this matrix is derived for the case of the nonconservative load discussed in previous chapter. Recall the Eq. (2.48):

$$\delta W_{\text{nc}} = \delta \mathbf{U}^{\text{T}} \big|_{x=l} \mathrm{f}_{\text{nc}} \tag{313}$$

Note that the above expression is only evaluated for the element into contact with the load. Thus, the virtual displacements can be expressed using Eq. (3.11) as follows:

$$\delta \mathbf{U}^{\text{T}} \Big|_{x=l} = \delta \mathbf{U}^{e^{\text{T}}} \, \mathbf{N}^{\mathbf{T}} \big|_{x=l} \tag{3.14}$$

where $\mathbf{N}^{\mathbf{T}} \big|_{x=l}$ is the transpose of the shape function matrix evaluated at the second node of the element, and $\delta \mathbf{U}^{e^{\text{T}}}$ is virtual nodal displacement. Now, the nonconservative force vector f_{nc} can be obtained in terms of the generalized nodal displacements using Figure 3.2. This figure shows the deformation of the

last element at which the nonconservative load is applied. The load rotates with the rotation at the tip of the cantilevered beam model and $\theta = \phi_{22}$.

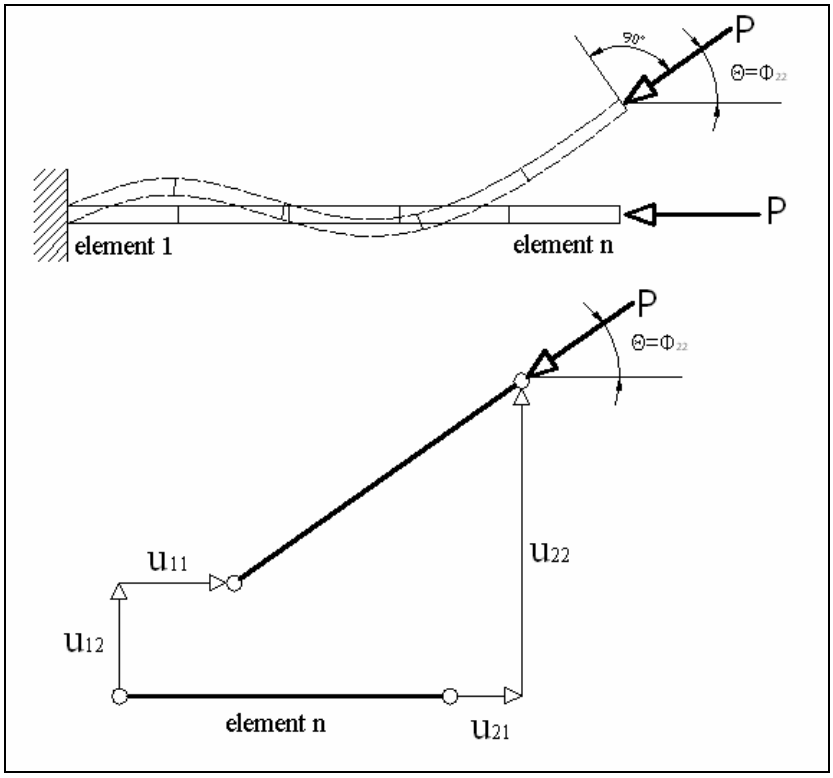

Figure 3. 2 Displacement of the beam element subjected to a follower load.

As shown in Fig. 3.2 at time ***t*** the load vector is:

$$\mathrm{f}_{\mathrm{nc}} = \left\{-\sin\theta, \cos\theta, 0\right\}^{\mathrm{T}} P \tag{3.15}$$

At the next time step, $t + \Delta t$ both *P* and its orientation θ will have changed. The new force is then:

$$\mathrm{f}_{\mathrm{nc}(t+\Delta t)} = \left\{-\sin\left(\theta + \Delta\theta\right), \cos\left(\theta + \Delta\theta\right), 0\right\}^{\mathrm{T}} \left(P + \Delta P\right) \tag{3.16}$$

Expanding the above equation and rearranging gives:

$$\begin{aligned} \mathrm{f}_{\mathrm{nc}(t+\Delta t)} = & \left\{-\sin(\theta), \cos(\theta), 0\right\}^{\mathrm{T}} (P) + \\ & \left\{-\sin(\theta), \cos(\theta), 0\right\}^{\mathrm{T}} \Delta P + \left\{-\cos(\theta), -\sin(\theta), 0\right\}^{\mathrm{T}} P \Delta\theta + \ldots \end{aligned} \tag{3.17}$$

Neglecting the higher order terms, the first term is the load at the previous time, the second is the load increment but aligned with the previous orientation, and the third term includes the orientation increments. The last term acts as a contribution to the stiffness matrix because it depends on the deformation increment. This could be taken to the equilibrium equation to result in an effective stiffness, which then changes the finite element calculation. Then Eq. (3.21) can be rewritten as:

$$\delta W_{\mathrm{nc}} = \delta \mathbf{U}^{e^{\mathrm{T}}} \mathbf{N}_{\mathbf{L}}^{\mathbf{T}} \mathrm{f}_{\mathrm{nc}} \mathbf{U}^{e} \tag{3.18}$$

and the elemental nonconservative force is then defined as:

$$\mathbf{f}_{\mathrm{nc}}^{\mathrm{e}} = \mathbf{N}_{\mathbf{L}}^{\mathbf{T}} \mathrm{f}_{\mathrm{nc}} \mathbf{U}^{e} \tag{3.19}$$

and the loading stiffness matrix for the last element becomes:

$$\mathbf{K}_{\mathrm{L}}^{\mathbf{e}} = \frac{\partial \mathbf{f}_{\mathrm{nc}}^{\mathrm{e}}}{\partial \mathbf{U}^{e}} = \mathbf{N}_{\mathbf{L}}^{\mathbf{T}} \mathrm{f}_{\mathrm{nc}} \tag{3.20}$$

A symbolic computer program is developed to perform all the necessary computations. Reduced integration technique is adopted to avoid possible shear locking. The overall matrices $\mathbf{K}_{\mathrm{M}}^{\mathrm{e}}$, $\mathbf{K}_{\mathrm{G}}^{\mathrm{e}}$, $\mathbf{K}_{\mathrm{L}}^{\mathrm{e}}$ and M^{e} are obtained by assembling the corresponding element matrices.

3.4 Equations of Motion

Substituting of all the defined components for beam element into governing equation of motion yields to:

$$\mathbf{F}^e = \mathbf{K}_{\mathrm{E}}^e \mathbf{U}^e + \mathbf{K}_{\mathrm{G}}^e \mathbf{U}^e - \mathbf{K}_{\mathrm{L}}^e \mathbf{U}^e + \mathbf{M}^e \ddot{\mathbf{U}}^e \tag{3.21}$$

The elemental matrices and vectors can be assembled and the global matrices and vectors can be substituted into Eq. (3.21). Assuming the length of each element is the same, the above equation can be expressed in terms of the total length of the beam as follows:

$$l^e = \frac{l}{n} \tag{3.22}$$

where n is the number of elements and l is the total length of the beam. With transformation from element to global components:

$$\mathbf{F} = nl^e \mathbf{F}^e,\ \mathbf{K}_{\mathrm{E}} = nl^e \mathbf{K}_{\mathrm{E}}^e,\ \mathbf{K}_{\mathbf{G}} = nl^e \mathbf{K}_{\mathrm{G}}^e,\ \mathbf{K}_{\mathrm{L}} = nl^e \mathbf{K}_{\mathrm{L}}^e,\ \mathbf{M} = nl^e \mathbf{M}^e \tag{3.23}$$

Then Eq. (3.21) can be rearranged as in global system as:

$$\mathbf{M}\ddot{\mathbf{U}} + \mathbf{K}_{\mathrm{E}}\mathbf{U} + \mathbf{K}_{\mathrm{G}}\mathbf{U} - \mathbf{K}_{\mathrm{L}}\mathbf{U} = \mathbf{F} \tag{3.24}$$

where $\mathbf{F}$ is the global external force vector, $\mathbf{K}_{\mathrm{E}}$ the global elastic stiffness matrix, $\mathbf{K}_{\mathrm{G}}$ the global geometric stiffness matrix, $\mathbf{K}_{\mathrm{L}}$ the global loading stiffness matrix, and $\mathbf{M}$ the global mass matrix. For the case of an axially compressed beam with periodic load p:

$$P = P_0 + P_t \cos\theta t \tag{3.25}$$

where θ is the loading frequency, t is the time, P_0 is the amplitude of the static part of the load, and P_t is the amplitude of the dynamic part of the load. Then the loading stiffness matrix can be expressed as:

$$\mathbf{K}_{\mathrm{L}} = \mathbf{K}_{\mathrm{L}}^{0} + \mathbf{K}_{\mathrm{L}}^{\mathrm{t}} \cos\theta t \tag{3.26}$$

Then it yields to:

$$\mathbf{M}\ddot{\mathbf{U}} + \left(\mathbf{K}_{\mathrm{E}} + \mathbf{K}_{\mathrm{G}} - \mathbf{K}_{\mathrm{L}}^{0}\right)\mathbf{U} - \mathbf{K}_{\mathrm{L}}^{\mathrm{t}} \cos\theta t\mathbf{U} = \mathbf{F} \tag{3.27}$$

The governing equation (3.27) is a matrix form of Mathieu equation. By solving this equation the dynamic behaviour and regions of instability of the beam will be determined. In this equation the tangent stiffness matrix, the mass matrix, the force vectors all can be obtained using the symbolic computational processor MATLAB® software.

3.5 Evaluation of the proposed element: Linear vibration of beam about equilibrium position

In this section, the proposed beam element will be examined for free vibration of the beam with different boundary conditions and the result will be compared with the results available in literature. The equilibrium position of the beam is studied and equation of motion in this state is derived.

In correspondence of studying of the equation of motion of the beam about equilibrium position, the discretized equation of motion (Eq.3.27) can be rewritten as:

$$\mathbf{M}\ddot{\mathbf{U}} + \left\{\left(\mathbf{K}_{\mathrm{E}} + \mathbf{K}_{\mathrm{G}} - \mathbf{K}_{\mathrm{L}}^{0}\right) - \mathbf{K}_{\mathrm{L}}^{\mathrm{t}} \cos\theta t\right\}\mathbf{U} = 0 \tag{3.28}$$

In general linear form by assuming the harmonic motion about equilibrium state $\mathbf{U} = \mathbf{U}_0 e^{\lambda t}$ as trial function and in the hypothesis that all the characteristic components of the equation of motion would be time invariant matrices, the resulting eigenvalue problem has the following form:

$$\left(\mathbf{M}\lambda^2 + \mathbf{K}\right)\mathbf{U}_0 = 0 \tag{3.29}$$

where the eigenvalues $\lambda t = i\theta t$ for different eigenfrequencies θ. Now, the free vibration of the beam in different cases with two different boundary conditions are calculated and the results are compared with those obtained using finite element method to evaluate the present beam element.

3.5.1 Case-1: Isotropic clamped-free beam

In the first case, the present beam element will be examined in case of free vibration of the cantilever isotropic beams (Clamped-Free Fig.3.3) to determine the natural frequencies and mode shapes and the results will be compared to exact solution of Euler-Bernouli beam and those have been done by previous studies. The symbolic toolbox of MATLAB® software has been employed to calculate the mass and stiffness matrices for descritized beam with present element and solve the eigenvalues problem.

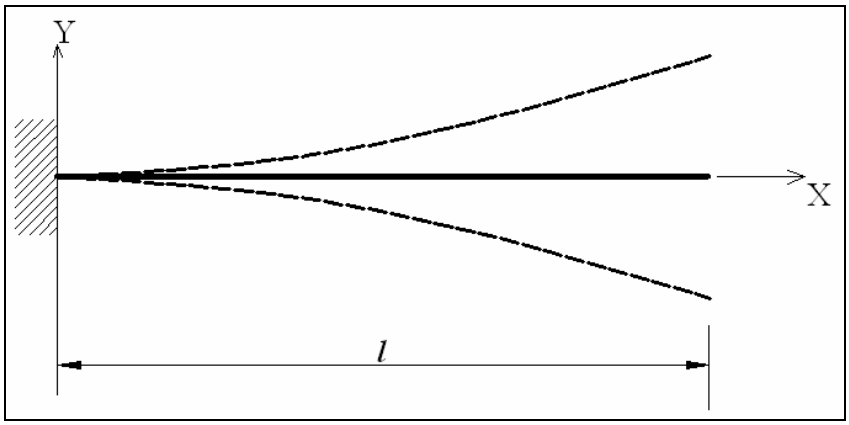

Figure 3. 3 The cantilever beam vibration

The boundary conditions for cantilever beam clamped at $x = 0$ are $u_{ij} = \phi_{ij} = 0$.

The exact solution of the eigenvalue of the cantilever uniform beam with $E_{xx}I_{xx} = E_{yy}I_{yy} = \text{constant}$, ρbh=constant given by Meirovitch (2001), and Logan (2002), the first two natural frequencies are as follows:

$$\omega_1 = 3.5160\sqrt{\frac{EI}{\rho bhl^4}}$$

$$\omega_2 = 22.0345\sqrt{\frac{EI}{\rho bhl^4}}$$

The calculated natural frequencies of the cantilever beam using the present element are compared with the above results from exact solutions in Table-3.1, and mode shapes in Fig.3.4, for beam with the following data:

$l = 30$	in^2,	$E = 3\times10^7$	psi
$I = 0.0833$	in^4,	$bh = 1$	in^2
$\rho = 0.00073$	$\text{lb-s}^2/\text{in}^4$,	$\nu = 0.3$	

Natural frequencies (rad/sec)	Exact solution	Logan (2003), using FE (10 elements)	Present, using FE (10 elements)
ω_1	228	227.5	228
ω_2	1434	1410	1426

Table 3. 1 The first two natural frequencies of the cantilever beam, computer solution compared with the exact solution.

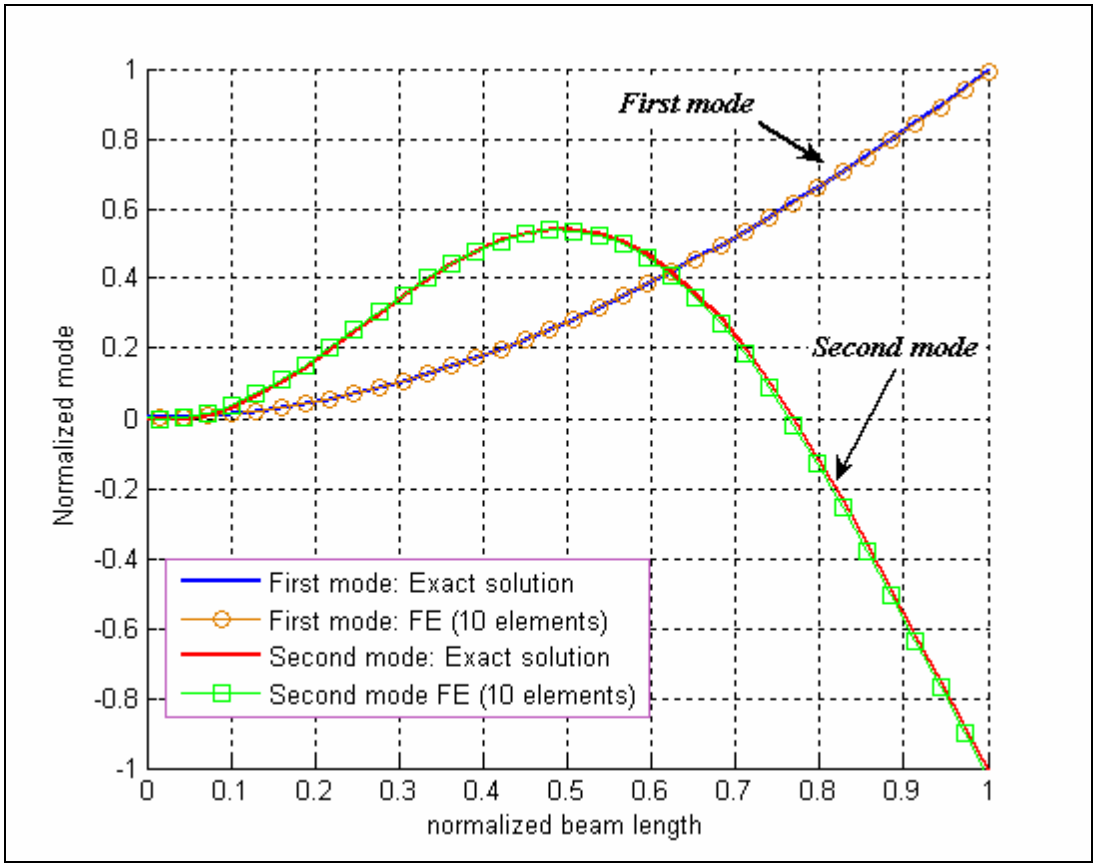

Figure 3. 4 The mode shapes of the cantilever beam, computer solution compared with the exact solution.

3.5.2 Case-2: Isotropic pinned-pinned beam

In second case, the present beam element will be examined in case of free vibration of the pinned-pinned isotropic beams, Fig.3.5, to determine the natural frequencies and mode shapes and the results will be compared to exact solution of Euler-Bernouli beam. The symbolic toolbox of MATLAB® software has been employed to calculate the mass and stiffness matrices for the descritized beam with present element and solve the eigenvalues problem.

The boundary conditions for the pinned-pinned beam clamped at $x = 0$ are $u_{ij} = \phi_{11} = 0$, and at $x = l$ are $u_{i2,3} = \phi_{i1} = 0$.

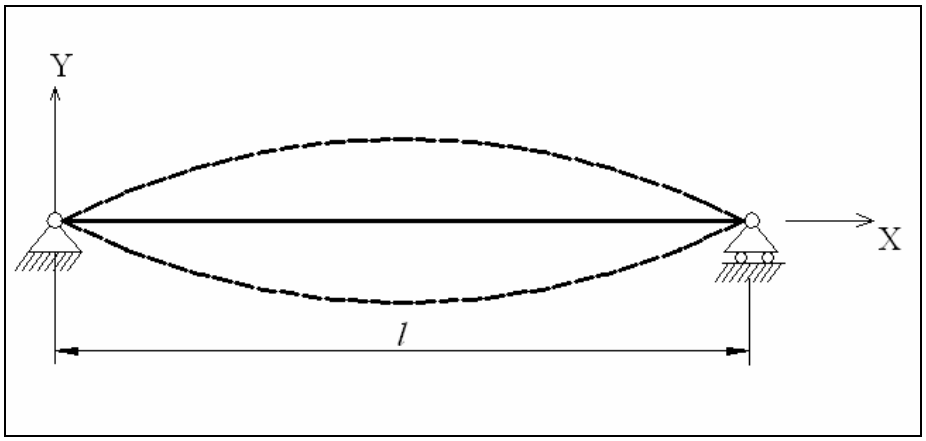

Figure 3. 5 The pinned-pinned beam.

The calculated natural frequencies of the pinned-pinned beam using MATLAB® program for present element are compared with the analytical results from exact solutions in Table-3.2, and mode shapes in Fig.3.6.

Natural frequencies	Exact solution	Present, using FE (10 elements) Using MATLAB®
ω_1	$\omega_1 = 9.870\sqrt{\frac{EI}{\rho AL^4}}$	$\omega_1 = 9.874\sqrt{\frac{EI}{\rho AL^4}}$
ω_2	$\omega_2 = 39.480\sqrt{\frac{EI}{\rho AL^4}}$	$\omega_2 = 39.489\sqrt{\frac{EI}{\rho AL^4}}$
ω_3	$\omega_3 = 88.830\sqrt{\frac{EI}{\rho AL^4}}$	$\omega_3 = 88.842\sqrt{\frac{EI}{\rho AL^4}}$

Table 3. 2 The first three natural frequencies of the pinned-pinned beam, computer solution compared with the exact solution.

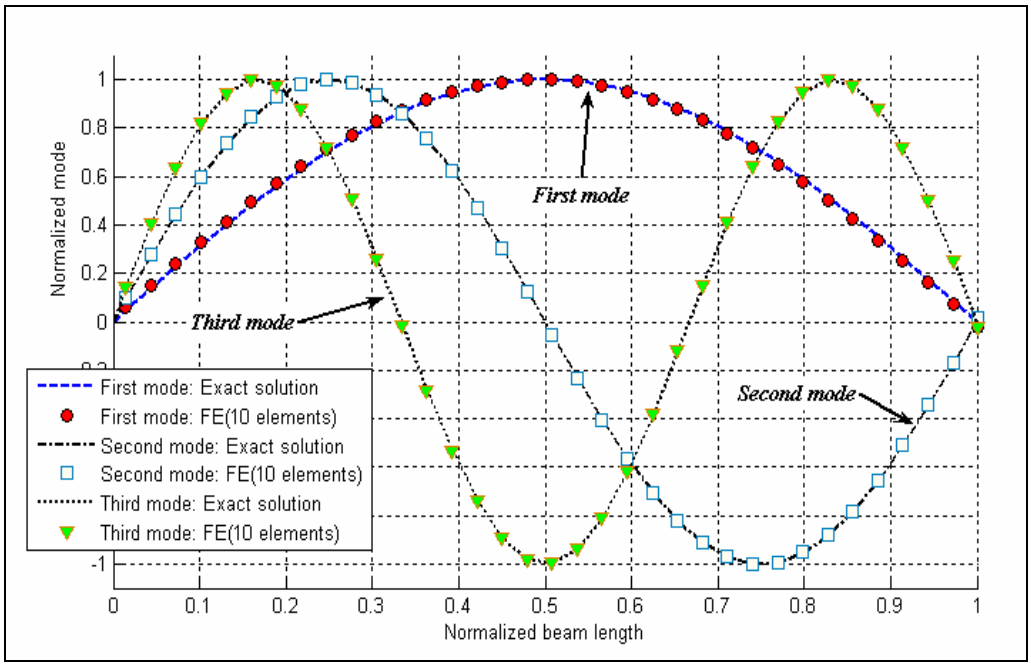

Figure 3. 6 The mode shapes of the pinned-pinned beam, computer solution compared with the exact solution.

The present beam element has been shown to yield results in good agreement with the results from analytical solution of the elastic isotropic beam, especially at low frequencies. It can be attributed to the fact that the beam becomes quite flexible under the clamped–free and pinned-pinned supports.

Now, the present model will be examined for the laminated composite beams and nondimensional natural frequencies $\hat{\omega}$ of the beam will be compared with the analytical and finite element solutions wherever are available in the literature.

3.5.3 Case-3: Orthotropic clamped-free and pinned-pinned asymmetric laminated composite beams

In this case, the natural frequencies of the asymmetric thin $\frac{l}{h_t} = 60$ and thick $\frac{l}{h_t} = 5$ orthotropic laminated composite beams are calculated. The total thickness of the beam h_t and each ply is assumed to have the same thickness. The laminates with the ply angle α are assumed to follow the $0^\circ / \alpha^\circ / \alpha^\circ / 0^\circ$ configuration. The finite element analysis results of the present model and the results obtained by Maiti and Sinha (1994) using a HSDT (higher order shear deformation theory) and FSDT (first order shear deformation theory) nine node element are compared. In this case, the material and geometric properties are defined as:

$E_{xx} = 129.20708$ GPa , $E_{yy} = 9.42512$ GPa ,
G_{xy}=5.15658 GPa , G_{xz}=4.30530 GPa , G_{yz}=2.54139 GPa ,
$\nu_{xy} = \nu_{xz} = 0.3$, $\nu_{yz} = 0.218837$, $\rho = 1550.0666$ Kg-m^3, $b_t = 0.0127$ m, $l = 0.1905$ m

The natural frequencies are calculated using the formulation obtained for proposed element and the results are compared with the results obtained from discretized beam with ten present beam elements and are shown in Table 3.3-3.6.

lamina lay up configuration	Maiti & Sinha		Present model, using FE (10elements)
	HSDT	FSDT	
$0^\circ/90^\circ/0^\circ/90^\circ$	8.843	8.854	8.863
$0^\circ/30^\circ/-30^\circ/0^\circ$	12.397	12.404	12.503
$0^\circ/45^\circ/-45^\circ/0^\circ$	12.268	12.271	12.312
$0^\circ/60^\circ/-60^\circ/0^\circ$	12.225	12.227	12.305

Table 3. 3 The first three natural frequencies for cantilever laminated composite beams with slender ratio $l/h_t = 60$.

lamina lay up configuration	Maiti & Sinha		Present model, using FE (10elements)
	HSDT	FSDT	
$0^\circ/90^\circ/0^\circ/90^\circ$	3.132	3.130	3.140
$0^\circ/30^\circ/-30^\circ/0^\circ$	3.493	3.546	3.550
$0^\circ/45^\circ/-45^\circ/0^\circ$	3.227	3.263	3.225
$0^\circ/60^\circ/-60^\circ/0^\circ$	3.154	3.178	3.158

Table 3. 4 The first three natural frequencies for cantilever laminated composite beams with slender ratio $l/h_t = 5$.

lamina lay up configuration	Maiti & Sinha		Present model, using FE (10elements)
	HSDT	FSDT	
$0^\circ/90^\circ/0^\circ/90^\circ$	26.331	26.378	26.389
$0^\circ/30^\circ/-30^\circ/0^\circ$	34.764	34.786	34.752
$0^\circ/45^\circ/-45^\circ/0^\circ$	34.380	34.403	34.289
$0^\circ/60^\circ/-60^\circ/0^\circ$	34.262	34.271	34.279

Table 3. 5 The natural frequencies for pinned-pinned laminated composite beams with slender ratio $l/h_t = 60$.

lamina lay up configuration	Maiti & Sinha		Present model, using FE (10elements)
	HSDT	FSDT	
$0^\circ/90^\circ/0^\circ/90^\circ$	16.955	17.350	17.210
$0^\circ/30^\circ/-30^\circ/0^\circ$	19.181	21.599	20.342
$0^\circ/45^\circ/-45^\circ/0^\circ$	18.475	20.092	19.788
$0^\circ/60^\circ/-60^\circ/0^\circ$	17.926	19.384	19.224

Table 3. 6 The natural frequencies for pinned-pinned laminated composite beams with slender ratio $l/h_t = 5$.

3.5.4 Case-4: Orthotropic clamped-clamped asymmetric laminated composite beams

In this case the three first natural frequencies of a clamped-clamped laminated beam with $\left(0^{\circ}/45^{\circ}/-45^{\circ}/0\right)$ layup configuration is investigated. The results obtained from discrettized ten elements beam model are compared with those results presented by Loja et al (2001). The mechanical and geometric properties of the beam are same as the beam properties in case-3. The results are shown in Table 3.7.

l/h_t	Model	First mode	Second mode	Third mode
10	Loja et al. (2001)	39.89	48.99	103.8
	Present, FE (10 elements)	42.56	55.37	112.47
30	Loja et al. (2001)	72.54	119.27	183.77
	Present, FE (10 elements)	74.33	127.66	195.72

Table 3. 7 The first three natural frequencies for clamped-clamped laminated composite $(0^{\circ}/45^{\circ}/-45^{\circ}/0)$ beam.

3.5.5 Case-5: Orthotropic clamped-free asymmetric laminated composite beams compare to literature and ANSYS results

The formulation and results of the proposed hybrid beam element for the asymmetric laminated shear deformable beams have been compared with the ones from two researchers Chen et al. (2004) and Aydogdu (2006), and also ANSYS simulation. Chen et al. studied the free vibration of generally laminated

composite beams. The vibration analysis of angle-ply laminated beams is investigated by Aydogdu.

Two asymmetric laminated orthotropic clamped-free and simply supported AS4/3501-6 graphite/epoxy composite beams used in the analysis. The material properties are: $E_{xx} = 9.65\ GPa$, $E_{yy} = 144.80\ GPa$, $G_{xy} = G_{xz} = 4.14\ GPa$, $G_{yz} = 3.45\ GPa$, $\upsilon_{xy} = 0.3$ and the $\frac{l}{h} = 15$. In ANSYS model, 3D shell element with 8 node and six degrees of freedom at each node was used (Fig. 3.7).

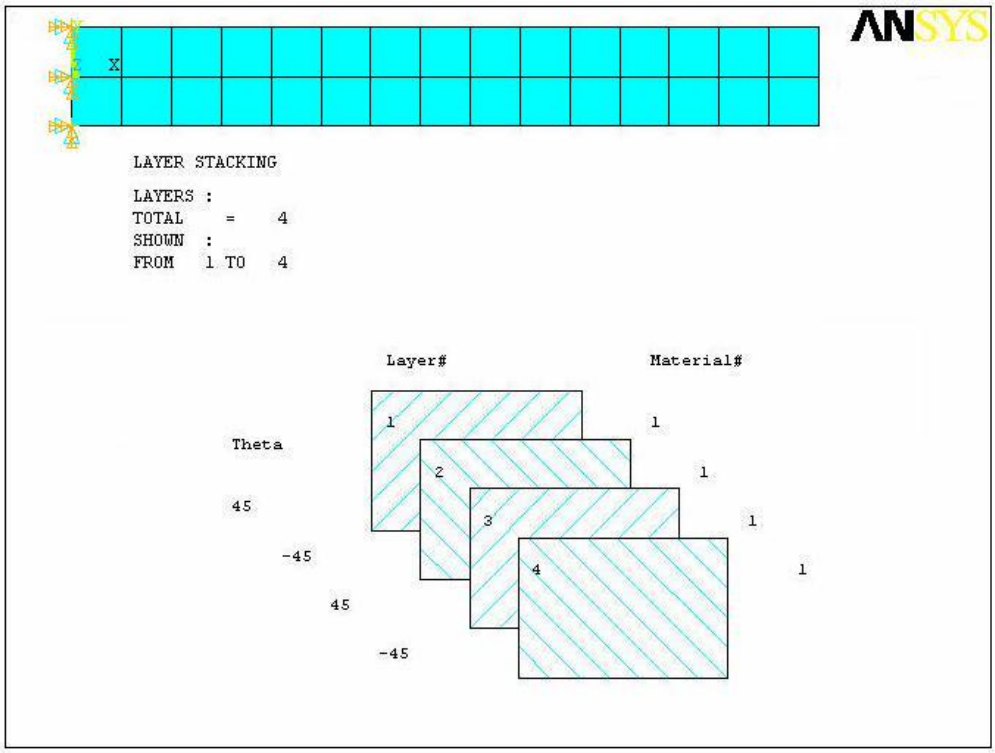

Figure 3. 7 The laminated asymmetric beam model in ANSYS using 80 shell elements.

The first three frequencies obtained with the proposed hybrid beam element and with the results reported by Chen et al. (2004) and Aydogdu (2006) compare well as shown in Table 3.8. Also in this table show well agreement of the proposed model results with that using ANSYS in higher frequencies. The results shows that when using only ten laminated hybrid beam elements are sufficient to capture the same effect obtained by other researchers and ANSYS. Only because of the properties and formulation of the eight nodes shell element provided by ANSYS are suitable to capture the membrane stresses and strain using the shell theory, which is far from the beam theory is used in this investigation, the results are not very close as it can be seen for the case of the simply supported beam.

Boundary Conditions	Model	Mode Numbers		
		1	2	3
CF	Chen et al.	0.297	1.778	4.895
	Aydogdu	0320	1.916	4.993
	ANSYS	0.738	1.550	4.672
	Present beam element	0.281	1.652	4.693
SS	Chen et al.	0.800	3.164	6.994
	Aydogdu	0.891	3.374	7.002
	ANSYS	1.626	4.585	6.447
	Present beam element	0.721	2.991	6.127

Table 3. 8 The first three non-dimensional frequencies ($\omega l^2\sqrt{\frac{\rho}{Eh^2}}$) for clamped-free (CF) and Simply-Supported(SS) asymmetric four-layer $(-45^\circ/45^\circ/-45^\circ/45^\circ)$ laminated composite beam.

3.6 Summary

In chapter-3, the integral form of the equation of motion of a laminated beam was descretized though a proposed five nodes beam element. Then, the equation of motion formulated using Lagrangian formulation. The presented element can capture the existing couplings (tension-bending, tension-twisting, bending-twisting) effects. The present model has been validated with the exact analytical solutions and those available in the literature for free vibration of both isotropic and orthotropic either symmetric or asymmetric laminated composite beams.

The results from present model, models available in literature, and the model simulated in commercial software ANSYS® show are in good agreement. Comparisons against experimental results and against alternative numerical analyses indicate that the present model can be used to perform extensive parametric studies.

In next chapter, the descretized equation of motion of the system, which is in Mathieu differential equation form, will be solved to determine the region of stabilities of the beam subjected to conservative and nonconservative loads. The stability regions of will be plotted for different cases.

CHAPTER 4

Dynamic Stability Analysis of Composite Laminated Beams

In the previous chapter, the integral form of the equations of motion of the laminated composite beams was discretized through a developed twenty degree of freedom beam element. Consequently, the Mathieu form differential equations of motion (Eq.3.28) were obtained using the extended Hamilton's principle. A presented five nodes beam element was examined and the results compared with the results available in literature.

In this chapter, the regions of stability of the composite laminated beams are determined. The effect of damping behaviour on stability of the beam is studied as well.

4.1 Stability analysis

A system is stable at an equilibrium state if for every small disturbance of the system the response remains small, otherwise it becomes unstable. Thus when studying the stability and vibration about the equilibrium state of the beam, the generalized displacements are perturbed by an infinitesimal displacement. The effects of the small displacements on displacement stiffness matrix are small and negligible and are not considered in this study.

Since the dynamic load P_t and the loading frequency θ cause dynamic strains and stresses, the stability of the beam is related to these parameters. This phenomenon is called dynamic instability and the regions of instability of the beam are determined and plotted in the plane loading-frequency $P-\theta$. In the other hand, dynamic stability analysis is essentially about determining of the boundaries of instability regions under loading conditions with periodic motion of *T* or *2T*, where $T=\frac{2\pi}{\theta}$.

4.2 Determination of Dynamic Instability regions of undamped system

Recall Eq. (3.28) and rearrange the descretized equations of motion about equilibrium state for undapmed system as:

$$\mathbf{M}\ddot{\mathbf{U}}+\left\{\left(\mathbf{K}_{\mathrm{E}}+\mathbf{K}_{\mathrm{G}}\right)-\mathbf{K}_{\mathrm{L}}^{0}-\mathbf{K}_{\mathrm{L}}^{\mathrm{t}}\cos\theta t\right\}\mathbf{U}=0 \tag{4.1}$$

Eq. (4.1) have the solution with period *2T* in Fourier series form for the components of vector $\mathbf{U}_{(t)}$ as follows:

$$\mathbf{U}_{(t)}=\sum_{m=1,3,5,\ldots}^{\infty}\left(\mathbf{A}_m\sin\frac{m\theta t}{2}+\mathbf{B}_m\cos\frac{m\theta t}{2}\right) \tag{4.2}$$

where $\mathbf{A}_m$ and $\mathbf{B}_m$ are vectors independent of time ***t*** and just depend on degrees of freedom.

Substituting Eq. (4.2) into Eq. (4.1) and equating the sum of the coefficients of identical $\sin\frac{m\theta t}{2}$ and $\cos\frac{m\theta t}{2}$ to zero leads to the following systems of matrix equations in terms of $\mathbf{A}_m$ and $\mathbf{B}_m$:

$$\begin{bmatrix} \mathbf{K}_E+\mathbf{K}_G-\mathbf{K}_L^0+\frac{\mathbf{K}_L^t}{2}-\frac{\mathbf{M}\theta^2}{4} & -\frac{\mathbf{K}_L^t}{2} & 0 & . \\ -\frac{\mathbf{K}_L^t}{2} & \mathbf{K}_E+\mathbf{K}_G-\mathbf{K}_L^0-\frac{9\mathbf{M}\theta^2}{4} & -\frac{\mathbf{K}_L^t}{2} & . \\ 0 & -\frac{\mathbf{K}_L^t}{2} & \mathbf{K}_E+\mathbf{K}_G-\mathbf{K}_L^0-\frac{25\mathbf{M}\theta^2}{4} & . \\ . & . & . & . \end{bmatrix} \begin{Bmatrix} \mathbf{A}_1 \\ \mathbf{A}_3 \\ \mathbf{A}_5 \\ . \end{Bmatrix} = \mathbf{0} \tag{4.3a}$$

and

$$\begin{bmatrix} \mathbf{K}_E+\mathbf{K}_G-\mathbf{K}_L^0-\frac{\mathbf{K}_L^t}{2}-\frac{\mathbf{M}\theta^2}{4} & -\frac{\mathbf{K}_L^t}{2} & 0 & . \\ -\frac{\mathbf{K}_L^t}{2} & \mathbf{K}_E+\mathbf{K}_G-\mathbf{K}_L^0-\frac{9\mathbf{M}\theta^2}{4} & -\frac{\mathbf{K}_L^t}{2} & . \\ 0 & -\frac{\mathbf{K}_L^t}{2} & \mathbf{K}_E+\mathbf{K}_G-\mathbf{K}_L^0-\frac{25\mathbf{M}\theta^2}{4} & . \\ . & . & . & . \end{bmatrix} \begin{Bmatrix} \mathbf{B}_1 \\ \mathbf{B}_3 \\ \mathbf{B}_5 \\ . \end{Bmatrix} = \mathbf{0} \tag{4.3b}$$

The nontrivial solutions of the above equations for $\mathbf{A}_m$ and $\mathbf{B}_m$ exist if the determinants of their coefficients are zero as follows:

$$\begin{vmatrix} \mathbf{K}_E+\mathbf{K}_G-\mathbf{K}_L^0\pm\frac{\mathbf{K}_L^t}{2}-\frac{\mathbf{M}\theta^2}{4} & -\frac{\mathbf{K}_L^t}{2} & 0 & . \\ -\frac{\mathbf{K}_L^t}{2} & \mathbf{K}_E+\mathbf{K}_G-\mathbf{K}_L^0-\frac{9\mathbf{M}\theta^2}{4} & -\frac{\mathbf{K}_L^t}{2} & . \\ 0 & -\frac{\mathbf{K}_L^t}{2} & \mathbf{K}_E+\mathbf{K}_G-\mathbf{K}_L^0-\frac{25\mathbf{M}\theta^2}{4} & . \\ . & . & . & . \end{vmatrix} = \mathbf{0} \tag{4.4}$$

In the same way, the solutions for the equations of motion Eq. (4.1) with period *T* in series form are as follows:

$$\mathbf{U}_{(t)} = \frac{1}{2}\mathbf{B}_0 \sum_{m=2,4,\ldots}^{\infty} (\mathbf{A}_m \sin\frac{m\theta t}{2} + \mathbf{B}_m \cos\frac{m\theta t}{2}) \tag{4.5}$$

Again, with substituting of Eq. (4.5) into Eq. (4.1) and using same approach, the conditions for existence of the non-trivial solutions for $\mathbf{A}_m$ and $\mathbf{B}_m$ are:

$$\begin{vmatrix} \mathbf{K}_E + \mathbf{K}_G - \mathbf{K}_L^0 - \mathbf{M}\theta^2 & -\frac{\mathbf{K}_L^t}{2} & 0 & . \\ -\frac{\mathbf{K}_L^t}{2} & \mathbf{K}_E + \mathbf{K}_G - \mathbf{K}_L^0 - 4\mathbf{M}\theta^2 & -\frac{\mathbf{K}_L^t}{2} & . \\ 0 & -\frac{\mathbf{K}_L^t}{2} & \mathbf{K}_E + \mathbf{K}_G - \mathbf{K}_L^0 - 16\mathbf{M}\theta^2 & . \\ . & . & . & . \end{vmatrix} = \mathbf{0} \tag{4.6a}$$

and

$$\begin{vmatrix} \mathbf{K}_E + \mathbf{K}_G - \mathbf{K}_L^0 & -\mathbf{K}_L^t & 0 & 0 & . \\ -\frac{\mathbf{K}_L^t}{2} & \mathbf{K}_E + \mathbf{K}_G - \mathbf{K}_L^0 - \mathbf{M}\theta^2 & -\frac{\mathbf{K}_L^t}{2} & 0 & . \\ 0 & -\frac{\mathbf{K}_L^t}{2} & \mathbf{K}_E + \mathbf{K}_G - \mathbf{K}_L^0 - 4\mathbf{M}\theta^2 & -\frac{\mathbf{K}_L^t}{2} & . \\ 0 & 0 & -\frac{\mathbf{K}_L^t}{2} & \mathbf{K}_E + \mathbf{K}_G - \mathbf{K}_L^0 - 16\mathbf{M}\theta^2 & . \\ . & . & . & . & . \end{vmatrix} = 0 \tag{4.6b}$$

Equations (4.4), (4.6a), and (4.6b) are eigenvalue problems of the system, which determines the boundaries of dynamic instability regions. It is important to note that these equations have symmetric coefficients and are useful for a system where damping is not taken into account. The analysis of systems with damping and determination of instability regions of such structures will be considered in the next section.

4.3 Determination of Dynamic Instability regions of damped system

Damping of composite laminated beams plays vital role in the dynamic behaviour analysis of structures as it controls the resonant vibrations and thus reducing the bounded instability regions. This damping depends on the lamina material properties as well as layer orientations and stacking sequence. Composite materials can store and dissipate energy. A damping process has been developed initially by Adams and Bacon (1973) in which the energy dissipation can be described as separable energy dissipations associated to the individual stress components. This analysis was refined in later paper of Ni and Adams (1984). In their study, the damping of orthotropic beams is considered as function of material orientation and the papers also consider cross-ply laminates and angle-ply laminates, as well as more general types of symmetric laminates. Rao and He (1993) presented closed-form solutions for the modal loss factors of the composite beam system under simple supports using the energy method. The finite element analysis has been used by Maheri and Adams (1994) to evaluate the damping properties of free–free fibre-reinforced plates. More recently the analysis of Adams and Bacon (1995) was applied by Yim et al. (1999) to different types of laminates then extended by Yim and Gillespie (2000) including the transverse shear effect in the case of 0° and 90° unidirectional laminates. The material damping of 0° laminated composite sandwich cantilever beams with a viscoelastic layer has been

investigated by Yim et al. (2003), and damping analysis of laminated beams and plates using the Ritz method has been studied by Berthelot (2004).

Goyal (2002) studied the deterministic and probabilistic stability analysis of laminated beams subjected to tangential loading using. He did not determine the region of dynamic instability and further the effects of damping in the dynamic instability of the shear deformable composite beams.

In this study, the damping of composite materials based on dissipation energy associated by strain energy is considered. The calculation of the elements of the damping matrix $\mathbf{C}$ for cross ply lay-up orthotropic laminated composite beam with material and geometry properties defined in previous cases is presented in Appendix A. The determinant of the damping matrix of the structure gives the total damping factor ξ of the system.

Therefore the equation of motion of the structure about equilibrium position with taking damping into account as additional term into matrix form differential equation Eq. (4.2) introduced as follows:

$$\mathbf{M}\ddot{\mathbf{U}} + \mathbf{C}\dot{\mathbf{U}} + \left\{\left(\mathbf{K}_{\mathrm{E}} + \mathbf{K}_{\mathrm{G}}\right) - \mathbf{K}_{\mathrm{L}}^{0} - \mathbf{K}_{\mathrm{L}}^{\mathrm{t}} \cos\theta t\right\}\mathbf{U} = 0 \qquad (4.7)$$

where $\mathbf{C}$ is damping matrix or energy dissipation matrix of the system. The periodic solutions (with period $2T$) of the Eq. (4.7) can be expressed as $\mathbf{U}_{(\mathrm{t})} = \sum_{m=1,3,5,\ldots}^{\infty} (\mathbf{A}_m \sin\frac{m\theta t}{2} + \mathbf{B}_m \cos\frac{m\theta t}{2})$ with same approach described in Eq. (4.2).

Substituting of the above equation in Eq.(4.7) and equating the sum of the coefficients of $\sin\frac{m\theta t}{2}$ and $\cos\frac{m\theta t}{2}$ to zero, leads to the following systems of matrix:

$$\begin{vmatrix} \mathbf{K}_{\mathrm{E}}+\mathbf{K}_{\mathrm{G}}-\mathbf{K}_{\mathrm{L}}^{0}+\frac{\mathbf{K}_{\mathrm{L}}^{\mathrm{t}}}{2}-\frac{\mathbf{M}\theta^{2}}{4} & -\frac{1}{2}\mathbf{C}\theta \\ \frac{1}{2}\mathbf{C}\theta & \mathbf{K}_{\mathrm{E}}+\mathbf{K}_{\mathrm{G}}-\mathbf{K}_{\mathrm{L}}^{0}-\frac{\mathbf{K}_{\mathrm{L}}^{\mathrm{t}}}{2}-\frac{\mathbf{M}\theta^{2}}{4} \end{vmatrix}=0 \qquad (4.8)$$

Leading expansion of the above determinant in second order form yields the equations of the boundary of principal instability regions of the system.

There are infinite numbers of determinants for the Eq. (4.8), in which the first principal instability region is important and is interested to determine hereon.

4.4 Conservative and nonconservative forces

As described in previous Chapter, a structure can be subjected to the forces that their directions don't change (conservative) and forces that follow the direction of the deformed structure (nonconservative). Consider a cantilever beam subjected to an axial force Fig. 4.1, this force can be tangential follower force P_{nc} or constant in direction P_{c}.

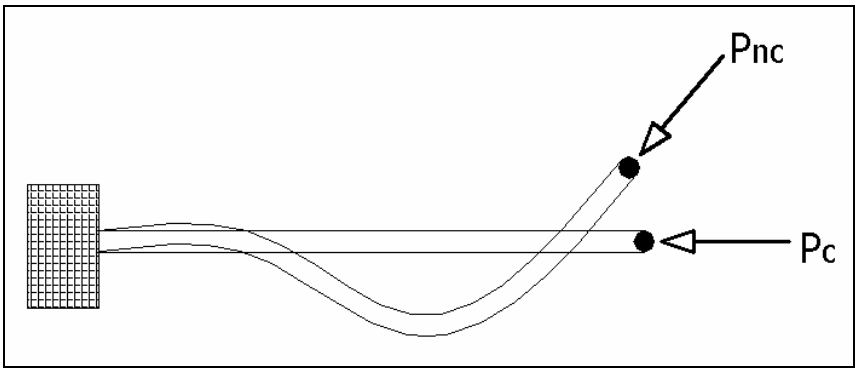

Figure 4. 1 The cantilever beam subjected to conservative or nonconservative load at free end.

For nonconservative forces the global loading stiffness matrix becomes unsymmetric and therefore the eigenvalues of the system consequence the change in regions of instability. If the conservativness of the system is defined by a factor η as $P_{\text{nc}} = \eta P,$ and $P_{\text{c}} = (1-\eta)P$, for pure conservative load $\eta = 0$ and for pure nonconservative load $\eta = 1$. Then the regions of instability may depend on the conservativness factor.

4.5 Verification of the present formulation

In literature little attention has been paid to the effect of nonconservativness in laminated composite beams. In order to verify the present beam model and formulation, an isotropic cantilevered beam subjected to a nonconservative load with same material and geometry properties defined by Vitaliani et al. (1997) and Gasparini et al. (1995) will be considered and the result compared to those presented by these researchers.

Consider a beam is subjected to an axial parametric loading $p = p_0 + p_t \cos\theta t$, where p_0 is static component of the load, p_t is dynamic component of the load, θ is loading frequency, and t is time. A prismatic beam under an axial load may undergo flexural buckling. The buckling load were defined by Kollar and Springer (2003) as $p_{cr}^{w} = \frac{k^2 \pi^2 E_{yy} bh^3}{12 l^2}$ for laminated beam without shear deformation, and $\frac{1}{p_{cr}} = \frac{1}{p_{cr}^{w}} + \frac{1}{\hat{S}}$ for laminated beam with shear deformation, where $\hat{S}$ is shear stiffness of the beam. For pinned-pinned beam $k = 1$, and for clamped-free beam $k = 1/2$. Also, the first natural frequency of lamiated beam without shear deformation is $\left(\omega_n^w\right)^2 = \frac{E_{yy} bh^3}{12 I_0}\left(\frac{\mu}{l}\right)^4$, and $\frac{1}{\omega_n^2} = \left(\frac{l}{\mu}\right)^4 \frac{12 I_0}{E_{yy} bh^3} + \left(\frac{l}{\mu}\right)^2 \frac{I_0}{\hat{S}}$ for beams with shear deformation have been carried out by Kollar and Springer (2003). The $I_0 = b\sum_{k=1}^{N} \rho^k \left(z_{k+1} - z_k\right)$ and N is the number of layers. For pinned-pinned beam $\mu = \pi$ and for clamped-free beam $\mu = \pi/2$.

For the beam with the following properties:

$l = 100$ cm	$E = 2.1\times10^7$ N/cm^2
$bh = 20$ cm^2	ν=0.3
ρ=0.1592 kg/cm	

the present formulation results are compared with the results calculated by Gasparini et al. (1995). In their study, the stability diagram is carried out by means of a finite element non-linear analysis supported with an eigenvalue

analysis of the deformed configuration and the system is considered without damping. Also, in their model, the beam element consists of four nodes, and each node has six degrees of freedom (three displacements and three rotations).

Recall the equation of eigenvalue problem of the system without damping, and substituting $-\lambda^2 = \omega^2$, where ω is the frequency of the beam, then the eigenvalue problem for all type of forces (conservative or nonconservative) becomes:

$$\left(\mathbf{K}_{\mathrm{E}} + \mathbf{K}_{\mathrm{G}} - \mathbf{K}_{\mathrm{L}} - \mathbf{M}\omega^2\right)\mathbf{U}_0 = 0 \tag{4.9}$$

with assuming that the geometry changing of the beam prior to the first critical load is zero and can be neglected, then the initial displacement stiffness matrix $\mathbf{K}_{\mathrm{D}} = 0$, consequently $\mathbf{K}_{\mathrm{E}} = \mathbf{K}_{\mathrm{M}}$ and eigenvalue problem can be rearranged as

$$\left(\mathbf{K}_{\mathrm{M}} + \mathbf{K}_{\mathrm{G}} - \mathbf{K}_{\mathrm{P}} - \mathbf{M}\omega^2\right)\mathbf{U}_0 = 0 \tag{4.10}$$

The loading stiffness matrix $\mathbf{K}_{\mathrm{L}}$ can be defined as the contribution of the conservativness factor as follows:

$$\hat{\mathbf{K}}_{\mathrm{L}} = \eta\mathbf{K}_{\mathrm{L}} \tag{4.11}$$

Therefore in case of conservative loading the eigenvalue problem becomes:

$$\mathbf{M}^{-1}\left(\mathbf{K}_{\mathrm{M}} + \mathbf{K}_{\mathrm{G}}\right) - \omega^2\mathbf{I} = 0 \tag{4.12}$$

where $\mathbf{I}$ is the unity matrix, and in case of nonconservative loading the eigenvalue can be expressed as:

$$\mathbf{M}^{-1}\left(\mathbf{K}_{\mathrm{M}} + \mathbf{K}_{\mathrm{G}} - \mathbf{K}_{\mathrm{L}}\right) - \omega^2\mathbf{I} = 0 \tag{4.13}$$

The frequencies ω are generally complex numbers and system stabilities depend on the value of this frequency. If ω is real or have positive imaginary

part, then the given position is stable. If among the roots ω there is at least one, which has a negative imaginary part, then the perturbation will increase unboundedly with time. Because of the matrices $\mathbf{M}$, $\mathbf{K}_{\mathrm{E}}$, $\mathbf{K}_{\mathrm{G}}$, and $\mathbf{K}_{\mathrm{L}}^{0}$ are symmetric, consequently, all $\omega^2 > 0$. Thus, for a such structure loaded by conservative forces, the system is statically and dynamically stable and stability concepts appears to be sufficient. The system will be unstable or in critical situation, if the mass and stiffness matrices are unsymmetric and/or the eigenvalue ω^2 is zero or negative. For the structure loaded by the following forces, which are nonconservative, the work done by external forces depends on the choice of the path through that the beam is brought to the final position and loss of dynamic stability is possible. Therefore, treating of the nonconservative system should be considered differently in compare to conservative system. In such problems involving the dynamic instability of nonconservative systems in equilibrium positions a nonlinear term on the basis of damping considerations has to be considered.

The results obtained by solving the eigenvalue problem of the conservative loading system Eq.(4.12) from the present model using symbolic manipulator MATLAB® are plotted in plane load vs. eigenvalue (frequency) and shown in Fig. 4.2, and Fig.4.3. Both results are in good agreement with the stability diagrams presented by Gasparini et al. (1995).

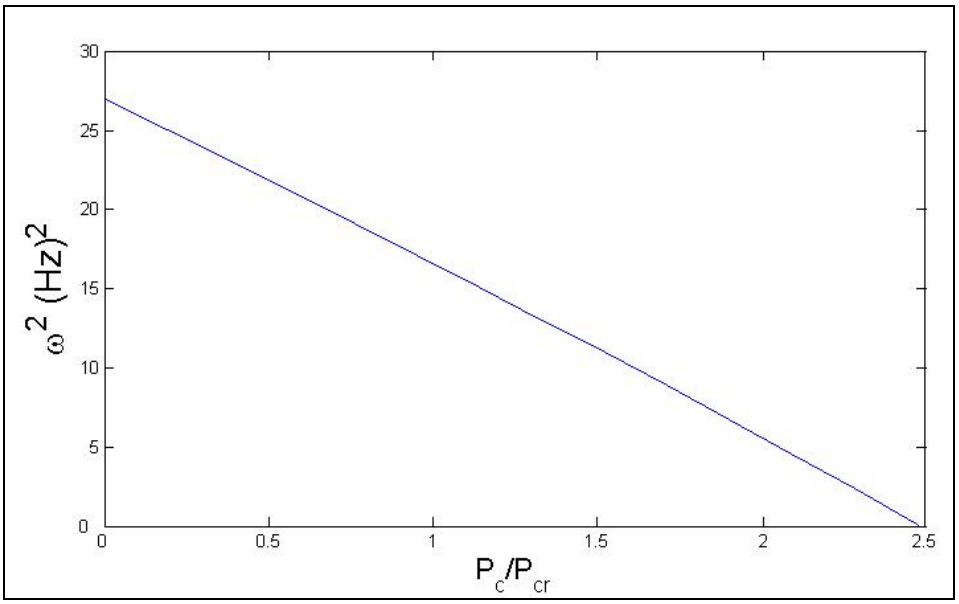

Figure 4. 2 Nondimensional load vs. eigenvalue frequency of isotropic cantilever beam subjected to perfectly conservative force.

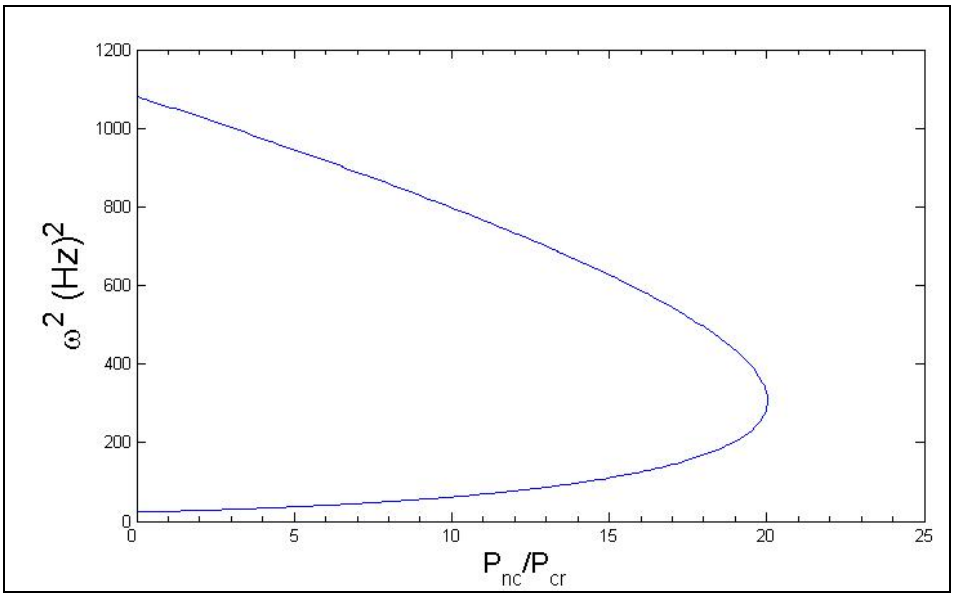

Figure 4. 3 Nondimensional load vs. eigenvalue frequency of isotropic cantilever beam subjected to perfectly nonconservative force.

Now with this verification of the present formulation with the result from literature, the stability analysis of the laminated beam can be presented and examined in different cases courageously.

4.6 Eigenvalue problem and characteristic diagram determination of laminated composite beams

To determine the dynamic stability regions of the laminated composite beams with arbitrary lamination subjected to periodic axial loading needs to calculate the stiffness and mass matrices of the structure. This has been done using the symbolic manipulator MATLAB® for lay-up configurations $0^\circ/\alpha^\circ/\alpha^\circ/0^\circ$. The material and geometry properties of the beam are same as the properties given in case-3 chapter3. The results for pure conservative loading are depicted and shown in Fig.4.4 for three different lay-up configurations. Also, the curves for pure nonconservative loading are shown in Fig.4.5 for symmetric laminated beam.

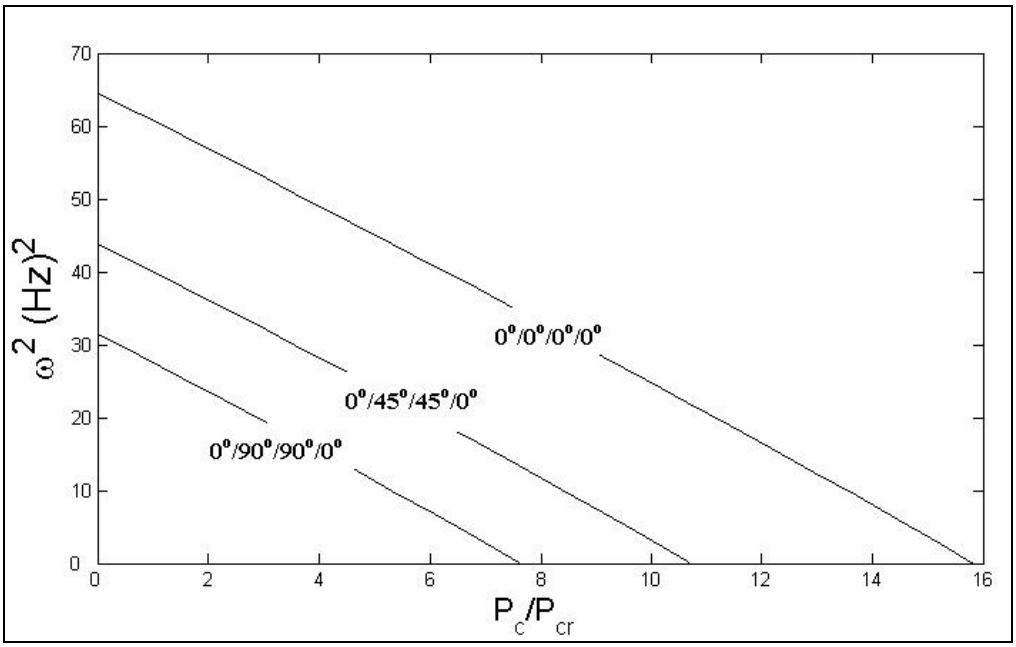

Figure 4. 4 Nondimensional loads vs. eigenvalue frequency of the laminated cantilever beam subjected to perfectly conservative force with lay-up $0^\circ/\alpha^\circ/\alpha^\circ/0^\circ$.

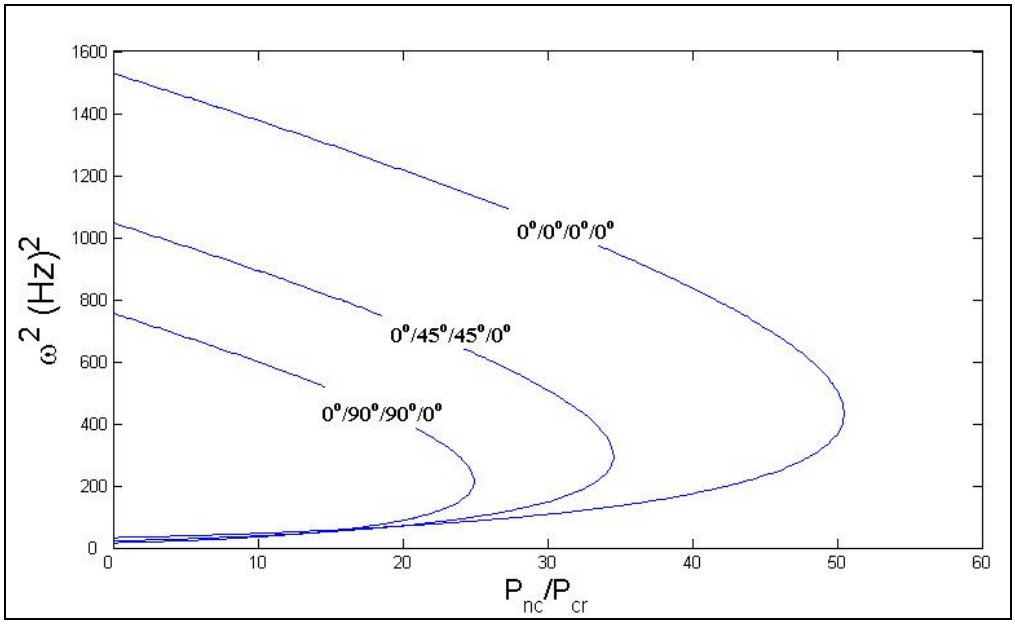

Figure 4. 5 Nondimensional load vs. eigenvalue frequency of the laminated cantilever beam subjected to perfectly nonconservative force with lay-up $0^\circ/\alpha^\circ/\alpha^\circ/0^\circ$.

The deterministic stability of isotropic and laminated beams was studied and the results depicted in different pictures. The present laminated beam model has been validated with those available in the literature. As it can be seen from the results of these cases of stability analysis, the ply orientations play important role in the stability of laminated beams. The analysis performed hereon is valid for deterministic systems.

4.7 Determination of instability regions of undamped cross-ply orthotropic laminated composite cantilever beam

The lay-up configuration of cross ply laminates is in form of $0^\circ/90^\circ/90^\circ/0^\circ$ and each lamina has equal thickness. The stiffness matrices $\mathbf{K}_{\mathrm{E}}, \mathbf{K}_{\mathrm{G}}, \mathbf{K}_{\mathrm{L}}^{0}, \mathbf{K}_{\mathrm{L}}^{\mathrm{t}}$ and mass matrix $\mathbf{M}$ are calculated using the symbolic computations. The approximate expression for the boundaries of the principal regions of instabilities is obtained by equating to zero the determinant of the first matrix element in the diagonal matrix, which is:

$$\left| \mathbf{K}_{\mathrm{E}} + \mathbf{K}_{\mathrm{G}} - \mathbf{K}_{\mathrm{L}}^{0} \pm \frac{\mathbf{K}_{\mathrm{L}}^{\mathrm{t}}}{2} - \frac{\mathbf{M}\theta^2}{4} \right| = 0 \tag{4.14}$$

This approximation is based on this fact that the periodic solution of the equation of motion is trigonometric form Eq. (4.2). The dynamic stability of the beam is considered initially when just the dynamic component p_t of the period load exists and load's direction changes with beams deformation (nonconservative or following load) and with constant direction, always in x-

direction. Then, the beam is subjected to static load p_0 as well as constant dynamic load p_t are considered.

Now, the Eq.(4.12) can be rewritten for only dynamic load in account as follows

$$\left| \mathbf{K}_{\mathrm{E}} + \mathbf{K}_{\mathrm{G}} \pm \frac{\mathbf{K}_{\mathrm{L}}^{\mathrm{t}}}{2} - \frac{\mathbf{M}\theta^2}{4} \right| = 0 \tag{4.15}$$

Upon expansion of the above determinants in second order form yields the two equations of the boundary of instability regions of the beam. With taking advantage of Bolotin's approach (1964), the first principal regions of instability can be determined.

The critical buckling loads and natural frequencies of the clamped-free beam with defined material and geometry properties for $\frac{l}{h} = 10$ are

$$p_{cr}^{w} = 4.7\,\mathrm{kN}, \text{ and } p_{cr} = 3.6\,\mathrm{kN}$$

$$\omega_n^{w} = 293\,\mathrm{Hz}, \text{ and } \omega_n = 163\,\mathrm{Hz}$$

The nondimensional parameters p_t / p_{cr}^{w}, and p_t / p_{cr} suppose to increase from 0 to 2.

The first principal region of instabilities is shown in the planes p_t / p_{cr}^{w} or $p_t / p_{cr}, \theta / 2\omega_n$ with dimensionless parameters in Fig. 4.6 for the beam subjected to the following load p_t without shear deformation and with shear deformation in account. As it can be seen, the beam without sear deformation in account

leads to a narrowing of the regions of dynamic instability, and the lower bound position of the beam with shear deformation in account is changing faster than upper bound.

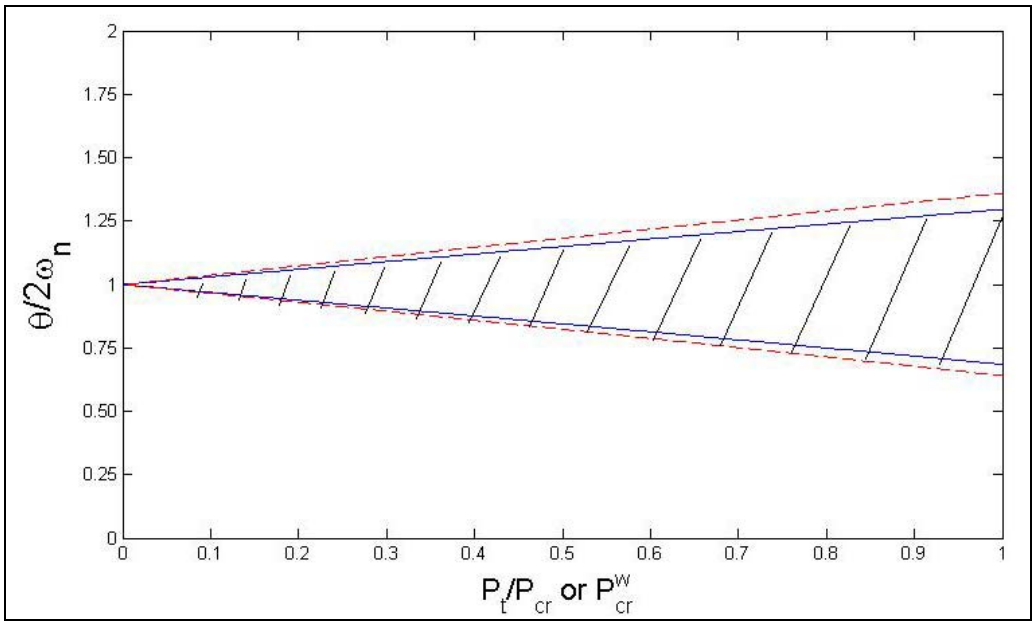

Figure 4. 6 Dynamic principal instability regions of a cantilever cross-ply laminated beam ($0^\circ / 90^\circ / 90^\circ / 0^\circ$) subjected to nonconservative load, without shear stiffness (crosshatched region) and with shear stiffness (dash lines).

Another obvious fact is the instability region of the beam subjected to the following (nonconservative) loading doesn't intersect axis p_t / p_{cr} or p_{cr}^w . This is because of such a problem involving the stability of equilibrium state of the structure subjected to the follower load must be investigated on the basis of damping and nonlinear considerations.

Now, the dynamic stability of the conservative system, when both the static and dynamic components of the load exist and the loads ratio p_t/p_0 is constant and p_0 is less than buckling load will be investigated. The instability regions for such a system, when the nondimensional parameter p_0/p_{cr} or p_{cr}^w increases from 0 to 0.8 are depicted and shown in Fig. 4.7. As it has been shown in Fig. 4.7, for the case when the load direction during vibration doesn't change, the regions of dynamic instability of the non-shear deformable beam becomes narrow.

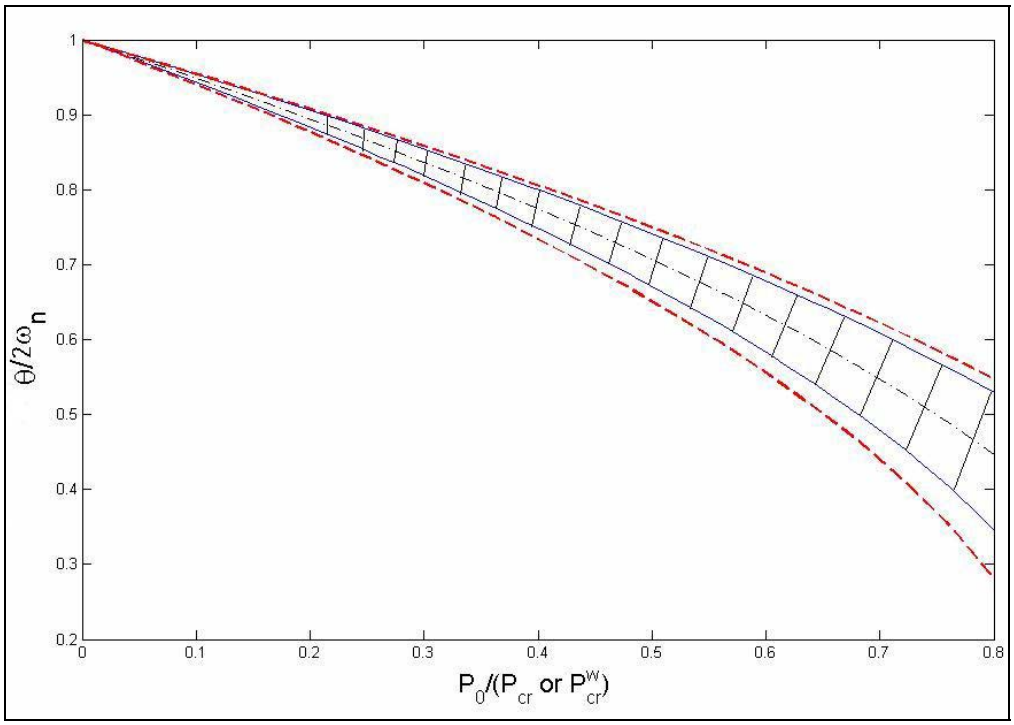

Figure 4. 7 Dynamic principal instability regions of a cantilever cross-ply laminated beam ($0^\circ/90^\circ/90^\circ/0^\circ$) subjected to conservative load, without shear stiffness (crosshatched region) and with shear stiffness (red dash lines).

In discussion of the results of this case and the graphs in Figures 4.6 and 4.7, it has to be considered that the results were obtained from equations based on the harmonic approximation and equilibrium state. As can be seen the regions of instability for nonconservative loading is enlarged in compare to conservative loading system.

4.8 Determination of instability regions of damped cross-ply orthotropic laminated composite cantilever beam

The first principal regions of instabilities for the beam subjected to the nonconservative loads and with shear deformation and damping in account are shown in the plane p_t/p_{cr}, $\theta/2\omega_n$ with dimensionless parameters in Fig. 4.8.

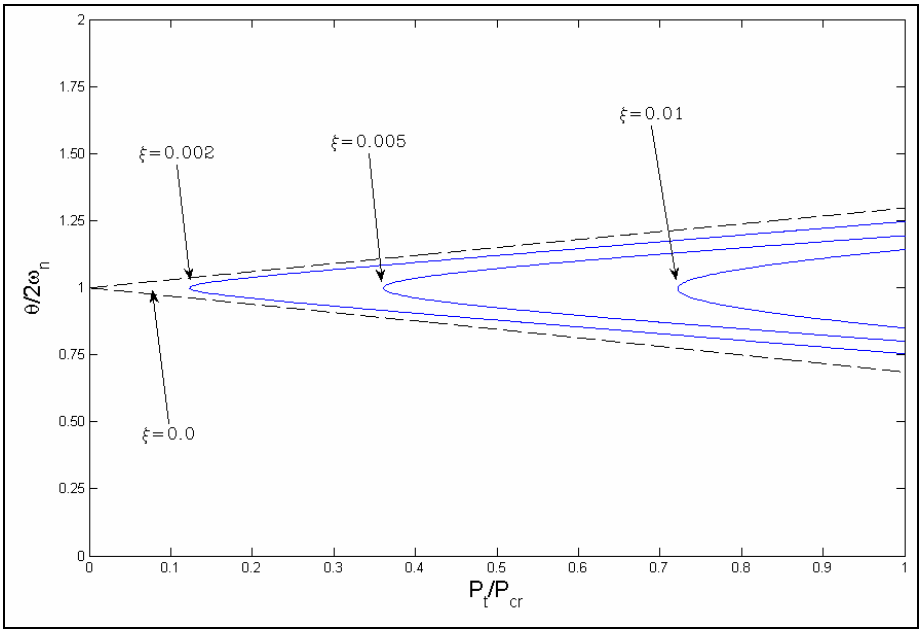

Figure 4. 8 Dynamic principal instability regions of a cantilever cross-ply laminated beam ($0^\circ/90^\circ/90^\circ/0^\circ$) subjected to nonconservative load, with shear stiffness and different damping factors in account.

As it can be seen from Fig. 4.8 the stable region becomes wider when the damping ratio of the structure is increased and the system will be in better stability situation. In the other hand, the greater of the damping, the greater of the amplitude of longitudinal force required to cause the beam dynamically unstable.

4.9 Determination of steady state amplitude of the laminated composite beams

In this section, the vibration of parametrically excited beam for the principal resonance of the system which causes the principal instability will be studied and the amplitude of the beam will be investigated. The parametric resonance of the system occurs in the near of frequency-ratios $\frac{\theta}{2\omega_n} = 1$. Having in view that within the framework of the principal resonance, the parametric excitation can excite only one mode at a time, it results that for each mode, infinity of instability regions could occur. Within these instability regions, the particular mode is excited in lateral motion with exponentially growing amplitude. For $\theta = 2\omega_n$ the resulted instability region is the largest and the most significant one. It is referred to as the principal parametric resonance. To determine the influence of loading frequency on the amplitude resonance, the first and most important instability region will be considered.

For describing the parametrically excited vibration system in general form with damping in account and the effects of the nonlinear factors such as

nonlinear damping, nonlinear inertia and nonlinear elasticity, the equation of motion can be expressed as follows:

$$\mathbf{M}\ddot{\mathbf{U}} + \mathbf{C}\dot{\mathbf{U}} + \left\{\left(\mathbf{K}_{\mathrm{E}} + \mathbf{K}_{\mathrm{G}}\right) - \mathbf{K}_{\mathrm{L}}^{0} - \mathbf{K}_{\mathrm{L}}^{\mathrm{t}} \cos\theta t\right\}\mathbf{U} + \Psi\left(\mathbf{U}, \dot{\mathbf{U}}, \ddot{\mathbf{U}}\right) = 0 \quad (4.16)$$

where Ψ is the nonlinear function of the system.

For the principal resonance, the influence of higher harmonics in the expansion of Eq.(4.2) can be neglected and the approximate solution of sub-harmonic system becomes:

$$\mathbf{U}_{(\mathrm{t})} = \mathbf{A}\sin\frac{\theta t}{2} + \mathbf{B}\cos\frac{\theta t}{2} \quad (4.17)$$

when amplitude of principal resonance $\mathbf{\Lambda}$ is defined as:

$$\mathbf{\Lambda} = \left(\mathbf{A}^2 + \mathbf{B}^2\right)^{1/2}$$

Substituting Eq. (4.17) into the general form of the equation of motion of the system with damping in account, Eq. (4.16), and follow the same approach described before the solution of the system in matrix form becomes:

$$\begin{vmatrix} \mathbf{K}_{\mathrm{E}} + \mathbf{K}_{\mathrm{G}} - \mathbf{K}_{\mathrm{L}}^{0} + \dfrac{\mathbf{K}_{\mathrm{L}}^{\mathrm{t}}}{2} - \dfrac{\mathbf{M}\theta^2}{4} - \Psi\Lambda^2 & -\dfrac{1}{2}\mathbf{C}\theta\left(1+\Lambda^2\right) \\ \dfrac{1}{2}\mathbf{C}\theta\left(1+\Lambda^2\right) & \mathbf{K}_{\mathrm{E}} + \mathbf{K}_{\mathrm{G}} - \mathbf{K}_{\mathrm{L}}^{0} - \dfrac{\mathbf{K}_{\mathrm{L}}^{\mathrm{t}}}{2} - \dfrac{\mathbf{M}\theta^2}{4} - \Psi\Lambda^2 \end{vmatrix} = 0 \quad (4.18)$$

The nonlinear function Ψ, including the nonlinear damping, inertia, and elasticity were defined by Bolotin, (1964) as:

$$\Psi\left(\mathbf{U}, \dot{\mathbf{U}}, \ddot{\mathbf{U}}\right) = \Theta\mathbf{U}^3 + \xi_{NL}\mathbf{U}^2\dot{\mathbf{U}} + \Upsilon U\left[\mathbf{U}\ddot{\mathbf{U}} + \left(\dot{\mathbf{U}}\right)^2\right] \quad (4.19)$$

where Θ is related to the nonlinear elasticity, ξ_{NL} is related to nonlinear damping, and Υ is related to nonlinear inertia. More discussion about these nonlinear parameters can be found in the literature. For instant result, the term

of the nonlinear elasticity is considered as described by Liberscu et al. (1990), and the lateral amplitude of the vibrating a cross ply laminated composite simply supported shear deformable beam with same material and geometry properties as defined for the beam in section 4.8 is solved and depicted in Fig. 4.9.

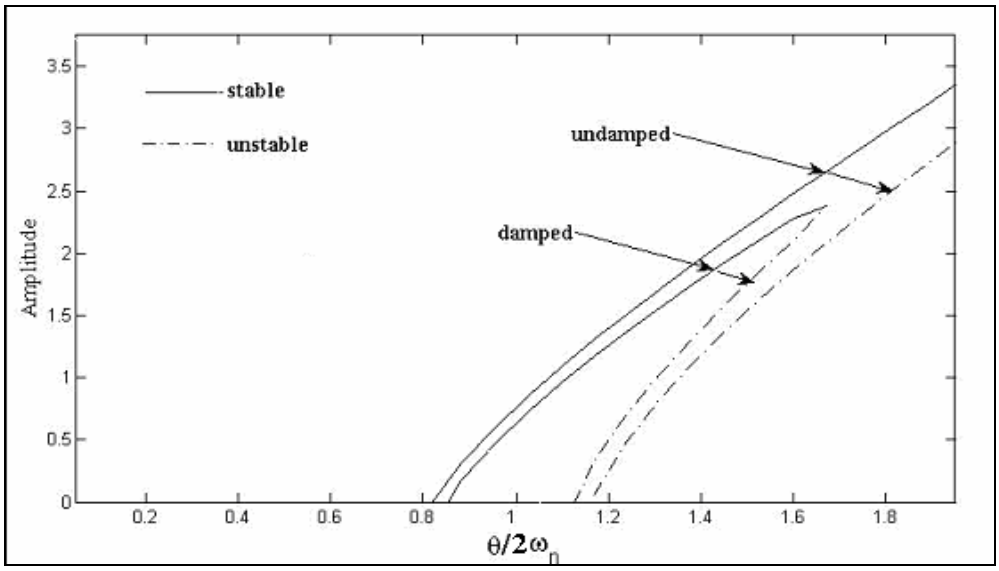

Figure 4. 9 The steady state resonance frequency-amplitude curve for a cross ply laminated composite beam.

As it can be seen from Fig.4.7, in case of nonlinear elasticity, the resonance curves are bent toward the increasing exciting frequencies. The damping factor has important role in diminishing of the amplitude of the vibrating beam, in contrast the increasing of the nonlinear elasticity of the system does not always reduce the resonance amplitudes.

4.10 Response of the laminated composite beams

The last section of this chapter proceeds to dynamic response of the beams subjected to varying time loading. The response of the structure will be investigated in stable and unstable zones and the result will be determined and plotted. The periodic solution of the Mathieu type equations of motion of the beam are established using the Floquet's theory. Recall the Equation of motion of undamped beam and rearrange in the form as:

$$\ddot{\mathbf{U}} + \left\{ \mathbf{M}^{-1} \left(\left(\mathbf{K}_{\mathrm{E}} + \mathbf{K}_{\mathrm{G}} \right) - \mathbf{K}_{\mathrm{L}}^{0} \right) - \mathbf{M}^{-1} \mathbf{K}_{\mathrm{L}}^{\mathrm{t}} \cos \theta t \right\} \mathbf{U} = 0 \qquad (4.20)$$

To simplify the above equation two parameters are defined in matrix form as:

$$\mathbf{R} = \mathbf{M}^{-1} \left(\left(\mathbf{K}_{\mathrm{E}} + \mathbf{K}_{\mathrm{G}} \right) - \mathbf{K}_{\mathrm{L}}^{0} \right), \quad \mathbf{Z} = \mathbf{M}^{-1} \mathbf{K}_{\mathrm{L}}^{\mathrm{t}}$$

and the Eq. (4.18) becomes:

$$\ddot{\mathbf{U}} + \left\{ \mathbf{R} - \mathbf{Z} \cos \theta t \right\} \mathbf{U} = 0 \qquad (4.21)$$

The Floquet solutions of the above Mathieu type equation can be expressed in Fourier series as:

$$\mathbf{U}_{(\mathrm{t})} = e^{i\lambda t} \sum_{n=-\infty}^{\infty} b_n e^{in\theta t} \qquad (4.22)$$

Substitute Eq. (4.22) into Eq. (4.21) and regrouping, the below equation is obtained:

$$\sum_{n=-\infty}^{\infty} \left\{ \frac{1}{2} b_{n-1} \left| \mathbf{Z} \right| + b_n \left[-\left(\lambda + n\theta \right)^2 + \left| \mathbf{R} \right| \right] + \frac{1}{2} b_{n+1} \left| \mathbf{Z} \right| \right\} e^{i(\lambda + n\theta)t} = 0 \qquad (4.23)$$

The above equation must be true for all times, therefore the term inside braces must be zero as well and leading to the recurrence relation:

$$\frac{1}{2}b_{n-1}\left|\mathbf{Z}\right|+b_n\left[-\left(\lambda+n\theta\right)^2+\left|\mathbf{R}\right|\right]+\frac{1}{2}b_{n+1}\left|\mathbf{Z}\right|=0 \tag{4.24}$$

This is a homogeneous set of equations, and to get a nontrivial solution the determinant is set to zero. This then specifies the characteristic value λ for a given set of material and geometry properties of the beam, $\mathbf{R}$ and $\mathbf{Z}$. With λ so determined, then b_n in terms of b_0 can be determined. Finally b_0 can be determined from the initial conditions $\mathbf{U}_0$.

The first three term approximation is used for investigating the motion of the beam subjected to varying time load with loading frequency θ. Approximate solution of the system with just the three terms, which leads to the set of equations:

$$\begin{bmatrix} -(\lambda-\theta)^2+\left|\mathbf{R}\right| & \frac{1}{2}\left|\mathbf{Z}\right| & 0 \\ \frac{1}{2}\left|\mathbf{Z}\right| & -\lambda^2+\left|\mathbf{R}\right| & \frac{1}{2}\left|\mathbf{Z}\right| \\ 0 & \frac{1}{2}\left|\mathbf{Z}\right| & -(\lambda+\theta)^2+\left|\mathbf{R}\right| \end{bmatrix}\begin{Bmatrix} b_{-1} \\ b_0 \\ b_1 \end{Bmatrix}=0 \tag{4.25}$$

For real value of λ the above determinant is solved for b_{-1} and b_1 in terms of b_0 as:

$$b_{-1}=\frac{-\frac{1}{2}\left|\mathbf{Z}\right|b_0}{\left[-\left(\lambda-\theta\right)^2+\left|\mathbf{R}\right|\right]}, \qquad b_1=\frac{-\frac{1}{2}\left|\mathbf{Z}\right|b_0}{\left[-\left(\lambda+\theta\right)^2+\left|\mathbf{R}\right|\right]}$$

Imposing the initial condition that $\mathbf{U}\left(t=0\right)=\mathbf{U}_0$ gives:

$$b_0 = \mathbf{U}_0 \Big/ \left[\frac{-\frac{1}{2}|\mathbf{Z}|}{\left[-(\lambda-\theta)^2 + |\mathbf{R}|\right]} + 1 + \frac{-\frac{1}{2}|\mathbf{Z}|}{\left[-(\lambda+\theta)^2 + |\mathbf{R}|\right]} \right] \tag{4.26}$$

and final solution will be:

$$\mathbf{U}_{(t)} = b_0 \left\{ \frac{-\frac{1}{2}|\mathbf{Z}|}{\left[-(\lambda-\theta)^2 + |\mathbf{R}|\right]} e^{i(\lambda-\theta)t} + e^{i\lambda t} + \frac{-\frac{1}{2}|\mathbf{Z}|}{\left[-(\lambda+\theta)^2 + |\mathbf{R}|\right]} e^{i(\lambda+\theta)t} \right\} \tag{4.27}$$

Now let examine the presented formulation to find the response of the nonconservative cross ply $\left(0^\circ/90^\circ/90^\circ/0^\circ\right)$ laminated composite beam in the regions of dynamic instability and stability found in section 4.7. The material and geometry properties are same as the case in section 4.7. Three points from Fig.4.4 are chosen to investigate the response of the middle of a simply supported beam:

1- Stable state: the response of the system for the first point in stable region with nondimensional parameters $\theta/2\omega_n = 1.75,\quad P_t/P_{cr} = 0.8$ is calculated and plotted in Fig. 4.10. Also the periodic loading is depicted to compare the frequency of the system to loading frequency. As it can be seen the response of the beam is pure periodic and follows the loading frequency history.

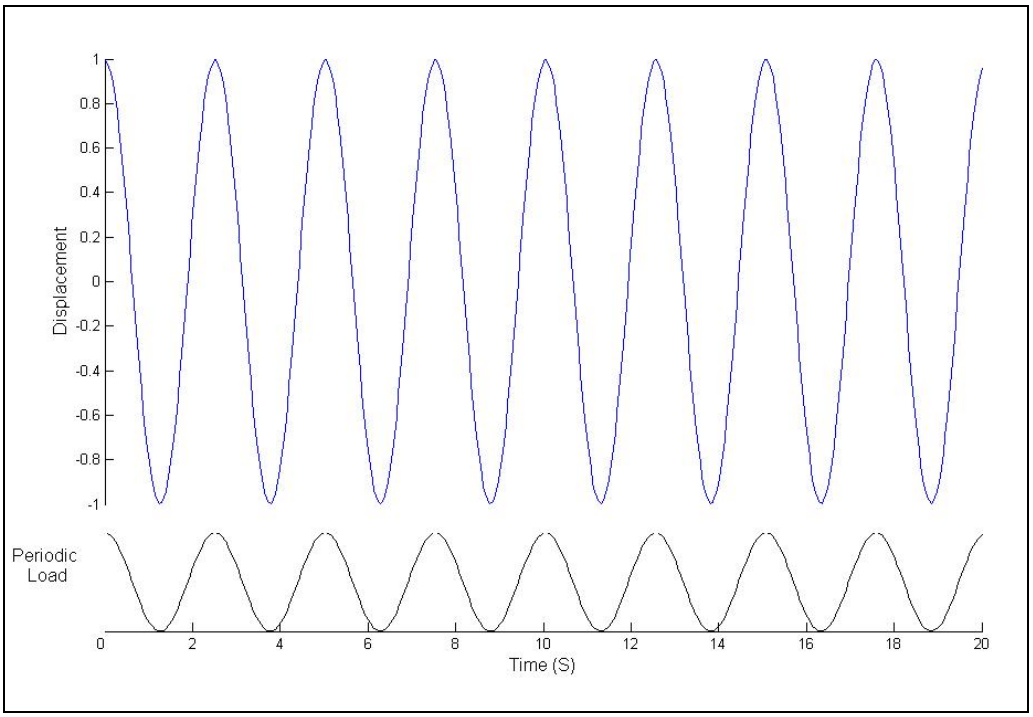

Figure 4. 10 Nondimensional displacement response of a cross ply simply supported laminated composite beam subjected to a periodic loading in stable region.

2- Asymptotically stable or dynamically critical: the response of the system for the second point is on the curve of instability region with nondimensional parameters $\theta/2\omega_n = 0.75,\quad P_t/P_{cr} = 0.8$ is calculated and plotted in Fig. 4.11. Also the periodic loading is depicted to compare the frequency of the system to loading frequency. As it can be seen the response of the beam is aperiodic and does not follow the loading frequency history.

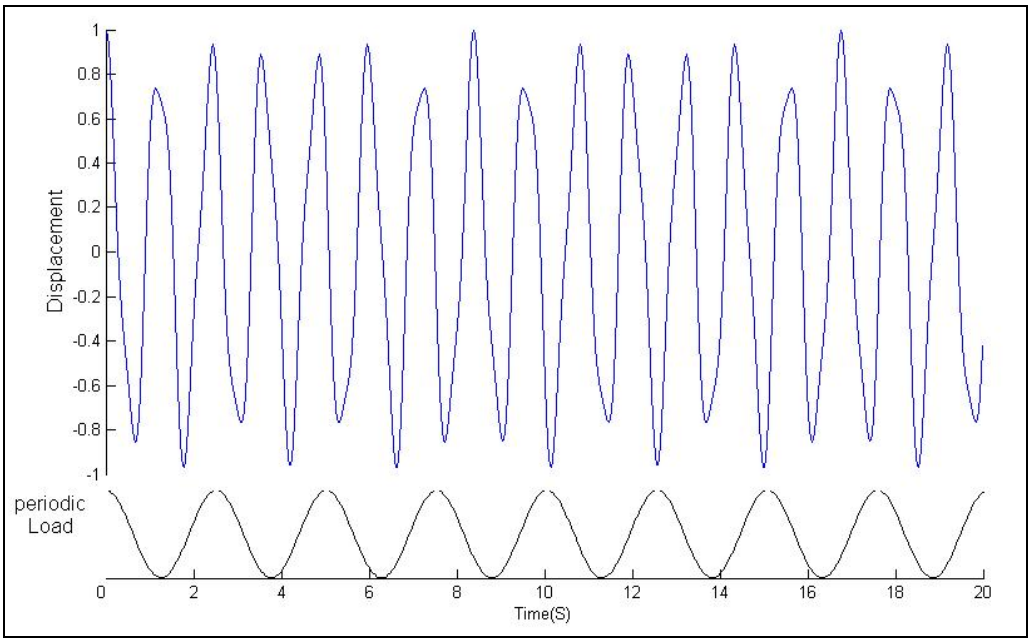

Figure 4. 11 Non dimensional displacement response of a cross ply simply supported laminated composite beam subjected to a periodic loading on dynamically critical curve.

3- Unstable state: the response of the system for the third point in instable region with nondimensional parameters $\theta/2\omega_n = 1,\quad P_t/P_{cr} = 0.8$ is calculated and plotted in Fig. 4.12. Also the periodic loading is depicted to compare the frequency of the system to loading frequency. The values of the characteristic λ are complex in this region and leading to unstable solution. As it can be seen the displacement shows an increasing due to the compressive periodic load, which is %80 of the lowest critical load. Another fact that it is obvious from the response curve, the beam frequency is higher than the loading frequency. It is clear that load parameters carrying the structure in unstable state is unreliable and hazardous and causes the structure failure. For this reason

structure designer try to eliminate the instability of the structure with load control and damping behaviour of the structure.

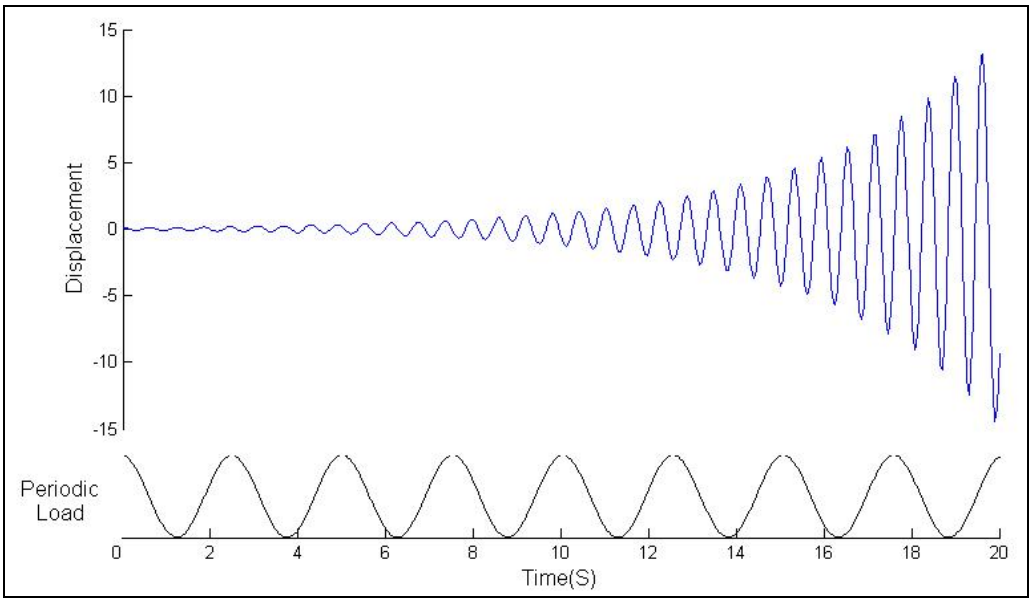

Figure 4. 12 Non dimensional displacement response of a cross ply simply supported laminated composite beam subjected to a periodic loading in unstable region.

Response of the forced system in unstable region depends on the excitation parameters and signature varies due to these parameters values. For example the amplitudes of the beam corresponded to substantial excitation loading parameters $P/P_{cr} > 1$ increase in a typical nonlinear manner accompanied by beats as shown in Fig. 4.13.

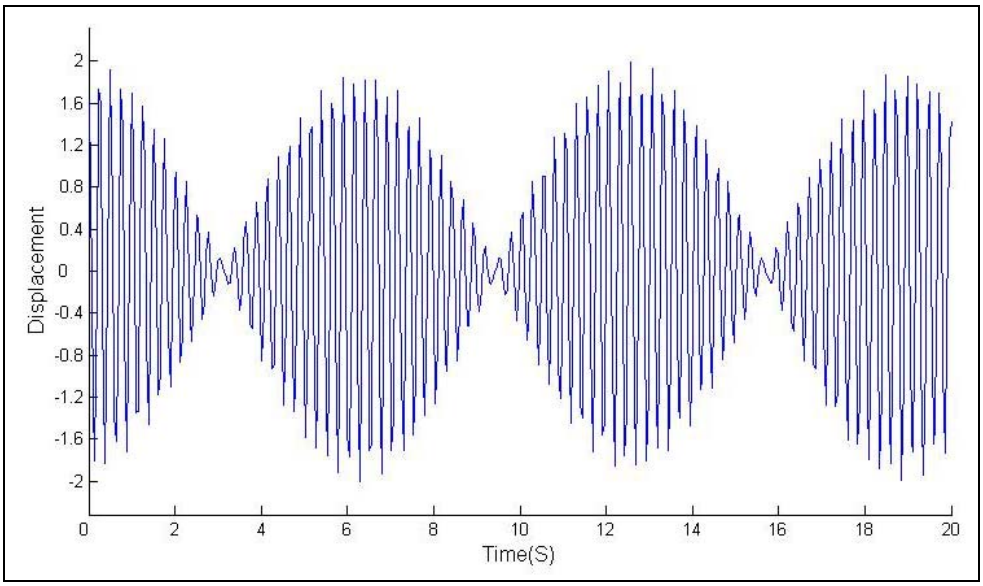

Figure 4. 13 Beat phenomena non dimensional displacement response of a cross ply simply supported laminated composite beam subjected to a periodic loading in unstable region with substantial loading parameters.

Then the equation of motion of the beam, Eq.4.23, becomes:

$$\ddot{\mathbf{U}} + \mathbf{C}\dot{\mathbf{U}} + \left\{\mathbf{R} - \mathbf{Z}\cos\theta t\right\}\mathbf{U} = 0 \tag{4.28}$$

where **C** is damping coefficients matrix. Thus approximate solution of the system with just the three terms, which leads to the set of equations:

$$\begin{bmatrix} -(\lambda-\theta)^2-(\lambda-\theta)+|\mathbf{R}|+|\mathbf{C}| & \frac{1}{2}|\mathbf{Z}| & 0 \\ \frac{1}{2}|\mathbf{Z}| & -\lambda^2-\lambda+|\mathbf{R}|+|\mathbf{C}| & \frac{1}{2}|\mathbf{Z}| \\ 0 & \frac{1}{2}|\mathbf{Z}| & -(\lambda+\theta)^2-(\lambda+\theta)+|\mathbf{R}|+|\mathbf{C}| \end{bmatrix} \begin{Bmatrix} b_{-1} \\ b_0 \\ b_1 \end{Bmatrix} = 0 \tag{4.29}$$

The response of the beam for small amount of damping and large excitation changes as shown in Fig. 4.14a and for large and very large amount of damping amplitude of the vibration will be back to zero quicker as shown in Fig.4.14b and c.

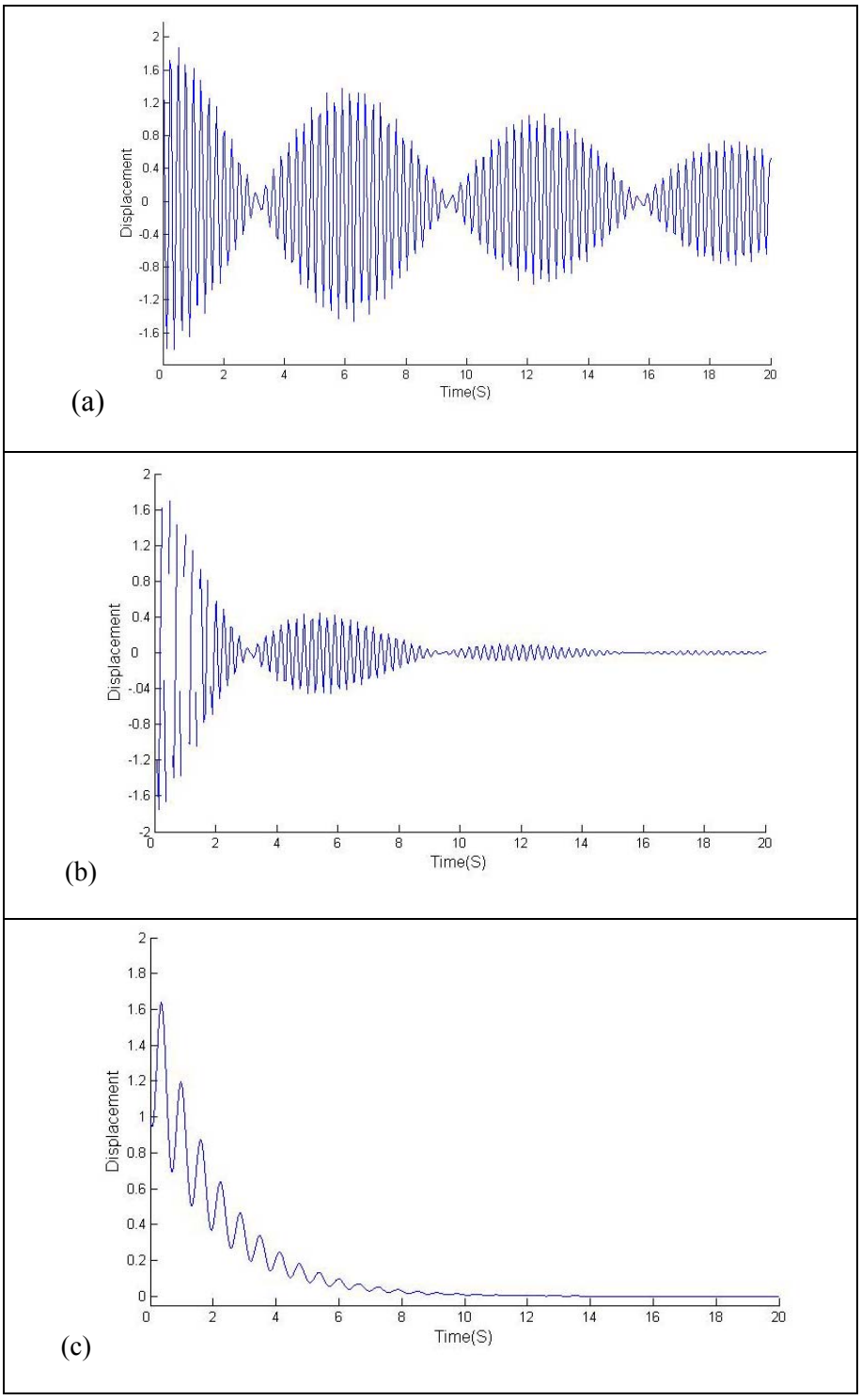

Figure 4. 14 Non dimensional displacement response of a cross ply simply supported laminated composite beam subjected to a periodic loading in unstable region with (a)small damping (b) large damping, and (c) very large damping ratio.

This fact can be determined that using appropriate damping in structures subjected to periodic loading can reduce the violation and unpredictable motion of the system in instability state.

4.11 Summary

In this chapter, dynamic stability analysis of isotropic and laminated composite beams under varying time loading was performed. The principal instability regions of the beam under conservative and nonconservative loading with and without damping taken into account have been determined and plotted. Subsequently the characteristic curves of cross ply laminated composite beam were calculated and plotted and the formulation verified and compared with the analytical and numerical analysis available in literature. Then, the response of the system with and without damping have been formulated and plotted. The results show the important roles of the damping in eliminating or reducing the dynamic instability regions and behaviour of the structure. The numerical and analytical results obtained in this chapter, are valued for deterministic system with the assumption that the structure is without imperfection. In the presence of imperfection and uncertainties, a new approach based on probability will be discussed in the next chapter.

CHAPTER 5

Reliability Analysis of Laminated Composite Laminated Beams with Random Imperfection parameters

Formulation and analysis in previous chapters were performed to study the deterministic stability and vibrational response of laminated beams without structural imperfections. However, in reality laminated composite structures have inbuilt uncertainties involved in the manufacturing process, and the end product may have significant variations in material and geometrical properties around the mean values.

The laminated composites are made of fibres and matrix, which are of two different materials. The way in which the fibres and matrix materials are assembled to make a lamina, as well as the lay-up and curing of laminae are complicated processes and may involve a lot of uncertainty. Such uncertainties can be in ply angles and/or the modulus of elasticity that lead to imperfections in the structure. Therefore, the material and geometry properties of a composite laminate are random in nature. In this case, the deterministic analysis may be no longer valid and it is intended to expand the deterministic formulation to account for uncertainties and perform a more accurate analysis.

In the previous chapters the stability analysis of laminated beams was formulated on basis of a finite element formulation, which didn't provide any information on how the uncertain parameters influence the overall dynamic

behaviour of the structure. A probabilistic formulation to take uncertainties in account is extended in this Chapter.

Because probabilistic models can capture the influence of the uncertainties, the chapter begins with a description of the probability approach through an imperfection modeling then the random variables and their characteristics are described. The rest of the chapter is dedicated to explain the probabilistic finite element analysis, and the Monte Carlo Simulation.

In a problem involving uncertainty, statistical analysis on the random variables shall be conducted first. This can be obtained experimentally or using sampling techniques. Then using this information the influence of the randomness of the random variables on the wanted response is intended to be calculated.

5.1 Imperfection Modeling

Questions about the modeling of imperfections arise when a structure is designed for the first time and no information is available about the initial imperfections. Usually, a maximum allowable limit on the imperfection at any point on the structure is specified by a design code or dictated by the manufacturing process used to build the structure itself, or the various members in the structure. The objective is to model the imperfections in a realistic manner, by treating the imperfections as random fields, so that a resulting distribution of the imperfect structure may be calculated.

The first step in applying imperfections to a discretized structural model is to define which joints or nodes will be allowed to have imperfections. The next step is to create a matrix of eigenvectors that only contains the components corresponding to the imperfect degrees of freedom. For the uncertain analysis of laminated beams the probabilistic finite element model shall be developed. The analysis uses the sensitivity derivatives and gives the mean and standard deviation directly.

Uncertainties in laminated composites exist because of material defects such as interlaminar voids, delamination, incorrect orientation, damaged fibers, and variation in thickness. If the uncertainty is due to imprecise information and/or statistical data cannot be obtained, then the non-probabilistic approaches such as fuzzy sets can be used. These approaches have been studied by Elishakoff et al. (2001). On the other hand, the uncertain parameters are treated as random variables with known (or assumed) probability distributions, then the theory of probability or random processes can be used, which is scope of this study.

Probabilistic models can capture the influence of noncognitive sources of uncertainty because they are based on probability principles rather than on experience. These principles are mainly based on the following three axioms ,Papoulis (1991): (i) the probability of any single event occurring is greater or equal to zero: (ii) the probability of the universal set is one: (iii) the probability of the union of mutually exclusive events is equal to the sum of the probabilities.

Several probabilistic methods have been used to analyze an uncertain unsymmetrically laminated beam by integrating uncertain aspects into the finite element modelling such as the perturbation technique using Taylor Series expansion and simulation methods (e.g., the Monte Carlo Simulation). Vinckenroy et al. (1995) presented a new technique to analyze these structures by combining the stochastic analysis and the finite element method in structural design. However they did not extend their work to dynamic problems. Stochastic methods were also studied by Haldar and Mahadevan (2000). They applied the concepts to reliability analysis using the finite element method.

The probabilistic of the structural behaviour by including uncertainties into the problem through the probabilistic finite element method (PFEM), exact Monte Carlo simulation (EMCS), and sensitivity-based Monte Carlo simulation (SBMCS) has been studied by Goyal (2002). He studied the axial modulus of elasticity and ply angle uncertainties on free vibration and eigenfrequencies of the beam using the Gaussian distribution.

To the best of the author's knowledge, there has been no reported study on the dynamic instability problem of the shear deformable laminated composite beams in the presence of uncertainties by taking dynamic stiffness force effects into account. In this research, both material properties and geometric parameters are treated as random variables in a stochastic finite element analysis for predicting the dynamic instability region of the beam subjected to the dynamic axial varying time load. Also, the effects of various

parameters on the region of instability (i.e. mean, standard deviation and coefficient of variation) of beams are investigated.

The both stochastic finite element and the Monte Carlo method are used to predict the reliability of laminated composite plates. The present finite element analysis of laminated composite beams with random parameters is formulated on the basis of the first order shear deformation theory.

5.2 System Random Variables

A composite laminate is a stack of layers of fiber-reinforced laminae. The fiber-reinforced laminae are made of fibers and matrix, which are of two different materials. The way in which the fibers and matrix materials are assembled to make a lamina, as well as the layup and curing of laminae are complicated processes and may involve a lot of uncertainty. Therefore, the material and geometry properties of a composite laminate can be considered as random in nature.

In the following presented probabilistic finite element analysis (PFEA), the elastic moduli of the material and the beam length are treated as independent random variables, and their statistics are used to predict the mechanical behaviour of the composite laminate. In the previous studies, it has been shown that the small variations of fiber orientations have insignificant effects on the variation of the laminate strength. Hence, without loss of generality, fiber orientations are treated as constants while laminate thickness l is considered to

be random. The uncertainty of each lamina can be expressed in the following form:

$$\chi = \frac{\overline{\chi}}{N}(1+\varsigma) \tag{5.1}$$

where χ represents the random parameter of the beam, $\overline{\chi}$ is the mean value of the property χ and ς represents the fluctuations around the mean value, and N number of layers.

There are a number of commonly used theoretical distribution functions, which have been derived for ideal conditions. In most cases characteristics of composites can be well described by the use of the Weibull distribution. The Weibull distribution is one which appears in an incredible variety of statistical applications. A good reason for this is the central limit theorem. This theorem tells us that sums of random variables will, under the appropriate conditions, tend to be approximately normally distributed. Even when the right conditions are not met however, the distributions found for many experimentally generated sets of data still tend to have a bell shaped curve that often looks quite like that of a normal. In this case, the entire distribution can be described by simply a mean and a variance. The Weibull distribution has become a convenient standard to use. Thus the present analysis will assume that all random variables obey the distribution:

$$f(\chi) = \frac{\alpha}{\beta}\left(\frac{\chi}{\beta}\right)^{(\alpha-1)} \exp\left[-\left(\frac{\chi}{\beta}\right)^{\alpha}\right] \tag{5.2}$$

where α and β are the shape and scale parameters, respectively.

The shape parameter provides indications of scatter and is related to the relative variance of the distribution. The shape parameter can be correlated to the coefficient of variation (COV). Random numbers with a uniform distribution were first generated using a random number generator. MATLAB® has the capability to generate uniformly distributed random numbers χ between 0 and 1.

5.3 Stochastic Finite Element Analysis

Finite element analysis is a commonly used tool within many areas of engineering and can provide useful information in structural analysis of mechanical systems. However, most analyses within the field of composite laminated usually take no account either of the wide variation in material properties and geometry that may occur in manufacturing imperfections in composite materials. This study discusses the method of incorporating uncertainty in finite element models. In this method, probabilistic analysis enables the distribution of a response variable to be determined from the distributions of the input variables.

In dealing with composite laminae manufacturing, no material properties are known exactly and no component can be fabricated to an infinitesimal tolerance and a problem lies in the loss of uncertainty in FE modelling. It is becoming recognized that these uncertainties can result in significant changes to

the dynamic stability regions of the system because of changes in stiffness matrices calculation associated with the degree of uncertainty in the results.

The probabilistic finite element analysis is a method that allows uncertainty and natural variation to be incorporated into a deterministic finite element model. The underlying principle of the method is that the input parameters of the model are defined by a statistical distribution. This distribution can take any form that can be defined mathematically. A common method is the Weibull distribution that can be uniquely defined by a mean and standard deviation.

The values of each input parameter are then sampled randomly from the appropriate distribution and used in the model. The model is solved many times to build up a distribution of the output of interest. One advantage of obtaining a distribution over the single value obtained from a deterministic model is that confidence limits, giving an indication of the spread of the response can be found. Another advantage is that it is possible to find the most likely response of the system which, if the output is not normally distributed, will not necessarily be the same as the mean value, Marczyk (1999).

The present stochastic finite element analysis of laminated composite plates consisting of random parameters is based on the mean-centered first-order perturbation technique. The present model can be applied to the analysis of slender beam. Based on the mean-centered second-order perturbation technique, the stiffness matrix **K**; is expanded in terms of the random

variables χ , which represent structural uncertainty existing in the beam, as follows:

$$K = K^{(0)} + \sum_{i=1}^{n} K_i^{(1)} \delta\chi_i + \frac{1}{2} \sum_{i=1}^{n} \sum_{j=1}^{n} K_{ij}^{(2)} \delta\chi_i \delta\chi_j \tag{5.3}$$

where $\delta\chi_i = \chi_i - \bar{\chi}_i$ with $\bar{\chi}_i$ denoting the mean value of the random variable χ_i , $K^{(0)}$ is the zeroth-order of structural stiffness matrix, which is identical to the deterministic structural stiffness matrix, $K_i^{(1)} = \frac{\partial K}{\partial \chi_i}$ the first-order structural stiffness matrix with respect to random variables χ_i , and $K_{ij}^{(2)} = \frac{\partial^2 YK}{\partial \chi_i \partial \chi_j}$ the second-order of structural stiffness matrix with respect to random variables with respect to random variables χ_i and χ_j . The nodal displacements, mass matrix, and loading matrix are also influenced by the structural uncertainty and thus the displacement vector, and mass matrix posses the similar expression:

$$D = D^{(0)} + \sum_{i=1}^{n} D_i^{(1)} \delta\chi_i + \frac{1}{2} \sum_{i=1}^{n} \sum_{j=1}^{n} D_{ij}^{(2)} \delta\chi_i \delta\chi_j \tag{5.4}$$

$$M = M^{(0)} + \sum_{i=1}^{n} M_i^{(1)} \delta\chi_i + \frac{1}{2} \sum_{i=1}^{n} \sum_{j=1}^{n} M_{ij}^{(2)} \delta\chi_i \delta\chi_j \tag{5.5}$$

In the present reliability study of a laminated composite beam, it is assumed that the beam is composed of identical laminae with the same material properties and is subjected to an axial load.

Substituting Eqs.(5.3), (5.4), and (5.5) into the differential equation of motion of the beam about equilibrium position , truncating the third- and fourth-

order terms, and equating equal order terms, the zeroth, first, and second-order equations are obtained, respectively.

5.4 Monte Carlo Method for Probability Analysis

Conventional Monte Carlo simulation (MCS) is the most common and traditional method for a probabilistic analysis. Extensive reviews of the method have been done by Haldar and Mahadevan (2000). In brief, the method uses randomly generated samples of the input variables for each deterministic analysis, and estimates response statistics after numerous repetitions of the deterministic analysis. The main advantages of the method are: (1) only a basic working knowledge of probability and statistics is needed, and (2) it always provides correct results when a very large number of simulation cycles are performed. However, the method has disadvantage: it needs an enormously large amount of computation time.

The MCS technique is based on the use of random variables and probability statistics to investigate problems. This technique combining with the finite element method is preferable to first and second order reliability methods since non-linear complex behaviour does not complicate the basic procedure. The main advantages of the method are: 1- engineers with only a basic working knowledge of probability and statistics can use it , and 2- It always provides correct results when a very large number of simulation cycles are performed (one simulation cycle represents a deterministic analysis). However, the method

has one drawback: it needs an enormously large amount of computation time and is extremely time consuming and expensive in obtaining acceptable results especially for problems having many random variables

The larger the number of simulations conducts the higher the confidence in the probability distribution of the obtained results. Therefore, for the present analysis, at least ten thousand realizations of the uncertain beam are performed, increasing the accuracy of the material and geometric properties of distribution fit to the sample data. The results are presented in frequency density diagrams or histograms, which show the distribution of the eigenfrequencies. Once the histograms are obtained, a density function is selected that best fits the response. This probabilistic density function can be used to perform the reliability analysis of uncertain structures.

Briefly, the objective is to study the influence uncertainty parameters in the dynamic behaviour of the beam. Both material properties and geometric parameters are treated as random variables. The effects of various parameters (i.e. mean standard deviation and coefficient of variation) of beams are investigated using the Monte Carlo method. For the sake of brevity, only the results corresponding to the mean values $\overline{\chi}_i$, standard deviations σ , and coefficients of variation (COV) and the data obtained from the finite element analyses are compared using the Weibull distribution function for two cases: Case-1, the material property (E) are treated as random, Case-2, the geometric property (l) are treated as random.

CASE-1 : $E = 4 = E_{xx} / E_{yy}$, σ=0.1, COV=0.05

CASE-2 : $l = 1$ m , σ=0.1, COV=0.05

The probability density functions are depicted for case-1 and case-2 as shown in Fig. 5.1 and 5.2.

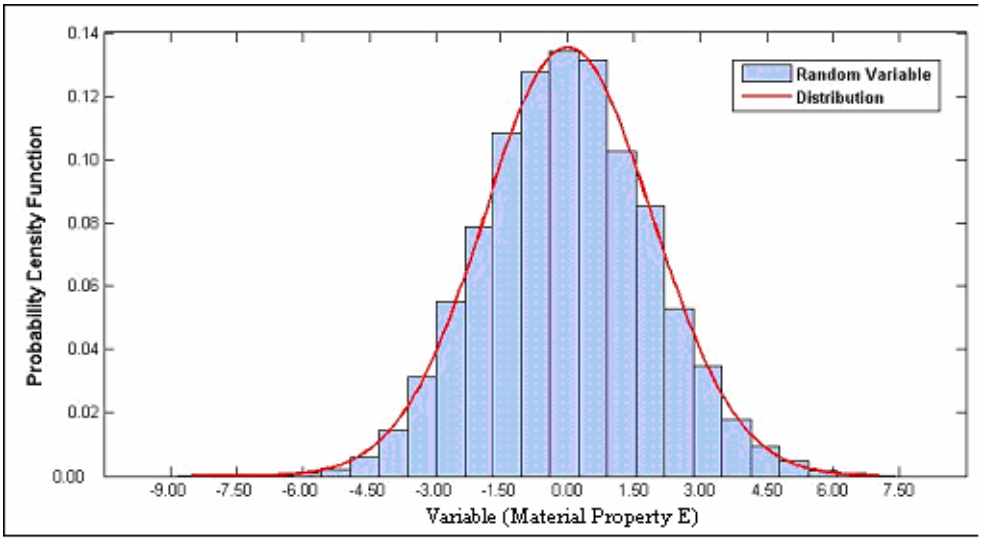

Figure 5. 1 Probability density functions for the beam with material property variable.

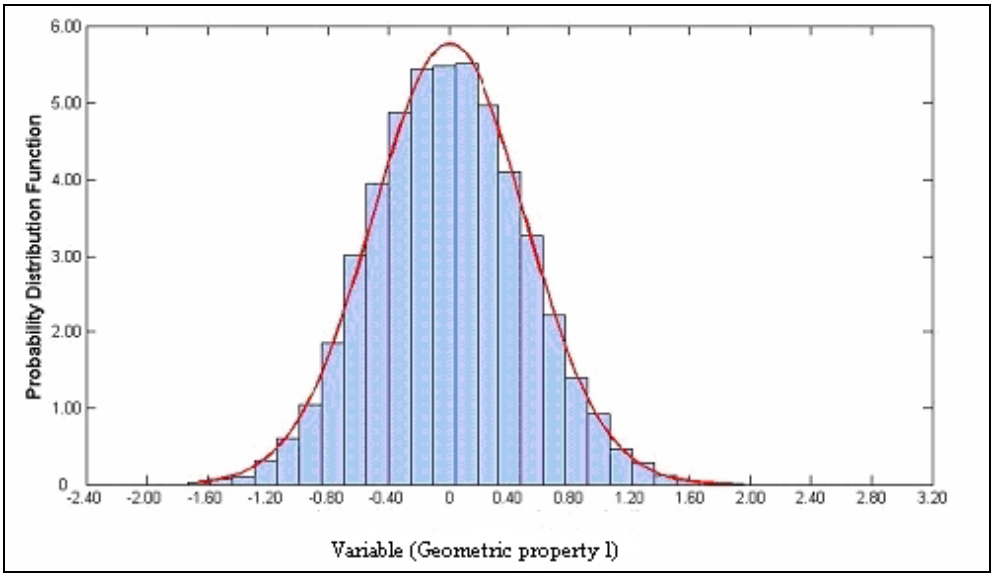

Figure 5. 2 Probability density functions for the beam with geometry property variable.

5.5 Reliability Analysis of Laminated Beams

Now the probabilistic finite element analysis of the laminated beam with ten elements is computed and compare to the result of Monte Carlo Simulation. The beam with two sets of boundary conditions is considered same as those mentioned in Chapter 3, clamped-free (cantilever) and pinned-pinned (simply-supported).

5.5.1 Uncertain material property

The cases when the material property E may become uncertain are considered here. For this case the two laminated composite beams with a layout of $\left(0^\circ, 30^\circ, 30^\circ, 0^\circ\right)$ and $\left(0^\circ, 90^\circ, 90^\circ, 0^\circ\right)$ are considered.

In models, the Monte Carlo Simulation (MCS) and the probabilistic finite element analysis (PFEA), the mean values and the coefficient of variations were close, Figures 5.3 and 5.4. However, the PFEA is conservative in the sense of overestimate the variation of the natural frequencies. The MCS would have been the most accurate approach but also a very expensive one. However, in both cases it can be shown that the material property uncertainties can play an important role in affecting free vibrations of symmetrically and unsymmetrically laminated beams.

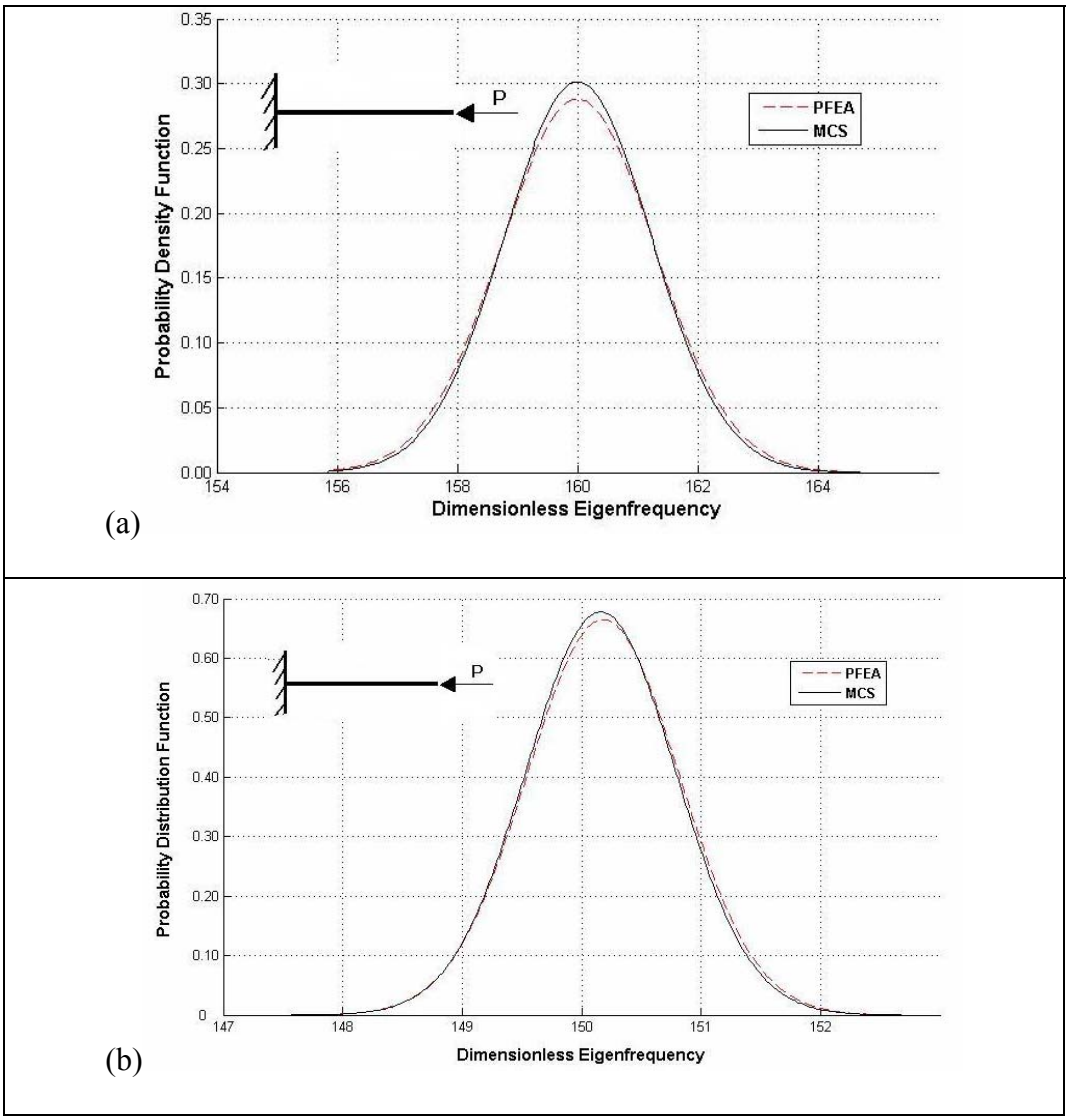

Figure 5. 3 Probability density function of the eigenfrequency for a cantilevered laminated beam (a)-$\left(0^{\circ},30^{\circ},30^{\circ},0^{\circ}\right)$, (b)-$\left(0^{\circ},90^{\circ},90^{\circ},0^{\circ}\right)$ with material uncertainty.

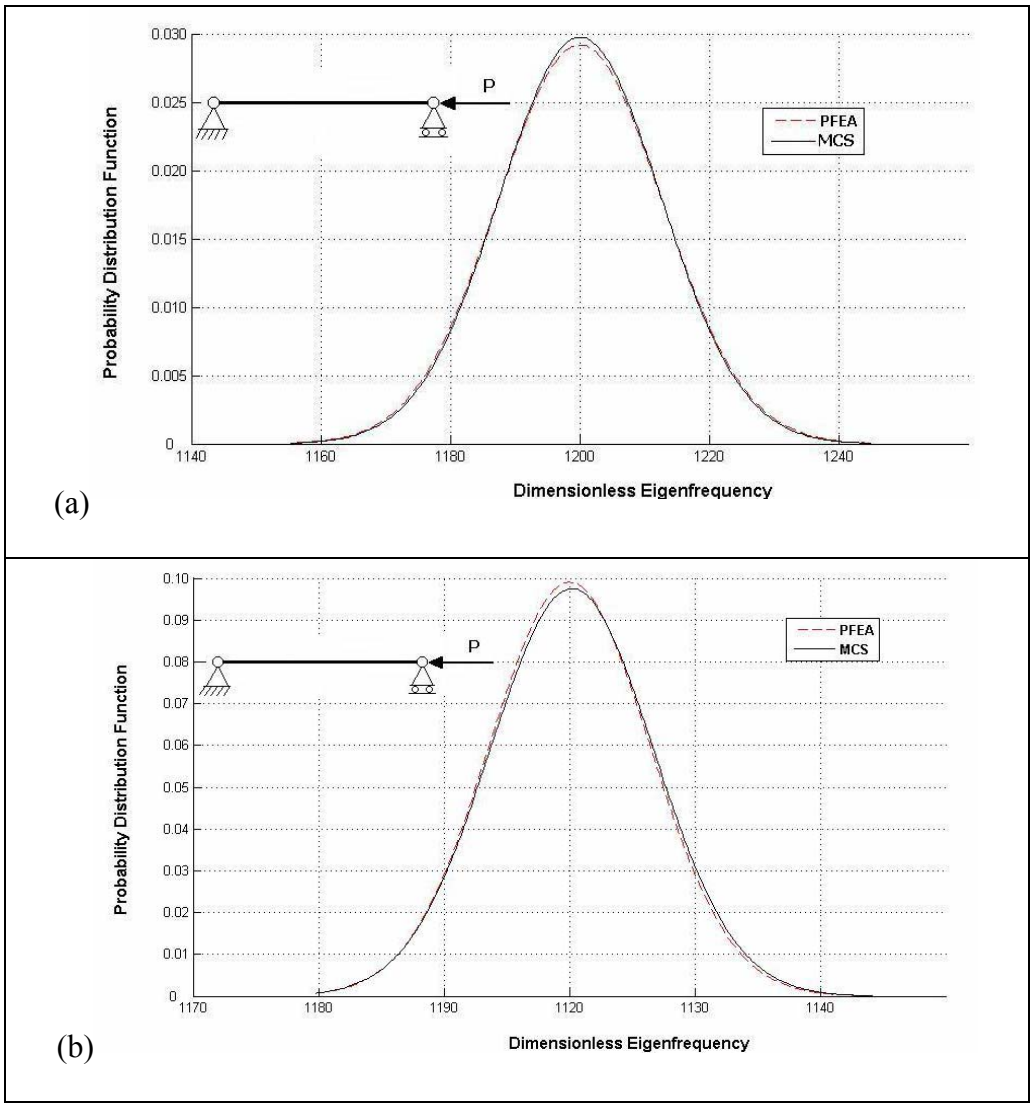

Figure 5. 4 Probability density function of the dimensionless eigenfrequency for a pinned-pinned laminated beam (a)-$\left(0^\circ,30^\circ,30^\circ,0^\circ\right)$, (b)- $\left(0^\circ,90^\circ,90^\circ,0^\circ\right)$with material uncertainty.

5.5.2 Uncertain geometric property

The probability distribution functions of the eigenfrequencies for laminated composite beams with geometric cross section uncertainty for two boundary conditions, Clamped–Free and Pinned-Pinned, and layup of$\left(0^\circ,30^\circ,30^\circ,0^\circ\right)$ and

$\left(0^\circ, 90^\circ, 90^\circ, 0^\circ\right)$ have been studied. The results are shown in Figures 5.5 and 5.6.

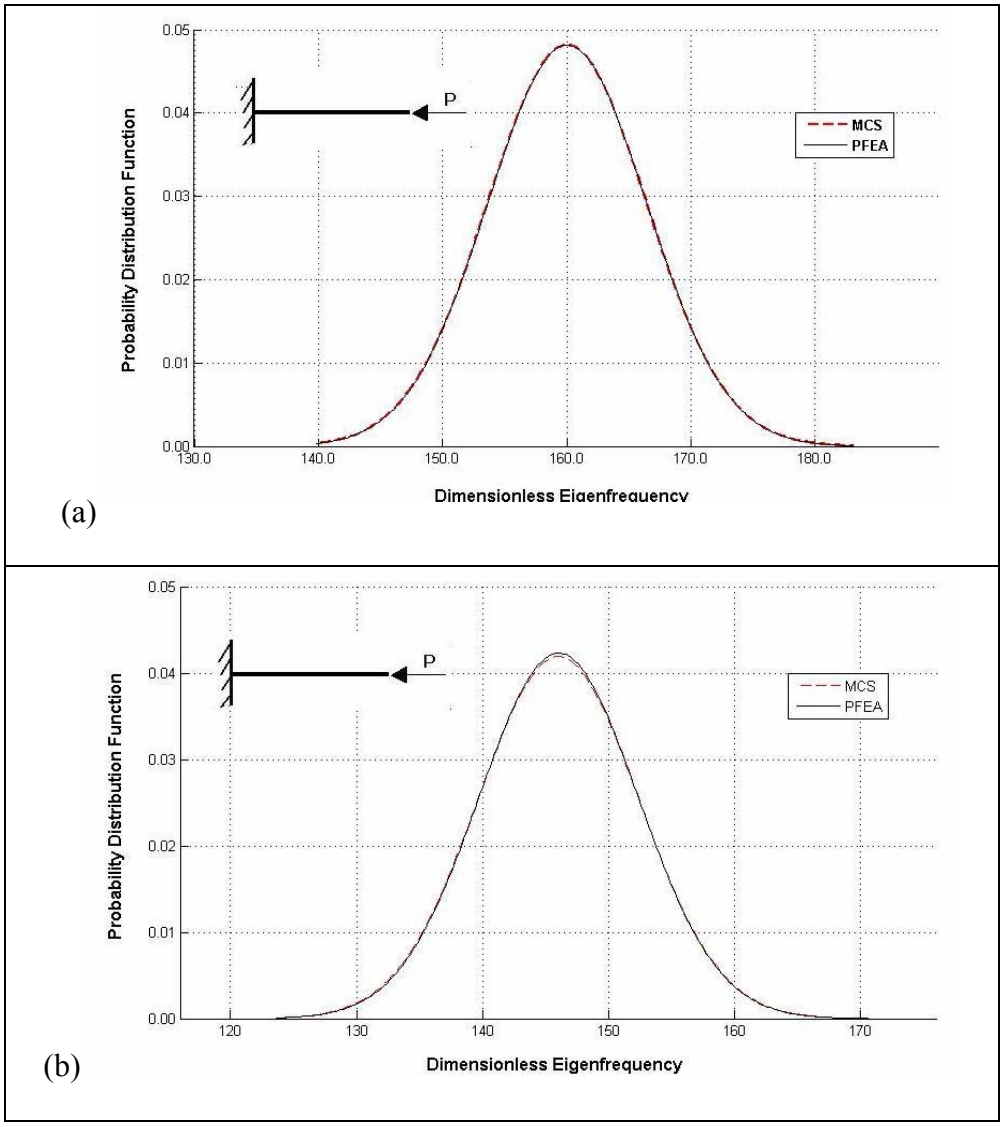

Figure 5. 5 Probability density function of the eigenfrequency for a cantilevered laminated beam (a)-$\left(0^\circ, 30^\circ, 30^\circ, 0^\circ\right)$, (b)- $\left(0^\circ, 90^\circ, 90^\circ, 0^\circ\right)$ with geometry uncertainty.

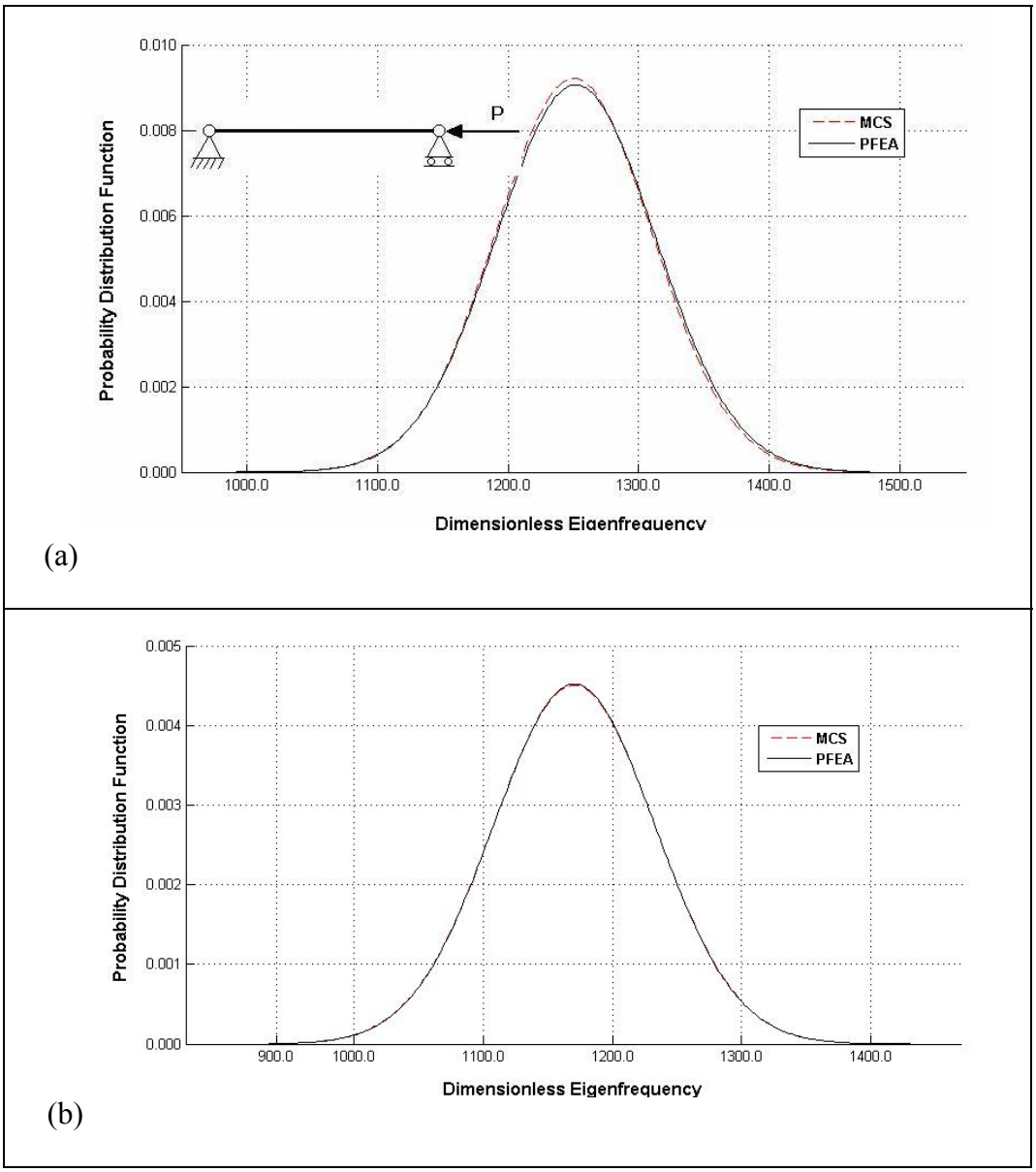

Figure 5. 6 Probability density function of the eigenfrequency for a simply-supported laminated beam (a)-$(0^\circ, 30^\circ, 30^\circ, 0^\circ)$, (b)- $(0^\circ, 90^\circ, 90^\circ, 0^\circ)$ with geometry uncertainty.

As it can be seen, the variation in the fundamental frequency of the laminated beam with geometry uncertainty is smaller for ply angle

layup $(0^\circ, 90^\circ, 90^\circ, 0^\circ)$ compare to layup $(0^\circ, 30^\circ, 30^\circ, 0^\circ)$. Once again the results show a very good agreement between both methods, PFEA and MCS.

5.6 Numerical Results

5.6.1 Cross ply uncertain composite laminated beams

The numerical applications presented here concern the prediction of the principal dynamic instability region of laminated composite beam associated with the geometric and material properties uncertainty. The boundary equations of instability regions, Eqs. (4.7 and 4.9) joint with the probabilistic stiffness and mass matrices involve an infinite number of calculations. However, approximate solutions can be obtained by truncating the series. The results generated from the MATLAB® software package are presented graphically. Applications are presented in the order of a simply supported (pinned-pinned) cross-ply laminated beams with the uncertain modulus of elasticity and beam length as per distribution function shown in Figures 5.1 and 5.2. The laminates are assumed to have equal thickness for each ply. The material properties of the plies are $E_{yy} = 10^6$ lb/in^2, $G_{xy}/E_{yy} = G_{xz}/E_{yy} = G_{yz}/E_{yy} = 0.5$, and $\nu_{xy} = 0.3$ with shear correction factor equal to $5/6$. The laminates have square cross section form with $b/h = 5$. The uncertain material property E of the beam and the geometric

property l of the laminates will be calculated for each application. For convenience the mass density is assumed to have a unit value of 1 lb/in^3.

The first application concerns a laminate beam with elastic modulus uncertainty of 0.05 standard deviation of mean value $4x10^6$ lb/in^2. The fundamental natural frequency of the unloaded laminate are calculated to be $\omega_n = 75$ rad/s. The dynamic instability of the laminate is considered initially when the nonconservative component of the load exists. The nondimensional loading parameter increases from 0 to 1 and the boundary resonance frequencies are determined. Numerical results in the graphical form are presented in Fig. 5.7 in the plane nondimensional frequency vs. nondimensional loading. It is noted that in this figure the boundary resonance frequencies are normalized against the fundamental frequency. Very close agreement is observed between the PFEA, MCS predictions and those of a deterministic solution. The dynamic instability regions are bounded by the two upper and lower curves. When load is very small the resonance frequency approaches of natural frequency for all three MSC, PFEA, and deterministic solutions. With the load increasing, the upper boundary of MCS increases faster than PFEA while the lower boundary of MCS decreases slower than PFEA. The distance between the two boundaries is termed the dynamic instability opening. It represents the range of parametric resonance frequency of the dynamic load at a particular load level.

The dynamic instability of the laminate when the conservative components of the load exist is studied next. The nondimensional loading component increases from 0 to 1.5. The predicted values of boundary resonance

frequencies are given in Fig. 5.7(a) in the plane nondimensional frequency vs. nondimensional loading. Again, the boundary resonance frequencies are normalised against the fundamental frequency. The dynamic instability regions in Fig. 5.7(b) starts at a point where the resonance frequency is equal to fundamental natural frequency.

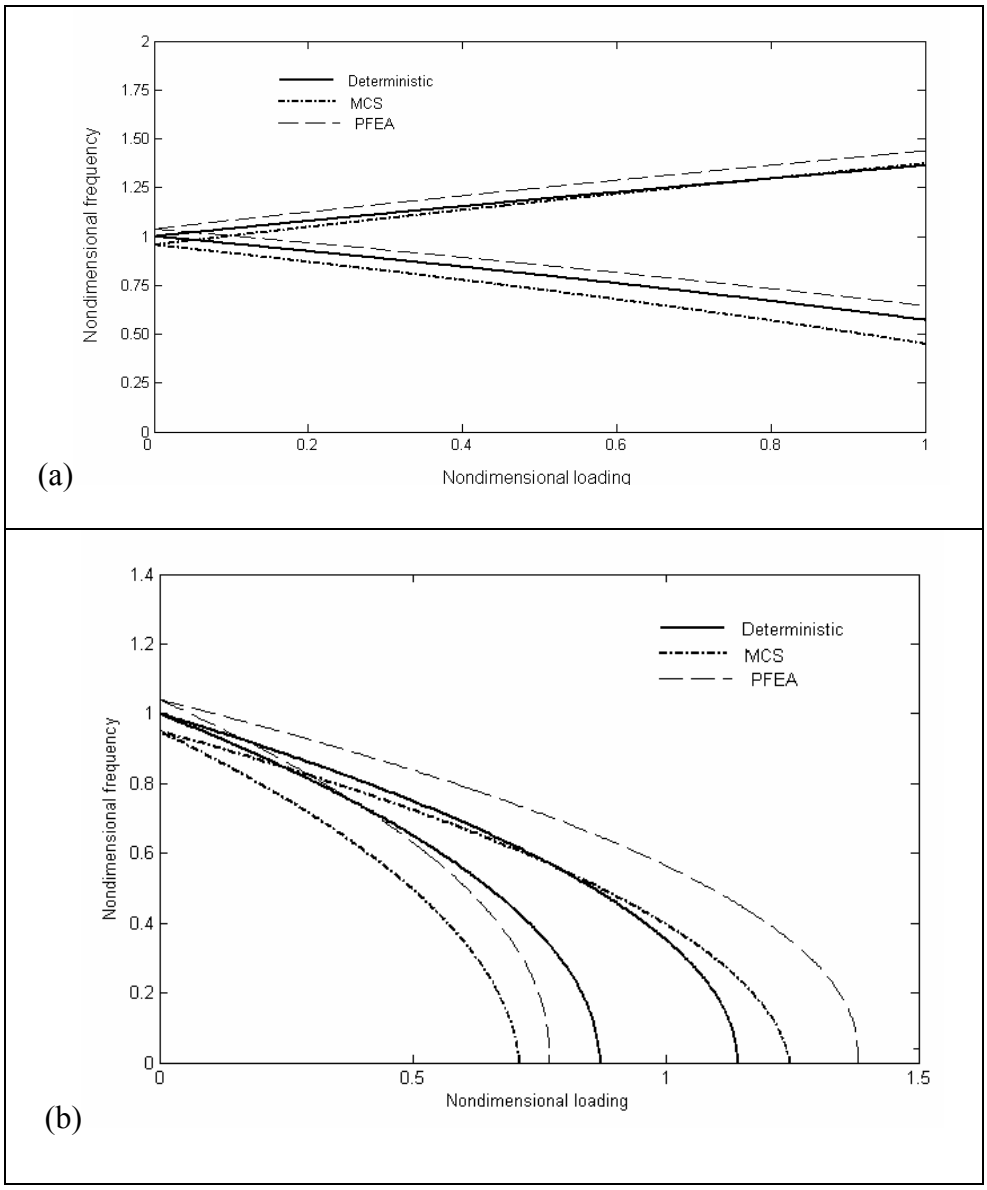

Figure 5. 7 Dynamic instability regions of a cross ply laminated composite beam with uncertain material parameters E for (a) Nonconservative loading. (b) Conservative loading.

When the load increases, the upper boundaries of the instability regions of MCS decrease faster in compare to PFEA. This implies that the presence of the compressive conservative load reduces the stiffness of the laminate, and thus shifts the resonance frequencies or the instability regions downwards. By comparing PFEA, MCS, and deterministic results in Figures 5.7 (a) and (b), it can be seen that the dynamic instability opening in the former is smaller than that in the latter for nonconservative system and upper bound for MCS increases faster than two others. But for conservative system the instability opening is bigger than MCS and deterministic one. It means that in studying the sensitive cases, Monte Carlo simulation shall be considered to predict the instability regions.

Next, two applications are concerned with studying the effect of the uncertain geometric property of the beam length l on the dynamic instability of the cross-ply laminates. The effect of geometric uncertainty of 0.05 is considered. The beam layup is same as the application presented before, so that effectively two different laminates are considered for conservative and nonconservative system. The dynamic instability regions of the two laminates are shown in Figure 5.8 (a) and (b) in the plane of nondimensional frequency vs. nondimensional loading. Figure 5.8 (a) shows that the instability region determined using the MCS method shifts to downward faster than using the PFEA method, then their natural frequencies become smaller in nonconservative system. The instability regions of the beam rapidly reach to the horizontal axes, then the beam becomes totally unstable.

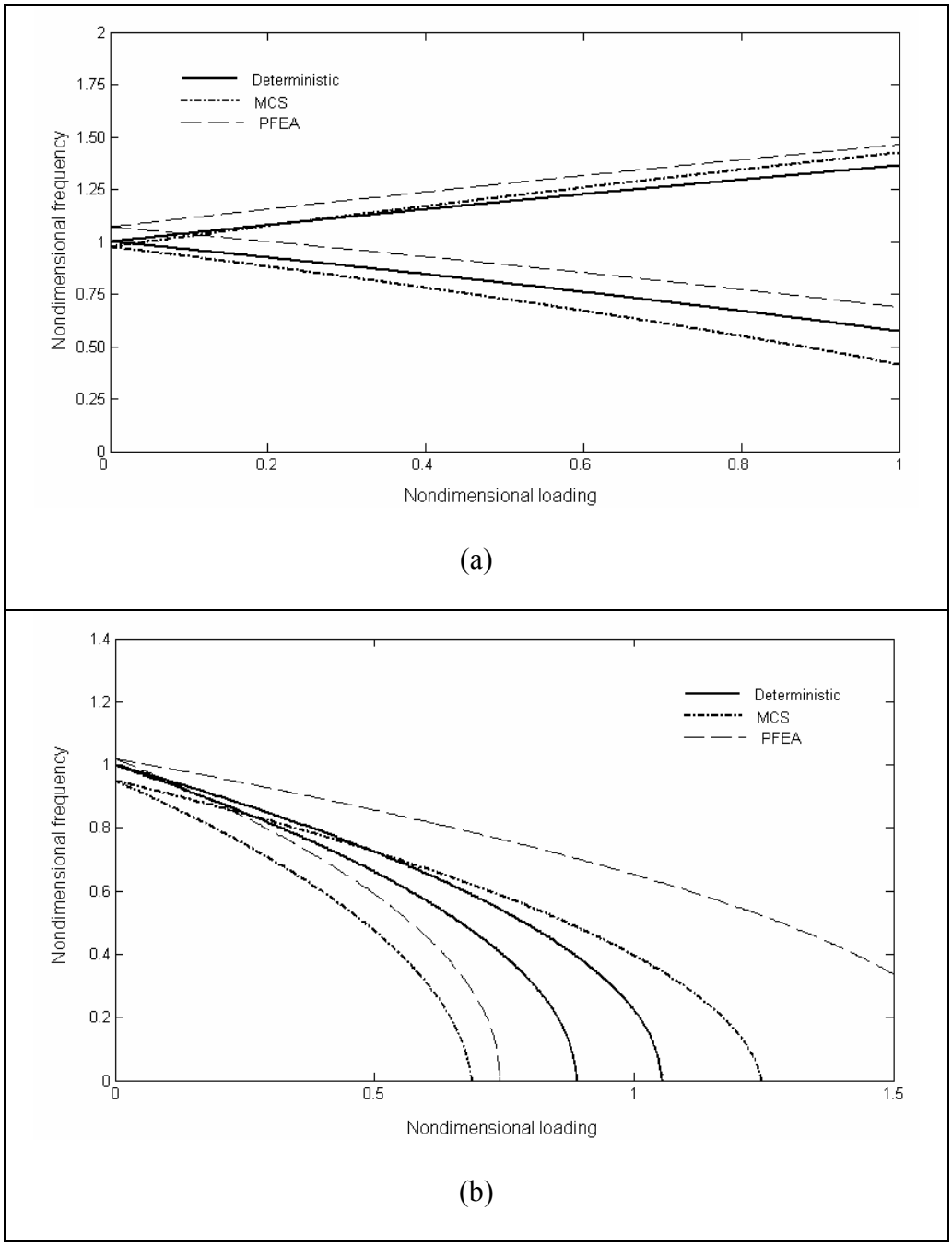

Figure 5. 8 Dynamic instability regions of a cross ply laminated composite beam with uncertain geometry parameter for (a) Nonconservative loading. (b) Conservative loading.

5.7 Beam failure

A composite laminate is assumed to fail when any ply in the laminate fails. In the sense of structural stability, a structure is safe only if the actual load applied to the component does not exceed the critical load. Most of the work pertaining to stability analysis with random imperfections deals with the modeling of imperfections which are known at discrete points on the structure, or with finding a critical imperfection shape that causes the largest reduction in the critical load for the structure. Questions about the modeling of imperfections arise when a structure is designed for the first time and no information is available about the initial imperfections. Usually, a maximum allowable limit on the imperfection at any point on the structure is specified by a design code or dictated by the manufacturing process used to build the structure itself, or the various members in the structure.

The objective in modeling the initial geometric imperfections is to obtain the variance of the modal imperfection amplitudes. Modeling of the initial geometric imperfections is accomplished using the assumption that only allows translational imperfections at the imperfect nodes. This means that crooked members are modeled by translational movements of the nodes of the finite elements used to discretize each structural member. In this study, the reliability or probability of a beam is defined as the probability that an imperfect structure will become unstable at a load greater than a specified percentage of the critical load, p_{cr} , for the perfect structure. The probability density function of failure is defined as:

$$F(\chi) = 1 - \exp\left[-\left(\frac{\chi}{\beta}\right)^{\alpha}\right] \tag{5.6}$$

where α and β are the shape and scale parameters, respectively. The shape parameter can be correlated to the coefficient of variation (COV) as (Winsum, 1998):

$$\text{COV} \approx \frac{1.2}{\alpha} \tag{5.7}$$

The above will be used to assess the Weibull shape parameter for probability failure analysis. Using the shape and scale parameters with 0.05 standard deviation σ defined by Karbhari et al., 2007), the probability of failure for a beam designed for various loading fraction $\chi = \frac{p}{p_{cr}}$ can be found. Figure 5.9 shows the probability density functions of the dimensionless critical load for the beam.

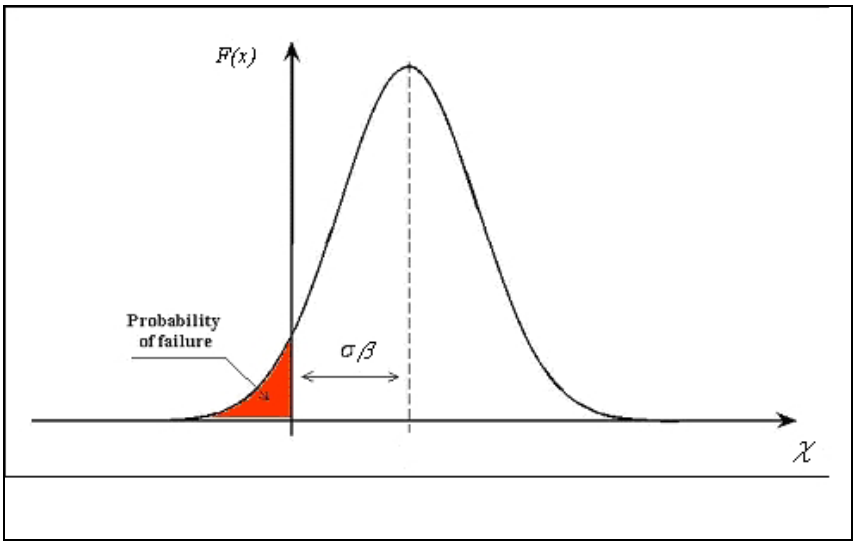

Figure 5. 9 Probability density function for the beam with variable critical load fraction $\chi = \frac{p}{p_{cr}}$.

5.8 Summary

Probabilistic stability analysis of a beam with random initial geometric imperfections was studied in Chapter 5. The problem of approximating or simulating initial geometric imperfections is a relatively new field of research. With the increasing use of lightweight structures, a method for approximating the imperfections must be available for structures where there is no exact imperfection data. Once an appropriate initial imperfection pattern is determined, an efficient technique must be used to determine the probability of failure for the structure. Two methods, probability finite element analysis (PFEA) and Monte Carlo simulation (MCS), for approximating the geometric imperfections and calculating the instability regions for laminated composite beams with uncertain material and geometry parameters were presented. The results show that in nonconservative system the chance for the beam to be unstable at same boundary conditions with uncertain material property predicted by MCS are higher than using the PFEA method. However, for conservative system is vice versa.

It was determined that the uncertain geometry parameter has more effect than uncertain material property such as modulus of elasticity on instability of the beam subjected to both conservative and nonconservative loads.

Both methods, MCS and PFEA, produce acceptable imperfection patterns and are relatively efficient in calculating the probability of failure of the beam.

Chapter 6

Conclusion and Future Work

6.1 Conclusion

Composites structures have found many applications in aeronautical, mechanical and civil engineering, where high strength and stiffness with low weight are of primary importance. Many structural members made of composites have the form of beams. These kinds of members are the most common load-carrying systems in engineering applications. The unstable composite beams may fail laterally or twists out of the plane of loading in a flexural and/or torsional modes. The failure of the beam structures is caused by the coupling among bending, twisting and stretching deformations. The linear dynamic behaviour analysis of the beam problems is the omission of any consideration of the effect of nonlinearities corresponding to the large deformation with small strains of composite shear deformable beams. Also the classical analysis may lead to inaccurate predictions due to the nonlinearities effect increasing the frequency values in the dynamic response.

6.1.1 The perfect composite laminated beams analysis

In this study a new formulation has been presented to predict the accurate dynamic stability behaviour and stability analysis of laminated composite beams subjected to the axial varying time loads with considering all couplings among bending, twisting, and stretching deformation effects in account.

Deterministic finite element analysis of composite laminated beams was performed based on a developed non-linear five node hybrid beam model. The beam model can capture the axial, transverse, lateral, and torsional displacements corresponding to the extension, bending, twisting couplings effects. A distinctive feature of the present study over others available in the literature is that this beam model incorporates, in a full form, the non-classical effects, such as warping, on stability and dynamic response of symmetrical and unsymmetrical composite beams. The accuracy of the developed beam model verified with those ones available in the literature and the model simulated in commercial software ANSYS.

It was observed that in general, axially loaded beam may be unstable not just in load equal to critical load and/or loading frequency equal to beam natural frequency. In fact there are infinite points in region of instability in plane load vs. frequency that the beam can be unstable under such loading conditions. Also the load direction can be changed with the beam deformation, therefore the effects of loads conservativeness on the beams instability is important to be investigated. The results obtained from different cases show that the dynamic instability behaviours of non-conservative and conservative system are

dissimilar. The fact is the damping and nonlinear parameters shall be considered in case of non-conservative system formulations. In case of conservative loading, the instability region intersects the loading axis, but in case of non-conservative loads the region will be increased with loading increases. The beam can be unstable in wider range, when the non-conservative load magnitude is less than the critical load.

Also the region of instability of the shear deformable beams is wider compare to the non-shear deformable beams. The lower bound of the instability region of the shear deformable beams changes faster than upper bound.

In the system with damping in account, the stable region is enlarged when the damping ratio of the beam is increased and it has more effect on stabilizing of the system. In the other hand, the greater the damping, the greater the amplitude of longitudinal force required to cause the beam to be unstable.

The influence of tangent and loading stiffness matrices of non-linear systems due to large displacement on the stability and free vibration behaviour of composite beams were investigated analytically and numerically. It has been observed that in case of nonlinear elasticity, the resonance curves are bent toward the increasing exciting frequencies. The damping factor has important role in diminishing of the amplitude of the vibrating beam, in contrast the increasing of the nonlinear elasticity of the system does not always reduce the resonance amplitudes.

In this research also the response of the composite laminated beams has been investigated in stable and unstable zones through a developed formulation.

It has been shown that the response of the stable beam is pure periodic and follow the loading frequency. When the beam is asymptotically stable the response of the beam is aperiodic and does not follow the loading frequency. In unstable state of the beam response frequency increases with time and is higher than the loading frequency, also the amplitude of the beam will increases, end to beam failure. The amplitude of the beam subjected to substantial excitation loading parameters increases in a typical nonlinear manner and leads to the beats phenomena. With adding the damping in formulation of the periodically loaded unstable composite beam the violation of motion will be reduced or eliminated.

6.1.2 Probabilistic analysis of imperfect composite laminated beams

The layup and curing of fibres and matrix are complicated process and may lead to imperfections in the structure and involve the material and geometry properties uncertainties. In this case, the deterministic analysis may be no longer valid and it is intended to expand a probabilistic formulation that can take these uncertainties in account. The probabilistic instability analysis of the laminated beams with uncertain geometric and material properties through Monte Carlo simulation and probabilistic finite element analysis was the second goal of this study.

Monte Carlo Simulation has been applied to laminated beams with randomness in beam length and the modulus of elasticity to study their effect on

the stability of the beams. The results from both approaches have been compared to the result obtained from deterministic finite element method. The MCS method predicts the wider instability regions than probabilistic finite element analysis.

The reliability of beams under uncertainties has been investigated. The reliability analysis showed that for the types of problems solved in this dissertation, both method MCS and finite element analysis, produce acceptable imperfection patterns and are relatively efficient in calculating the probability of failure of the beam.

Also it was observed that for nonconservative systems variations in uncertain material properties has a smaller influence than variations of geometric properties over the eigenfrequencies.

6.2 Future Work

In the present work the laminated composite structures with high slender ratio of the length to width was analyzed using one-dimensional model. However, real structures may be too complex to be modeled as beams. Thus a more rigorous study should expand the present study using plate and shell theory. In doing so, one can perhaps model and study a wide class of wings. Moreover, the use of a higher order theory will not require the approximations for the shear correction factors. Thus it is suggested that the present formulation be extended by using a higher order plate and/or shell theory.

In the present work it was assumed that the load applied to the beam is axial and in x-direction, but in real applications the loads can be applied in other direction as well. Therefore is recommended that a formulation to be improved and developed which can cover and analyze the multi axial loading.

It is suggested that the nonlinear post-buckling phenomena analysis be considered in stability analysis of the structure. The formulation for the post-buckling analysis has been included but not used because it was beyond the scope of this work. It would be most interesting to see how uncertainties affect the post-buckling behaviour of laminated structures.

The analytical approach to predict the damping property of the laminated beams here was the method developed by Ni and Adams (1994). It will be interesting to use the new approach verified through a new experimental technology to calculate the damping loss factors. One such approach for instance can be found in the recent work presented by J. Hee et al. (2007).

The stability regions in this study were determined using Bolotin's approach and just the first principal regions were plotted. It can be great if other methods are used for determining the higher level of stability regions.

When analyzing uncertain structures, creating a proper sampling for the purpose of Monte Carlo Simulation is an extremely important step. Some researchers have developed new and better methods for creating these samplings than those used in this dissertation. Among these methods is the Latin Hypercube Sampling, widely used at Sandia Laboratories (Wyss and Jorgensen,

1998). Thus it is recommended that these new methods of generating appropriate samples be integrated into the analysis of uncertain systems.

The reliability assessment for laminated composite structures usually involves many random variables such as anisotropic material properties, lamina thickness, fibre orientation angle, etc. It will be challenging to perform a reliability assessment with random variables other than the calculation of the limit state function done by a nonlinear code developed here.

The reliability estimation of the regions of instability of the compressive laminated composite plates can be another future work.

Appendix A

Prediction of the Damping in Laminated Composites

Ni and Adams (1995) developed a model to provide designers with a useful and accurate prediction method for damping of composites. Their model predicted damping in laminated composites related to the energy dissipation with respect to the inplane stresses in the fibre coordinate system under ply stress condition as shown in Fig. 1.

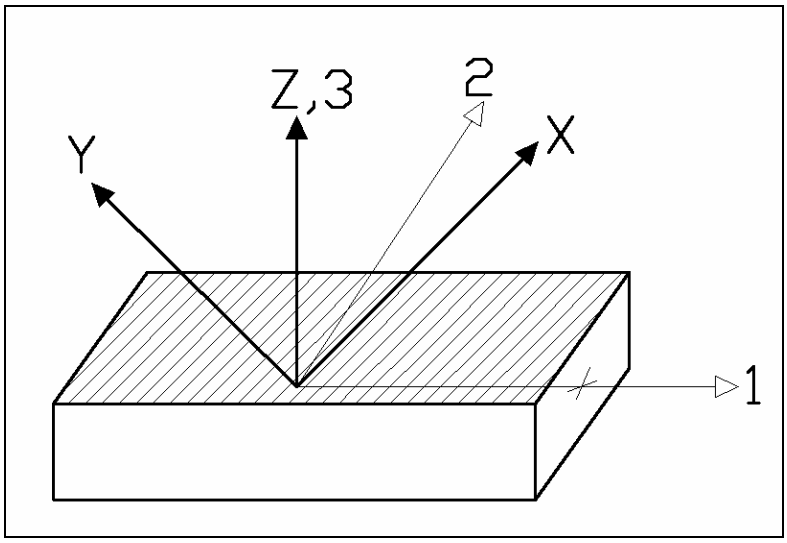

Fig . 1 Fibre and loading coordinate systems used in the analytical model.

Analytical approach

The analytical approach developed by Ni and Adams (1995) predicts the damping of the laminated composites. This method is based on the strain energy approach. The damping loss factor δ is defined as:

$$\delta = \frac{\Delta E}{2\pi E} \tag{A-1}$$

where ΔE is the energy dissipated during a stress cycle and E is the maximum strain energy. The analytical formulation is conducted on the coordinate system as shown in Fig. 1.

For axial loading, the basic damping property δ_l is represented by

$$\delta_l = \delta_m \left(1 - V_f\right) \frac{E_m}{E_l} \tag{A-2}$$

where δ_l is the axial damping loss factor in composites, δ_m is the damping loss factor of the matrix, V_f is the fibre volume fraction in composites, E_m is the Young's modulus of the matrix, E_l is the axial Young's modulus of the composites.

Appendix B

MATLAB Codes:

Some Matlab codes that were used in this study are brought here. The complete codes are available upon request.

```
% stability nonconservative loading laminates 0/0/0/0, 0/45/45/0,
0/90/90/0
clc
syms  a b c m;
a =0;
m = 12.7;
%============
hold on;
grid off;
A = [10-a-0.1366*b-7.2576*c 0.6366*b-6.1408*c
    -0.0236*b-0.6816*c 10-0.1111*a+0.0791*b-0.7584*c];
B = [10-a+0.1366*b-7.2576*c -0.6366*b-6.1408*c
    +0.0236*b-0.6816*c 10-0.1111*a-0.0791*b-0.7584*c];
d = det(A);
e = det(B);
%=====================================================
C = [m-a-0.1366*b-7.2576*c 0.6366*b-6.1408*c
    -0.0236*b-0.6816*c m-0.1111*a+0.0791*b-0.7584*c];
D = [m-a+0.1366*b-7.2576*c -0.6366*b-6.1408*c
    +0.0236*b-0.6816*c m-0.1111*a-0.0791*b-0.7584*c];
h = det(C)
i = det(D)
%=================
m=12.7
f = ('100-23/40*b-2004/25*c+42187/10000000*b^2-
141793/781250*b*c+515076/390625*c^2');
g = ('16129/100+2921/4000*b-
63627/625*c+42187/10000000*b^2+141793/781250*b*c+515076/390625*c
^2');

%=============================================================
===========
m=17.6
j = ('144-69/100*b-12024/125*c+42187/10000000*b^2-
141793/781250*b*c+515076/390625*c^2');
```

```
k = ('7744/25+253/250*b-
88176/625*c+42187/10000000*b^2+141793/781250*b*c+515076/390625*c
^2');
%=================================================================
==========
m=25.7
%l = ('225-69/80*b-3006/25*c+42187/10000000*b^2-
141793/781250*b*c+515076/390625*c^2');
m = ('66049/100+5911/4000*b-
128757/625*c+42187/10000000*b^2+141793/781250*b*c+515076/390625*
c^2');
%=======================
n = ('2601/25-1173/2000*b-51102/625*c+42187/10000000*b^2-
141793/781250*b*c+515076/390625*c^2');
%o = ('2601/25+1173/2000*b-
51102/625*c+42187/10000000*b^2+141793/781250*b*c+515076/390625*c
^2');
%================
p = ('88317187/400000-169861187/10000000*a-
18929293/156250*c+1111/10000*a^2+1222437/781250*a*c+515076/39062
5*c^2');
q = ('91767187/400000-163468813/10000000*a-
18645707/156250*c+1111/10000*a^2+1222437/781250*a*c+515076/39062
5*c^2');
%++++++++++++++++
ezplot(g,[0,600])

%===============
ezplot(k,[0,600])
%===============
ezplot(l,[0,300])
ezplot(m,[0,600])
%====================

ezplot(n,[0,300])
ezplot(o,[0,300])
%========
ezplot(p,[0,300])
ezplot(q,[0,300])
%========
xlabel('P_t/P_c_r or P^w_c_r ')
ylabel('\theta/\omega_n')
title('instability regions')
```

```
% Probability nonconservative beam%
clc
syms  a b c;
a = 0;
%============
hold on;
grid on;
A = [1-a-0.1366*b-7.2576*c 0.6366*b-6.1408*c
    -0.0236*b-0.6816*c 1-0.1111*a+0.0791*b-0.7584*c];
B = [1-a+0.1366*b-7.2576*c -0.6366*b-6.1408*c
    +0.0236*b-0.6816*c 1-0.1111*a-0.0791*b-0.7584*c];
```

```
d = det(A);
e = det(B);

%=================
f = ('.63-230/20*b-1002/125*c+42187/10000000*b^2-
141793/781250*b*c+515076/390625*c^2');
g = ('.63+210/20*b-
1002/125*c+42187/10000000*b^2+141793/781250*b*c+515076/390625*c^
2');
f1 = ('1-264/18*b-1002/125*c+42187/10000000*b^2-
141793/781250*b*c+515076/390625*c^2');
g1 = ('1+235/18*b-
1002/125*c+42187/10000000*b^2+141793/781250*b*c+515076/390625*c^
2');
f2 = ('-0.5-265/20*b-1002/125*c+42187/10000000*b^2-
141793/781250*b*c+515076/390625*c^2');
g2 = ('-0.5+200/20*b-
1002/125*c+42187/10000000*b^2+141793/781250*b*c+515076/390625*c^
2');

ezplot(f,[0,.5,4,9])
ezplot(g,[0,.5,4,9])

% stability of conservative laminates P0=0 (a=0)
clc
syms  a b c m;
b = 5;
m = 25.7;
%============
hold on;
grid off;
A = [10-a-0.1366*b-7.2576*c 0.6366*b-6.1408*c
    -0.0236*b-0.6816*c 10-0.1111*a+0.0791*b-0.7584*c];
B = [10-a+0.1366*b-7.2576*c -0.6366*b-6.1408*c
    +0.0236*b-0.6816*c 10-0.1111*a-0.0791*b-0.7584*c];
d = det(A);
e = det(B);
%=====================================================
C = [m-a-0.1366*b-7.2576*c 0.6366*b-6.1408*c
    -0.0236*b-0.6816*c m-0.1111*a+0.0791*b-0.7584*c];
D = [m-a+0.1366*b-7.2576*c -0.6366*b-6.1408*c
    +0.0236*b-0.6816*c m-0.1111*a-0.0791*b-0.7584*c];
h = det(C)
i = det(D)
%=================
m=10
f = ('100-23/40*b-2004/25*c+42187/10000000*b^2-
141793/781250*b*c+515076/390625*c^2');
g = ('100+23/40*b-
2004/25*c+42187/10000000*b^2+141793/781250*b*c+515076/390625*c^2
');

%=================================================================
===========
m=12
```

```
j = ('144-69/100*b-12024/125*c+42187/10000000*b^2-
141793/781250*b*c+515076/390625*c^2');
k = ('144+69/100*b-
12024/125*c+42187/10000000*b^2+141793/781250*b*c+515076/390625*c
^2');
%================================================================
===========
%m=15
l = ('225-69/80*b-3006/25*c+42187/10000000*b^2-
141793/781250*b*c+515076/390625*c^2');
m = ('225+69/80*b-
3006/25*c+42187/10000000*b^2+141793/781250*b*c+515076/390625*c^2
');
%======================
n = ('2601/25-1173/2000*b-51102/625*c+42187/10000000*b^2-
141793/781250*b*c+515076/390625*c^2');
o = ('2601/25+1173/2000*b-
51102/625*c+42187/10000000*b^2+141793/781250*b*c+515076/390625*c
^2');
%===============
%b=5, m=12.7
p = ('63097687/400000-144305887/10000000*a-
16048543/156250*c+1111/10000*a^2+1222437/781250*a*c+515076/39062
5*c^2');
q = ('91767187/400000-163468813/10000000*a-
18645707/156250*c+1111/10000*a^2+1222437/781250*a*c+515076/39062
5*c^2');
%+++++++++++++++++
r = ('121922187/400000-198749787/10000000*a-
22185793/156250*c+1111/10000*a^2+1222437/781250*a*c+515076/39062
5*c^2');
s = ('261282687/400000-288748887/10000000*a-
32331043/156250*c+1111/10000*a^2+1222437/781250*a*c+515076/39062
5*c^2');
%====================================
b=5, m=12.7
ezplot(q,[0,300])
%========
b=5, m=17.6 & 25.7

ezplot(r,[0,300])
ezplot(s,[0,300])
%==========

xlabel('P_c/P_c_r ')
ylabel('\omega^2 (Hz)^2')
title('')
```

```
% Beam element calculation %
nel = 5;
nnel = 10;
ndof = 6;
nnode = (nnel – 1)*nel + 1;
sdof = nnode*nodof;
el = 10*7;
sh = 3.8*10-6
```

```
tleng = 10;
leng = 10/nel;
heig = 1;
width = 1;
rho = 1;
bcdof(1) = 3;
bcval(1) = 0;
bcdof(2) = 16;
bcval(2) = 0;
bcdof(3) = 17;
bcval(3) = 0;
ff = zeros (sdof,1);
kk = zeros (sdof,sdof);
index = zeros (nnel*ndof,1);
ff(18)=50
for iel = l:nel
index = feeldofl (iel,nnel,ndof);
k = febeam3 (el,sh,leng,heig,width,rho);
kk = feasmbl1 (kk,k,index);
end
[kk,ff] = feaplyc2 (kk,ff,bcdof,bcval);
fsol = kk\ff;

e=10*7; l=20; xi=1/12; P=100;
for i =1:nnode
x = (i-1)*2;
c = P/(48*e*xi);
k = (i-1)*ndof+1;
esol(k+2)=c*(3*l-2 – 4*x-2)*x;
esol(k+1)=c*(3*1-2-12*x-2)*(-0.5);
esol(k)=c*(3*1-2-12*x-2)*(0.5);
end

num = 1:1:sdof;
store = [num'fsol esol']

function [febeam3(el,sh,leng,heig,width,rho)


a1=(sh*leng*width)/(4*heig);
a2=(sh*heig*width)/leng;
a3=(el*heig*width)/(6*leng);
a4=sh*width/2
k=[a1+2*a3 a4 a1-2*a3-a1-a3-a4;
-a1+a3 a1+2*a3-a4-a1-a3 a1-2*a3 a4;
a4 –a4 a2 a4 –a4 –a2; …
a1-2*a3 –a1-a3 a4 a1 +2*a3 –a1 +a3 –a4; …
-al-a3 a1-2*a3-a4 –a1+a3 a1+2*a3 a4; …
-a4 a4 –a2 –a4 a4 a2];

m=zeros(6,6);
mass=rho*heig*width*leng/4;
m=mass*diag([1 1 2 1 1 2]);
```

```
% Response of the beam with damping %

nel = 5;
nnel = 2;
ndof = 3;
nnode = (nnel - 1)*nel + 1;
sdof = nnode*ndof;
el = 10*7;
sh = 3.8*10-6;
tleng = 10;
leng = 10/nel;
heig = 1;
width = 1;
rho = 1;
bcdof(1) = 3;
bcval(1) = 0;
bcdof(2) = 16;
bcval(2) = 0;
bcdof(3) = 17;
bcval(3) = 0;
ff = zeros (sdof,1);
kk = zeros (sdof,sdof);
index = zeros (nnel*ndof,1);
ff(18) = 50;
for iel = 1:nel
% index = feeldofl (iel,nnel,ndof);
k = febeam3 (el,sh,leng,heig,width,rho);
kk = feasmbl1 (kk,k,index);
end
[kk,ff] = feaplyc2 (kk,ff,bcdof,bcval);
fsol = kk\ff;

e=10*7; l=20; xi=1/12; P=100;
for i =1:nnode
x = (i-1)*2;
c = P/(48*e*xi);
k = (i-1)*ndof+1;
esol(k+2)=c*(3*l-2 - 4*x-2)*x;
esol(k+1)=c*(3*1-2-12*x-2)*(-0.5);
esol(k)=c*(3*1-2-12*x-2)*(0.5);
end

num = 1:1:sdof;
store = [num, 'fsol, esol'];

function =  [febeam3(el, sh, leng, heig, width, rho)];


a1=(sh*leng*width)/(4*heig);
a2=(sh*heig*width)/leng;
a3=(el*heig*width)/(6*leng);
a4 = sh*width/2;
k=[a1+2*a3 a4 a1-2*a3-a1-a3-a4;
-a1+a3 a1+2*a3-a4-a1-a3 a1-2*a3 a4;
a4 - a4 a2 a4 - a4 - a2;
a1-2*a3 - a1-a3 a4 a1 +2*a3 -a1 +a3 -a4;
```

```
-al-a3 a1-2 *a3-a4 -a1+a3 a1+2*a3 a4;
-a4 a4 a2 a4 a4 a2];

m = zeros(6,6);
mass = rho*heig*width*leng/4;
m = mass*diag([1 1 2 1 1 2])
```

References

Abarcar R. B., Cunnif P. F (1972), "The Vibration of Cantilever Beams of Fiber Reinforced Material", Int. Journal of Composite Materials, 6:504-517.

Abramovich, H. (1992). "Shear Deformation and Rotatory Inertia Effects of Vibrating Composite Beams". Composite Structures 20, pp. 165–173.

Abramovich H., Livshits A. (1994) "Free vibration of non-symmetric cross ply laminated composite beams." Sound and Vibration, 176 pp 597–612.

Abramovich H., Eisenberger M., and Shulepov O.,(1995). "Dynamic Stiffness Matrix for Laminated Beams Using A First Order Shear Deformation Theory". Composite Structures 31, pp. 265–271.

Adams R.D., Bacon D.G.C., (1973) "Effect of fiber orientation and laminate geometry on the dynamic properties of CFRP", J. of Compos. Mater, pp.402–408.

Argyris, J. H., Symeondis S., (1981). "Nonlinear Finite Element Analysis of Elastic Systems Under Nonconservative Loading–Natural Formulation. PartI. Quasistatic Problems". Computer Methods in Applied Mechanics and Engineering 26, pp. 75–123.

Atkinson, A. C., Pearce M. C., (1976). “The Computer Generation of Beta, Gamma, and Normal Random Variables”. Journal of the Royal Statistical Society, A139, pp. 431–448.

Aydigdu, M., (2006). “Free vibration analysis of angle-ply laminated beams with general boundary conditions”. Journal of reinforced plastics and composites, Vol. 25, No.15.

Averill, R. C., Yip Y. C. ,(1996). “Development of Simple, Robust Finite Elements Based on Refined Theories for Thick Laminated Beams”. Computers and Structures 59 (3), pp. 529–546.

Banerjee J., Williams F. (1995) “Free vibration of composite beams – an exact method using symbolic computation”. Int. J. Aircraft ,32:636–42.

Bassiouni, A. S., Gad-Elrab R. M., Elmahdy T. H.,(1999). “Dynamic Analysis for Laminated Composite Beams”. Composite Structures 44 (2–3), pp. 81–87.

Berthelot, J. M., Sefrani, Y., (2004) “Damping analysis of unidirectional glass and Kevlar fibre composites”., Compos Sci Technol; 64: pp.1261–78.

Bhimaraddi A, Chandrashekhara K.,(1991) “Some observations on the modeling of laminated composite beams with general lay-ups.” Composite Structure,19:371–80 pp 651–60.

Bolotin V.V. (1964), Dynamic Stability of Elastic Systems, Holden-Day, San Francisco.

Cassenti, B. N. (1984). “Probabilistic static failure of composite material”. AIAA J 22: pp.103–10.

Cederbaum G., Aboudi J., Elishakoff I., (1991) “Dynamic instability of shear-deformable viscoelastic laminated plates by Lyapunov exponents.” Solids Structure, 28(3) pp 317-327.

Chakraborty A., Mahapatra D. R., Gopalakrishnan S. (2002) “Finite element analysis of free vibration and wave propagation in asymmetric composite beams with structural discontinuities.” J. Composite Structure, 55:23–36.

Chandrashekhara K., Krishnamurthy K., Roy S., (1990)”Free vibration of composite beams including rotary inertia and shear deformation.” Composite Structure, 14 pp 269 79.

Chandrashekhara K., Bangera K. M. (1992).”Free vibration of composite beams using a refined shear flexible beam element.” Composite Structure, 43 pp 719 27.

Chen, A. T. and T. Y. Yang (1985). “Static and Dynamic Formulation of A Symmetrically Laminated Beam Finite Element for A Microcomputer”. Journal of Composite Materials 19, pp. 459–475.

Chen W. Q., Bian Z. G. (2004) “Free vibration analysis of generally laminated beams via state-space-based differential quadrature.” J. Composite Structure, 63:417–25.

Doyle, J. F. (2001). Nonlinear Analysis of Thin-Walled Structures. New York: Springer-Verlag.

Eisenberger M., Abramovich H., Shulepov O. (1995). “Dynamic Stiffness Analysis of Laminated Beams Using A First Order Shear Deformation Theory”. Composite Structures 31 (4), pp. 265–271.

Elishakoff, I., Y. Li, and J. James H. Starnes (2001). Non-classical Problems in the Theory of Elastic Stability. New York: Cambridge.

Engelstad S. P., Reddy J.N, (1993)" Probabilistic Methods for the Analysis of Metal-Matrix Composites", Composites Science and Technology, 50 pp 91-107.

Frangopol, D. M. and K. Imai (2000). "Geometrically Nonlinear Finite Element Reliability Analysis of Structural Systems. II: Applications". Computers and Structures 77 (6), pp. 693–709.

Frangopol D. M. and Recek S. (2003) " Probabilistic Finite Element Analysis of Matrix Composites" Probabilistic Engineering Mechanics, 18(2), pp 119-137.

Gasparini, A. M., A. V. Saetta, and R. V. Vitaliani (1995). "On the Stability and Instability Regions of Non-Conservative Continuous System Under Partially Follower Forces". Computer Methods in Applied Mechanics and Engineering 124 (1–2), pp. 63–78.

Goyal, V. K. and Kapania, R. K. (2006). "A shear-deformable beam element for the analysis of laminated composites". Finite Elements in Analysis and Design 43, pp. 463 – 477.

Goyal, V. K. (2002). "Dynamic Stability of Uncertain Laminated Beams Subjected to Subtangential Loads". PhD thesis, Virginia Polytechnic Institute and State University.

Haldar, A. and S. Mahadevan (2000). Probability, Reliability, and Statistical Methods in Engineering Design. New York: John Wiley.

Haldar, A. and S. Mahadevan (2000). Reliability Assessment Using Stochastic Finite Element Analysis. New York: John Wiley.

Hansen, J.S. (2007), "Some Thoughts on the Theories of Layered Beams and Plates", CANCAM conference proceeding, pp.2-8.

Kam, T. Y. and R. R. Chang (1992). "Buckling of Shear Deformable Laminated Composite Plates". Composite Structures 22, pp. 223–234.

Kam T. Y., Jan T. B. (1995) "First-ply failure analysis of laminated composite plates based on the layerwise linear displacement theory", Composite Structures, 32 pp 583-591.

Kant T., Marur S.R., Rao G.S. (1997) "Analytical solution to the dynamic analysis of laminated beams using higher order refined theory." Composite Structure, 40 pp 1–9.

Kapania, R. K. and S. Raciti (1989a). "Nonlinear Vibrations of Unsymmetrically Laminated Beams". AIAA Journal 27 (2), pp. 201–210.

Kapania, R. K. and S. Raciti (1989b). “Recent Advances in Analysis of Laminated Beams and Plates, Part I: Shear Effects and Buckling”. AIAA Journal 27 (7), pp. 923–934.

Kapania, R. K. and S. Raciti (1989c). “Recent Advances in Analysis of Laminated Beams and Plates, Part II: Vibrations and Wave Propagation”. AIAA Journal 27 (7), pp. 935–946.

Karbhari, V.M. and Abanilla M. A. (2007). “Design factors, reliability, and durability prediction of wet layup carbon/epoxy used in external strengthening”. Composites: Part B 38, pp.10–23.

Khdeir, A. A. and J. N. Reddy (1994). “Free Vibration of Cross-Ply Laminated Beams with Arbitrary Boundary Conditions”. International Journal of Engineering Science 32, pp. 1971–1980.

Khdeir, A. A. and J. N. Reddy (1997). “An Exact Solution for the Bending of Thin and Thick Cross-Ply Laminated Beams”. Composite Structures 37 (2), pp. 195–203.

Khdeir, A. A. (1996). “Dynamic Response of Antisymmetric Cross-Ply Laminated Composite Beams with Arbitrary Boundary Conditions”. International Journal of Engineering Science 34, pp. 9–19.

Kollar L.P., Springer G.S. (2003) 'Mechanics of Composite Structures' New York, John Wiely.

Krishnaswamy S, Chandrashekhara K, Wu WZB. (1992) "Analytical solutions to vibration of generally layered composite beams." Sound and Vibration, 159 pp 85–99.

Law, A. M. and W. D. Kelton (2000). Simulation Modeling and Analysis (Thirded.). New York: McGraw-Hill.

Librescu, L. and A. A. Khdeir (1987). "An Exact Solution to the Aeroelastic Divergence of Sweptforward Composite Wings Accounting for Their Warping Restraint Effect". CCMS Review, Virginia Polytechnic Institute and State University, Blacksburg, VA.

Librescu, L. and O. Song (1991). "Behaviour of Thin-Walled Beams Made of Advanced Composite Materials and Incorporating Non-Classical Effects". Applied Mechanics Reviews 44 (11), pp. 174–180.

Lin C. Y., Chen L.W. (2002). "Dynamic stability of rotating composite beams with a viscoelastic core" Composite Structures, 58 pp185–194.

Loja M. A. R., Barbosa J. I. and Soares C. M. M. (2001) “Static and dynamic behaviour of laminated composite beams.", J. of Structural Stability and Dynamics, 545-560.

Loja M. A. R., Barbosa J. I. and C. Soares M. M. (1997) “Buckling behaviour of laminated beam structures using a higher-order discrete model." Composite Structure 38, pp. 119-131.

Loja M/. A. R. (1995) “Higher-Order Shear Deformation Models- Development and Implementation of Stiffness Coefficients for T, I, Channel and Rectangular Box Beams” Report IDMEC/IST, Project STRDA/C/TPR/592/92, Lisbon.

Logan D. L., Finite Element Method, Brooks/Cole, CA, USA, 2002.

Mahapatra D.R., Gopalakrishnan S., Sankar T. S. (2000) “Spectral-element based of multiply connected unsymmetric laminated composite beams.” Int. J. Sound and Vibration;237:819–36.

Mahapatra D. R., Gopalakrishnan S. (2003) “A spectral finite element model for analysis of axial–flexural–shear coupled wave propagation in laminated composite beams.” J. Composite Structure, 59:67–88.

Maiti, D. K. and P. K. Sinha (1994). “Bending and Free Vibration Analysis of Shear Deformable Laminated Composite Beams by Finite Element Method.” Composite Structures 29, pp. 421–431.

Manjunatha, B. S. and T. Kant (1993). “New Theories for Symmetric/ Unsymmetric Composite and Sandwich Beams with C0 Finite Elements” Composite Structures 23 (1), pp. 61–73.

Matsunaga H. (2001) “Vibration and buckling of multilayered composite beams according to higher order deformation theories.” J. Sounds and Vibration, 246:47–62, 2001.

Meirovitch, L. (2001), Fundementals of Vibrations, New York, NY: McGraw-Hill.

Miller A. K., Adams D. F. (1975), “An analytic means of determining the flexural and torsional resonant frequencies of generally orthotropic beams. J. Sound and Vibration, 41:433–49.

Murin, J. (1995). “The Formulation of A New Non-Linear Stiffness Matrix of A Finite Element”. Computers and Structures 54 (5), pp. 933–938.

Nabi S.M., Ganesan N. (1994) “A generalized element for the free vibration analysis of composite beam.” Computer Structure, 51 pp607–10.

Nakayasu H., Maekawa Z. (1997) “A comparative study of failure criteria in probabilistic fields and stochastic failure envelopes of composite materials”, Reliability Engineering and System Safety, 56 pp 209-220.

Ni, R.G., Adams, R.D. (1984) “The damping and dynamic moduli of symmetric laminated composite beams, theoretical and experimental results.”, Journal of Composite Materials, 18:104–121.

Ramtekkar G. S., and Desai Y. M. (2002) “Natural vibrations of laminated composite beams by using mixed finite element modeling.”, J. Sound and Vibration, 635–651.

Rao M. K., Desai Y. M., Chitnis M. R. (2001) “Free vibrations of laminated beams using mixed theory.” Composite Structure, 52:149–60.

Reddy, J. N. (1992). An Introduction to the Finite Element Method (Second ed.). New York, NY: McGraw-Hill.

Reddy, J. N. (1997). Mechanics of Laminated Composite Plates and Shells: Theory and Analysis. New York, NY: CRC Press.

Reddy, J. N. (2002). Energy Principles and Variational Methods in Applied Mechanics. John Willey & Sons, Inc.

Ruotolo R. (2004) "A spectral element for laminated composite beams: theory and application. J. Sound and Vibration, 270:149–69.

Schueller, G. I. (1997). "A State-of-the-Art Report on Computational Stochastic Mechanics". Probabilistic Engineering Mechanics 12 (4), pp. 197–321.

Shames, I. H. and Dym, C. L., (1985). Energy and Finite Element Methods in Structural Mechanics,McGraw-Hill, New York.

Shi, G., K. Y. Lam, and T. E. Tay (1998). "On Efficient Finite Element Modeling of Composite Beams and Plates Using Higher-Order Theories and An Accurate Composite Beam Element". Composite Structures 41 (2), pp. 159–165.

Shimpi R.P., Ainapure A.V. (1999) "Free vibration analysis of two layered cross-ply laminated beams using layer-wise trigonometric shear deformation theory." Communication Numerical Method in Engineering, 15 pp 651–60.

Soldatos KP, Elishako. I. (1992) “A transverse shear and normal deformable orthotropic beam theory.” Sound and Vibration, 154 pp 528–33.

Song S.J., Waas A.M. (1997) “Effects of shear deformation on buckling and free vibration of laminated composite beams.” Composite Structure, 37 pp 33–43.

Subramanian, P. (2001). “Flexural Analysis of Symmetric Laminated Composite Beams Using C1 Finite Element”. Composite Structures 54 (1), pp. 121–126. Technical Note.

Subramanian P. (2006) “Dynamic analysis of laminated composite beams using higher order theories and finite elements”, Composite Structures, pp.342–353.

Teboub, Y. and P. Hajela (1995). “Free Vibration of Generally Layered Composite Beams Using Symbolic Computations”. Composite Structures 33 (3), pp 123–134.

Teoh L.S., Huang C.C. (1976) “The vibration of beams of fibre reinforced material.” Sound and Vibration, 51 pp 467–73.

Teoh L.S. (1975), Thesis, Department of MechanicalEngineering, University of Western Australia, Nedlands, Western Australia. 'The vibration of cantilever beams of fiber reinforced material.'

Timoshenko, S. P., (1921), On the correction for shear of the differential equation for transverse vibrations of prismatic bars, Philosophical Magazine and Journal of Science, 41, pp. 744—747.

Timoshenko, S. P.,(1922), On the transverse vibrations of bars of uniform cross-section, Philosophical Magazine and Journal of Science, 43 (1922), pp. 125-131.

Timoshenko, S. P. and J. N. Goodier (1970). Theory of Elasticity (Third edition), New York, McGraw-Hill.

Truesdell, C. A. and W. Noll (1965). The Non-linear Field Theories of Mechanics (S. Fl¨ugge ed.), Volume III/3. Berlin: Springer-Verlag.

Vinckenroy, G. V., W. P. de Wilde, and J. Vantomme (1995). "Monte Carlobased Stochastic Finite Element Method: A New Approach for Structural Design". Vrije Universiteit Brussel.

Vinckenroy, G. V. and W. P. de Wilde (1995). “The Use of Monte Carlo Techniques in Statistical Finite Element Methods for the Determination of the Structural Behaviour of Composite Materials Structural Components”. Composite Structures 32, pp. 247–253.

Vinckenroy, G. V. (1994). Monte Carlo-Based Stochastic Finite Element Method: An Application to Composite Structures. Ph. D. thesis, Departement Analyse van Strukturen, Vrije Universiteit Brussel, Brussels, Belgium.

Vinson J. R., Sierakowski RL. (1986) “Behaviour of structures composed of composites materials”. Kluwer Academic Publishers.

Vitaliani, R. V., A. M. Gasparini, and A. V. Saetta (1997). “Finite Element Solution of the Stability Problem for Nonlinear Undamped and Damped Systems Under Nonconservative Loading”. International Journal of Solids and Structures 34 (19), pp. 2497–2516.

Wu Y., Youalin Z., Yuanming L., Weideng P. (2002) “Analysis of shear lag and shear deformation effects in laminated composite box beams under bending loads.” Composite Structures, 55 pp145-156.

Wyss, G. D. and K. H. Jorgensen (1998). A User's Guide to LHS: Sandia's Latin Hypercube Sampling Software, SAND98-0210. Albuquerque, NM: Risk Assessment and Systems Modeling Department, Sandia National Laboratories.

Yildirim, V. and E. Kiran (2000). "Investigation of the Rotatory Inertia and Shear Deformation Effects on the Out-of-Plane Bending and Torsional Natural Frequencies of Laminated Beams". Composite Structures 49 (3), pp. 313–320.

Yildirim, V. (2000). "Effect of the Longitudinal to Transverse Moduli Ratio on the In-Plane Natural Frequencies of Symmetric Cross-Ply Laminated Beams by the Stiffness Method". Composite Structures 50 (3), pp. 319–326.

Yuan F. and Miller R. E. (1990) "A higher order finite element for laminated beams". Composite Structure 14: pp.125-150.